UNIVERSITEIT VAN PRETORIA
UNIVERSITY OF PRETORIA
YUNIBESITHI YA PRETORIA

BIOAUGMENTATION OF COAL GASIFICATION STRIPPED GAS LIQUOR WASTEWATER IN A HYBRID FIXED-FILM BIOREACTOR

ELEONORA MARIA ELIZABETH RAVA

A thesis submitted in partial fulfilment of requirements for the degree of

DOCTOR OF PHILOSOPHY (CHEMICAL TECHNOLOGY)

in the

FACULTY OF ENGINEERING, BUILT ENVIRONMENT AND INFORMATION TECHNOLOGY

UNIVERSITY OF PRETORIA

2017

ABSTRACT

Title: Bioaugmentation of Coal Gasification Stripped Gas Liquor Wastewater in a Hybrid Fixed-Film Bioreactor

Author: Eleonora ME Rava
Supervisor: Professor Evans Chirwa
Department: Chemical Engineering
University: University of Pretoria
Degree: Doctor of Philosophy (Chemical Technology)

Coal gasification stripped gas liquor (CGSGL) wastewater contains large quantities of complex organic and inorganic pollutants which include phenols, ammonia, hydantoins, furans, indoles, pyridines, phthalates and other monocyclic and polycyclic nitrogen-containing aromatics, as well as oxygen- and sulphur-containing heterocyclic compounds. The performance of most conventional aerobic systems for CGSGL wastewater is inadequate in reducing pollutants contributing to chemical oxygen demand (COD), phenols and ammonia due to the presence of toxic and inhibitory organic compounds.

There is an ever-increasing scarcity of freshwater in South Africa, thus reclamation of wastewater for recycling is growing rapidly and the demand for higher effluent quality before being discharged or reused is also increasing. The selection of hybrid fixed-film bioreactor (H-FFBR) systems in the detoxification of a complex mixture of compounds such as those found in CGSGL has not been investigated. Thus, the objective of this study was to investigate the detoxification of the CGSGL in a H-FFBR bioaugmented with a mixed-culture inoculum containing *Pseudomonas putida*, *Pseudomonas plecoglossicida*, *Rhodococcus erythropolis*, *Rhodococcus qingshengii, Enterobacter cloacae, Enterobacter asburiae* strains of bacteria, as well as the seaweed (*Silvetia siliquosa*) and diatoms.

The results indicated a 45% and 79% reduction in COD and phenols, respectively, without bioaugmentation. The reduction in COD increased by 8% with inoculum PA1, 13% with inoculum PA2 and 7% with inoculum PA3. Inoculum PA1 was a blend of *Pseudomonas, Enterobacter and Rhodococcus* strains, inoculum PA2 was a blend of *Pseudomonas putida*

strains and inoculum PA3 was a blend of *Pseudomonas putida* and *Pseudomonas plecoglossicida* strains. The results also indicated that a 70% carrier fill formed a dense biofilm, a 50% carrier fill formed a rippling biofilm and a 30% carrier fill formed a porous biofilm. The autotrophic nitrifying bacteria were out-competed by the heterotrophic bacteria of the genera *Thauera, Pseudaminobacter, Pseudomonas* and *Diaphorobacter.* Metagenomic sequencing data also indicated significant dissimilarities between the biofilm, suspended biomass, effluent and feed microbial populations. A large population (20% to 30%) of unclassified bacteria were also present, indicating the presence of novel bacteria that may play an important role in the treatment of the CGSGL wastewater.

The artificial neural network (ANN) model developed in this study is a novel virtual tool for the prediction of COD and phenol removal from CGSGL wastewater treated in a bioaugmented H-FFBR. Knowledge extraction from the trained ANN model showed that significant non-linearities exist between the H-FFBR operational parameters and the removal of COD and phenol. The predictive model thus increases knowledge of the process inputs and outputs and thus facilitates process control and optimisation to meet more stringent effluent discharge requirements.

Keywords: Artificial Neural Network (ANN)**,** Bioaugmentation**,** Biofilm, Coal Gasification, Chemical Oxygen Demand (COD), Microbial Diversity, Next Generation Sequencing (NGS), Phenols, Predictive Modelling, *Pseudomonas.*

DECLARATION

I, Eleonora Maria Elizabeth Rava, declare that this thesis which I hereby submit for a Doctor of Philosophy in Chemical Technology degree at the University of Pretoria is my own work and has not been previously submitted by me for any degree at this institution or any other institutions.

_____ _____

Eleonora Maria Elizabeth Rava Date

ACKNOWLEDGEMENTS

I would like to thank Buckman Africa and in particular, Peter Wheeler, for his support, as well as Minkie Mmola, Michelle Taylor, Maria Tigeli, Ayanda Dladla and Thaira Gany for their assistance in terms of laboratory work in the Enstra and Hammarsdale laboratories.

I also would like to thank the following people and institutions:

- University of Pretoria for funding the metagenomic, 16S rRNA and 18S rRNA studies.
- Dr. Gueguim Kana for his assistance in the development of the intelligent model for the prediction of COD and phenol removal.
- Michael van Niekerk and Ronel Augustyn from Sasol Group Technology (Pty) Ltd for the use of the pilot plant.
- Denver Karshagen from East Rand Water (ERWAT) for all the GC-MS analysis.
- Hamilton Govender and Christiaan Labuschagne from Inqaba Biotechnical Industries (Pty) Ltd for the metagenomic and PCR sequencing of the bioaugmentation inocula and research samples.
- Elsevier Inc. for granting permission for the reproduction of excerpts and figures used in Chapter 2 under license number 3774650368525.

Finally, a huge thanks to all my family, Matthew and Daisy for their patience and support.

TABLE OF CONTENTS

Table of Contents continued

Table of Contents continued

Table of Contents continued

Table of Contents continued

LIST OF FIGURES

List of Figures continued

LIST OF TABLES

List of Tables continued

LIST OF ABBREVIATIONS

AAP	aminoantipyrine
AHL	*N-acyl* homoserine lactone
AIs	auto-inducers
ANN	artificial neural network
ANOVA	analysis of variance
AOA	ammonia-oxidising Archaea
AOB	ammonia-oxidising bacteria
APHA	American Public Health Association
API	American Petroleum Industry
AR	analytical reagent grade
ATP	adenosine triphosphate
BFW	boiler feed water
BLAST	Basic Local Alignment Search Tool
BLASTn	Basic Local Alignment Search Tool nucleotide
BOD_5	biological oxygen demand (5 day)
CGSGL	coal gasification stripped gas liquor
CGWW	coal gasification wastewater
CLL™	Chemie Linz and Lurgi (CLL) ammonia recovery process
COD	chemical oxygen demand
CTL	coal-to-liquor
DCM	dichloromethane
DCS	data collection system
DIPE	diisopropyl ether
DMH	5,5-dimethyl-hydantoin
DNA	deoxyribonucleic acid
DO	dissolved oxygen
DWAF	Department of Water Affairs and Forestry
EDX	energy-dispersive X-ray
EI	electron impact
EMH	5-ethyl-5-methyl-hydantoin
EPS	extracellular polymeric substance

List of Abbreviations continued

ERWAT	East Rand Water Care Company
EWG	electron withdrawing groups
F/M	food-to-mass ratio
FBDB™	Fixed-Bed Dry-Bottom
FEG-SEM	field-emission gun scanning electron microscopy
FE-SEM	field-emission scanning electron microscopy
FT-IR	Fourier transform infrared
FTRW	Fischer-Tropsch Reaction Water
GC-MS	gas chromatography-mass spectrometry
gDNA	genomic deoxyribonucleic acid
GLS™	Gas Liquor Separation
H-FFBR	hybrid fixed-film bioreactor
H-MBBR	hybrid moving-bed biofilm reactor
HMBP	hybrid membrane biofilm process
HPC	heterotrophic plate counts
HRT	hydraulic retention time
IC	ion chromatography
ICP	inductively coupled plasma
ICP-OES	inductively coupled plasma-optical emission spectroscopy
IEC	International Electrotechnical Commission
IFAS	integrated fixed-film activated sludge
ISO	International Organization for Standardization
LP	low pressure
MBBR	moving-bed biofilm reactor
MBR	membrane bioreactor
MCRT	mean cell retention time
MINAS	Minimum National Standards
MLP	multi-layer perceptron
MLSS	mixed liquor suspended solids
MLVSS	mixed liquor volatile suspended solids
MSD	mass selective detector

List of Abbreviations continued

MSE	mean square error
NCBI	National Center for Biotechnology Information
NGS	next-generation sequencing
NIST	National Institute of Standards and Technology
NOB	nitrogen-oxidising bacteria
OECD	Organisation for Economic Co-operation and Development
OLR	organic loading rate
OTU	operational taxonomic units
OUR	oxygen uptake rate
PAHs	polycyclic aromatic hydrocarbons
PCoA	principal coordinates analysis
PCR	polymerase chain reaction
PERMANOVA	permutational analysis of variance
QS	quorum sensing
r/min	revolutions per minute
RAS	return activated sludge
RBC	rotating biological contactor
rDNA	ribosomal deoxyribonucleic acid
RMSE	root mean square error
RNA	ribonucleic acid
rRNA	ribosomal ribonucleic acid
SABS	South African Bureau of Standards
SANAS	South African National Accreditation System
SANS	South African National Standard
SCST	specific capillary suction test
SEM	scanning electron microscopy
SGL	stripped gas liquor
SRT	sludge retention time
SS	suspended solids
SVOC	semi-volatile organic compounds
TDS	total dissolved solids

List of Abbreviations continued

TKN	total Kjeldahl nitrogen
TSS	total suspended solids
UniFrac	unique fraction metric
UPGMA	Unweighted Pair Group Method with Arithmetic Mean
USEPA	United States Environmental Protection Agency
WAS	waste activated sludge
WHO	World Health Organization
ZLD	zero liquid discharge

CHAPTER 1
INTRODUCTION

1.1 Background

Coal gasification wastewater, such as stripped gas liquor, is generated during the coal-to-liquid Lurgi-Phenosolvan® process. The wastewater contains large quantities of complex organic and inorganic pollutants such as phenols, ammonia, thiocyanate, cyanide (Park et al., 2008; Cui et al., 2017), monocyclic and polycyclic nitrogen-containing aromatics, and oxygen- and sulphur-containing heterocyclic compounds (Gubuza, 2008; Ji et al., 2015a). Phenol and its derivatives induce genotoxic, carcinogenic, immunotoxic, haematological and physiological effects (Nahed and Saad, 2008) in organisms living in the receiving water bodies and higher-order organisms (Li and Han, 2013; Pal and Kumar, 2014). The guideline value for phenols is <30 µg/L for freshwater bodies (DWAF, 1996) and <1 µg/L for drinking water (Pishgar et al., 2012).

Biological treatment has been used to treat coal gasification stripped gas liquor (CGSGL) mostly after pretreatment by the process of phenol solvent extraction and ammonia stripping to avoid inhibition of the biological process. Biological treatment is considered more environmentally compatible and therefore sustainable in the long term (Lim et al., 2013). However, most conventional aerobic systems for coal gasification wastewater treatment are not sufficient in reducing chemical oxygen demand (COD), phenols and ammonia due to the presence of refractory organics (Ji et al., 2015a). For this reason, a more robust biological system such as the hybrid fixed-film bioreactor (H-FFBR) system was considered.

Efficient removal of pollutants in biofilm systems using carriers was demonstrated by Jeong and Chung (2006) who reported the removal of COD, thiocyanate, cyanide and nitrogen from coal processing wastewater using a fluidised biofilm process. High removal efficiencies of 97%, 99%, 99% and 93% were obtained for COD, cyanide, thiocyanate and ammonia, respectively. Mazumder (2010) reported removal efficiencies of 80% and 90% for COD and ammonia, respectively, from high-strength wastewater using a shaft-type aerobic hybrid bioreactor. Li et al. (2011) reported the removal of phenols, thiocyanate and ammonia-nitrogen from coal gasification wastewater using a moving-bed biofilm reactor (MBBR).

Li et al. (2011) also reported that biofilm processes were reliable for the removal of organic carbon and nitrogen without some of the problems associated with conventional activated sludge processes since nitrifying bacteria in the biofilm would be more resistant to inhibitory constituents in the wastewater. However, the selection of hybrid fixed-film bioreactor systems in the detoxification of a complex mixture of compounds such as those found in CGSGL wastewater has not been investigated. The proposed system in this study relies on improved contact of pollutants in the wastewater with the biofilm and bioaugmented microbial community.

1.2 Problem statement

Coal gasification stripped gas liquor (CGSGL) wastewater from a petrochemical refinery does not meet effluent standards with respect to COD, phenols and ammonia-nitrogen when treating the effluent using the conventional activated sludge process. The removal of COD, phenols and ammonia-nitrogen can be achieved biologically by bioaugmenting a hybrid fixed-film bioreactor (H-FFBR) with strains of *Pseudomonas putida*, *Pseudomonas plecoglossicida*, *Rhodococcus erythropolis*, *Rhodococcus qingshengii, Enterobacter cloacae* and *Enterobacter asburiae,* as well as the seaweed *Silvetia siliquosa* and diatoms.

1.3 Aims and objectives

The main objective of this study was to investigate the removal of chemical oxygen demand (COD), phenols and ammonia-nitrogen in a hybrid fixed-film bioreactor (H-FFBR) inoculated with a mixed inoculum containing *Pseudomonas putida*, *Pseudomonas plecoglossicida*, *Rhodococcus erythropolis*, *Rhodococcus qingshengii, Enterobacter cloacae, Enterobacter asburiae* strains and other unidentified species of bacteria, seaweed and diatoms.

To achieve the above objective, the following tasks and targets were set:

- Quantifying the removal of COD, phenols and ammonia-nitrogen in the H-FFBR by the indigenous microbial community.
- Determining the main parameters affecting the biofilm structure and biological activity.
- Characterising the H-FFBR indigenous population by next-generation sequencing (NGS).

- Using 16S rRNA gene sequence analysis to characterise the specific strains of *Pseudomonas putida*, *Pseudomonas plecoglossicida*, *Rhodococcus erythropolis*, *Rhodococcus qingshengii, Enterobacter cloacae* and *Enterobacter asburiae* selected as bioaugmentation inocula.
- Quantifying the removal of COD and phenols in the H-FFBR inoculated with the selected strains of *Pseudomonas putida*, *Pseudomonas plecoglossicida*, *Rhodococcus erythropolis*, *Rhodococcus qingshengii, Enterobacter cloacae* and *Enterobacter asburiae.*
- Using 18S rRNA gene sequence analysis to characterise the seaweed (*Silvetia siliquosa*) and quantifying the removal of suspended solids.
- Developing a predictive intelligent model for the removal of COD and phenol from CGSGL wastewater in a bioaugmented H-FFBR.

1.4 Methodology

The removal of COD, phenols and ammonia-nitrogen in the H-FFBR inoculated with specific blends of *Pseudomonas putida*, *Pseudomonas plecoglossicida*, *Rhodococcus erythropolis*, *Rhodococcus qingshengii, Enterobacter cloacae* and *Enterobacter asburiae* strains was studied. The methodology employed to achieve these aims and objectives of the study included:

a) Undertaking a detailed literature review of the generation of the coal gasification stripped gas liquor (CGSGL) wastewater and biological processes used for the treatment of this complex wastewater.
b) Determination of the chemical composition of the CGSGL wastewater to identify biodegradable and non-biodegradable compounds specific to the petrochemical refinery wastewater.
c) Carrying out next-generation sequencing (NGS) studies of the indigenous microbial community in the H-FFBR to gain an understanding of the community structure and diversity at different taxa levels.
d) Conducting experiments to determine the removal of COD, phenols and ammonia-nitrogen in the H-FFBR by the indigenous microbial population.
e) Determination of the main parameters affecting the biofilm structure.
f) Conducting experiments to determine the removal of COD, phenols and ammonia-nitrogen in the H-FFBR bioaugmented with specific blends of *Pseudomonas putida*, *Pseudomonas*

plecoglossicida, *Rhodococcus erythropolis*, *Rhodococcus qingshengii, Enterobacter cloacae* and *Enterobacter asburiae* strains.

1.5 Organisation of the thesis

This thesis consists of the following chapters and appendices:

- Chapter 1 presents an introduction to the study; it explains the motivation, main aims, objectives and scope of the study, highlighting the importance of the research study. It also provides an outline of the organisational structure of the thesis.
- Chapter 2 provides an extensive review of the literature relevant to the present research, with technical information on the theoretical background of CGSGL wastewater composition and biodegradation by biological processes.
- Chapter 3 presents technical details of the pilot H-FFBR operating parameters, materials used, as well as the analytical and experimental methods used.
- Chapter 4 describes the characterisation of the indigenous microbial communities in the H-FFBR by next-generation sequencing, phylogenetic diversities and lineages (phylogenetic tree).
- Chapter 5 presents the composition of the feed and effluent, factors affecting the structure of the biofilm, and quantifies the removal of COD, phenols, and ammonia-nitrogen in the H-FFBR by the indigenous microbial community.
- Chapter 6 describes the characterisation of the strains of *Pseudomonas putida*, *Pseudomonas plecoglossicida*, *Rhodococcus erythropolis*, *Rhodococcus qingshengii, Enterobacter cloacae* and *Enterobacter asburiae* by 16S rRNA gene sequencing and the characterisation of the seaweed (*Silvetia siliquosa*) by 18S rRNA gene sequencing. Chapter 6 also presents the quantification of the removal of COD and phenol in the H-FFBR.
- Chapter 7 presents a predictive intelligent model based on an artificial neural network for the removal of COD and phenol in the bioaugmented H-FFBR.
- Chapter 8 provides a summary of the key findings of this study and the conclusions drawn from the findings; also included in this chapter are recommendations for further studies.
- Chapter 9 presents a listing of all cited reference materials.
- Appendices.

CHAPTER 2
LITERATURE REVIEW

2.1 Background

Sasol is a signatory to the Responsible Care® initiative, the global chemical industry's environmental, health and safety (EHS) initiative to drive continuous improvement in performance (Beloff et al., 2005). The Sasol refinery is currently expanding its operations both locally and internationally and, in line with global standards, all new operational designs employ total reuse or zero liquid discharge (ZLD) approaches. This approach results in the reduction of water demand through recycling and avoidance of possible off-site impacts on the surrounding environment (Meerholz and Brent, 2013). Compounding the problem are the unique characteristics of the effluent streams, thus case studies and best practices in related industries cannot be applied directly to this petrochemical refinery effluent (Meerholz and Brent, 2013).

2.2 Sasol-Lurgi Fixed-Bed Dry Bottom (FBDB^{TM}) process generating coal gasification stripped gas liquor wastewater stream

The Sasol process starts at the gasification plant where low rank coal (lignite) is converted to crude gas under pressure and at a high temperature in the presence of steam and oxygen (Gai et. al., 2016). At both Sasolburg and Secunda, synthesis gas (syngas) is produced from coal using the Sasol-Lurgi Fixed-Bed Dry Bottom (FBDB^{TM}) gasifiers. Coal is loaded from an overhead bunker into a lock hopper that is isolated from the reactor during loading, then closed, pressurised with syngas, and opened to the reactor. The coal from the lock hopper is distributed over the area of the reactor by a mechanical distribution device, and then moves slowly down through the bed, undergoing the processes of drying, devolatilisation, gasification and combustion. The ash from the combustion of ungasified char is removed from the reactor chamber via a rotating grate, and is discharged into an ash lock hopper. In the grate zone the ash is pre-cooled by the incoming blast (oxygen and steam) to about 300 ℃ to 400 °C. The blast enters the reactor at the bottom and is distributed across the bed by the grate. Flowing upwards, it is pre-heated by the ash before reaching the combustion zone in which oxygen (O_2) reacts with the char to form carbon dioxide (CO_2). At this point in the reactor the temperatures reach their highest level (Figure 2.1).

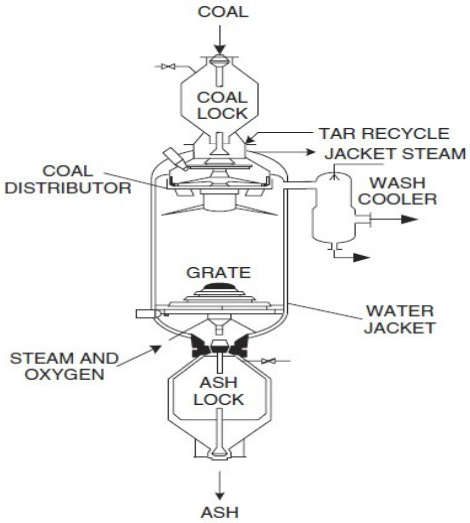

Figure 2.1: Sasol-Lurgi FBDB^{TM} gasifier (Higman and Van der Burgt, 2008)

The O_2 and steam then react with the coal in the gasification zone to form CO_2, hydrogen and methane. The gas composition at the outlet of the gasification zone is governed by the three heterogeneous gasification reactions: water-gas, Boudouard, and methanation. The gas leaving the gasification zone then enters the upper zones of the reactor where the heat of the gas is used to devolatilise, pre-heat and dry the incoming coal. In the process, the coal is cooled from 800 ºC at the outlet of the gasification zone to about 550 ºC at the reactor outlet (Figure 2.2).

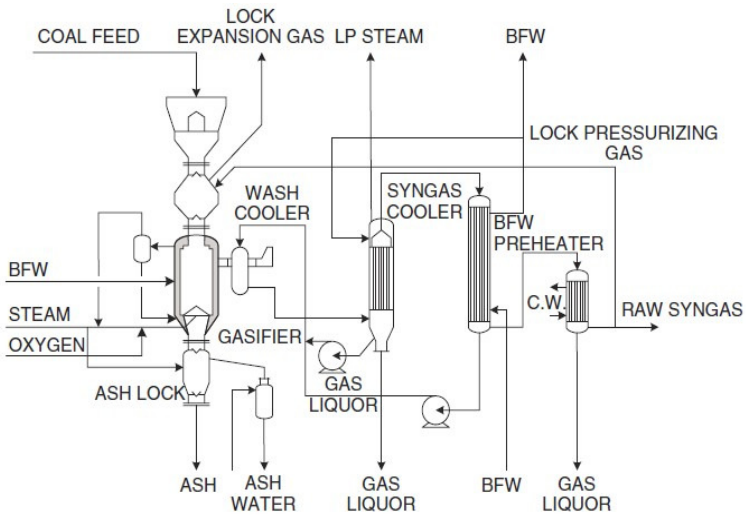

Figure 2.2: Sasol-Lurgi FBDB^{TM} gasification loop (Higman and Van der Burgt, 2008)

A result of the counter-current flow is the relatively high methane content of the outlet gas. On the other hand, part of the products of devolatilisation are contained unreacted in the synthesis gas, particularly tars, phenols and ammonia, but also a wide range of other hydrocarbon

species. Bulk removal of this material takes place immediately at the outlet of the reactor by means of a quench cooler in which most of the high-boiling hydrocarbons and dust carried over from the reactor are condensed and/or washed out with gas liquor from the downstream condensation stage. The gas liquor from the quench cooler typically contains suspended matter (1 000 mg/L), sulphur (600 mg/L), chlorides (50 mg/L), ammonia-nitrogen (10 000 mg/L), cyanides (50 mg/L), phenols (1 000 mg/L to 5 000 mg/L) and COD (10 000 mg/L) (Higman and Van der Burgt, 2008). Lurgi developed two processes for the recovery of phenols and ammonia, i.e. Phenosolvan® and Lurgi CLL™ (Gai et al., 2016) (Figure 2.3).

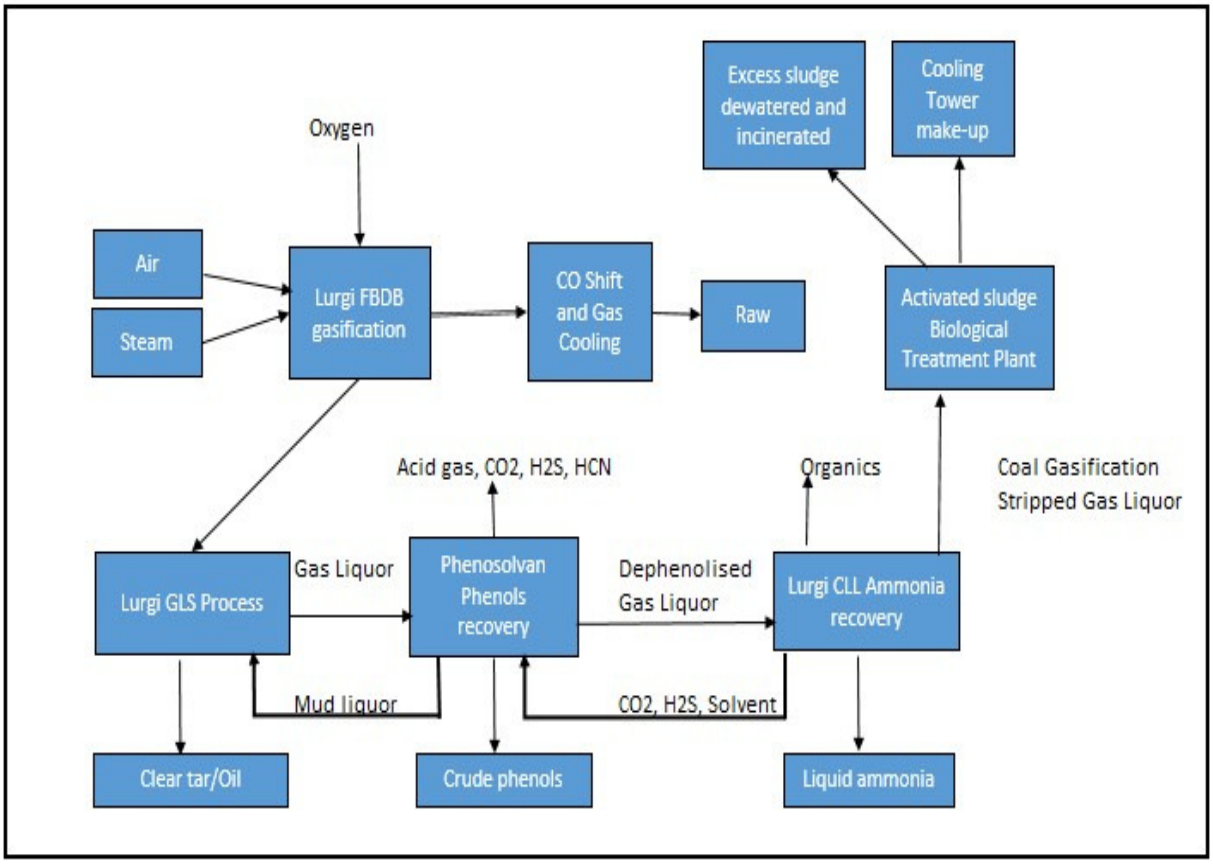

Figure 2.3: Flow diagram of the Sasol-Lurgi gasification loop and generation of the CGSGL wastewater stream

The Phenosolvan® process is a proprietary solvent extraction process developed by Lurgi for the removal of phenols from coke oven and coal gasification process wastewaters (Gai et al., 2016). The Phenosolvan® process consists of three parts: filtration, extraction and solvent recovery. Gas liquor from the Gas Liquor Separation™ (GLS) process unit is filtered through a gravel bed to remove suspended matter. The liquor then enters a counter-current extractor where phenols are extracted from the liquor by counter-current contact with a solvent such as

diisopropyl ether (DIPE) (Lin et al., 2005; Gai et al., 2008) or butyl ethanoate (Anastasi, 1980). Diisopropyl ether is mainly used in South African refineries and in most coal-gasification plants in China (Yang et al., 2013). The extract containing the solvent and phenols is distilled to separate the solvent. The distilled solvent is then recycled to the extractors. The solvent contained in the phenol after distillation is recovered by steam stripping and recycled to a distillation column. The crude phenols are mixed with tar, oil and naphtha recovered from the GLS process. The dephenolised liquor (raffinate) is gas-stripped with nitrogen (N_2) in a stripping column to remove any residual solvent in the liquor (Yu et al., 2010; Gai et al., 2016).

The N_2/solvent is washed with phenol to recover the solvent for recycling (Beychok, 1974). After N_2 stripping, the dephenolised gas liquor is fed to the Ammonia Recovery Unit (Lurgi CLL^{TM}) for the recovery of ammonia (fixed and free). The gas liquor is fed into a free ammonia still where free ammonia and acid gases (hydrogen sulphide and carbon dioxide) are recovered by live steam injection (Beychok, 1974). The liquid leaving the bottom of the free ammonia still is fed to a lime mixing vessel where a lime slurry is added to free the fixed ammonia. The mixture from the lime slurry vessel is fed to a fixed ammonia still to recover the remaining ammonia using steam stripping (Gai et al., 2008; Feng et al., 2009).

The ammonia vapours leaving the top of the fixed ammonia still are combined with the vapour leaving the free ammonia still and fed to the Phosam-W absorber (ammonium phosphate solution) for the recovery of ammonia. Upon leaving the ammonia stripping process the wastewater is known as stripped gas liquor (SGL) (Wernberg et al., 1984; Van Zyl, 2008). In general, the Phenosolvan® process extracts 99% of the monohydric phenols, 60% of the polyhydric phenols and 15% of other organics. Approximately 95% of the total organic carbon is removed by the coal liquefaction process (Higman and Van der Burgt, 2008).

2.3 Characterisation of coal gasification stripped gas liquor wastewaters

The inorganic and organic constituents of coal conversion wastewaters (gasification, liquefaction and coking) are very similar; however, these constituents are found at different ratios and concentrations (Kapusta and Stanczyk, 2011; Li et al., 2011). The composition will depend on the type of coal, the process and operating conditions, including the degree of recycling of the wastewater. Lignite coals (low rank) are a source of high levels of aromatic compounds with a higher oxygen content than higher-ranking coals (Skonde, 2009). Low-

ranking coal used in the Sasol-Lurgi process (Ginster and Matjie, 2005) contains large amounts of hydrophilic polar groups such as -OH, -COO, -O, -N, -S (Molva, 2004). A number of coal gasification plants in China also use lignite coals as a raw material to produce gas via the Lurgi process (Yang et al., 2006). Jin et al. (2013) observed the presence of phenols, cyanides, thiocyanates, polycyclic aromatic hydrocarbons (PAHs), nitrogen-, oxygen- and sulphur-containing heterocyclic compounds in the coking wastewater. Gai et al. (2008) reported the presence of hydrogen sulphide (H_2S), ammonia (NH_3) and fatty acids (carboxylic acids), while Liu et al. (2013) and Ji et al. (2015) observed the presence of long-chain alkanes.

2.3.1 Organic compounds

Numerous reports have been published since the 1970s indicating the presence of various organics in the wastewater. In terms of the identification and classification of the organics, it is important to understand which compounds are present and which are biodegradable. The organic compounds identified were dependent on the sample preparation and instrumentation used at the time of reporting.

Beychok (1974) classified the term phenols to include monohydric phenols (cresols, xylenols and ethyl-phenols) which contain one hydroxyl group, and polyhydric phenols which contain two or more hydroxyl groups (catechol and resorcinol). Schmidt et al. (1974) detected the presence of various organic compounds in acid and alkali extracts of the wastewater analysed by high-resolution mass spectrometry combined with gas chromatography. Phenols, cresols, indoles, benzofuranols and xylenols were detected in both acid and alkali fractions, whereas catechols and dihydroxybenzenes were detected only in the acid fractions and the pyridines were detected only in the alkali fractions.

Stamoudis and Luthy (1980) classified organic compounds into acid fractions, base fractions and neutral fractions. The acid fraction consisted of phenols and cresols, the base fraction consisted of nitrogen heterocyclic compounds and the neutral fraction consisted of toluenes and alkylated cycloalkanes. Stamoudis and Luthy (1980) found that 99% of the acid fractions, 96% of the base fractions and 93% of the neutral fractions would be removed by biological treatment. Wei and Goldstein (1977) and Liu et al. (2013) reported that phenols were readily biodegradable and effectively removed by optimising technology and operating parameters.

Phenolics were reported to comprise 40% to 80% of the organic carbon in the wastewater of which 70% to 80% were monohydric phenols and 20% to 30% were dihydric phenols (Beychok, 1974; Bryant et al., 1988; Ji et al., 2015). Yang et al. (2006) reported dihydric and trihydric phenols to be resistant to biological degradation. Wang et al. (2012) and Fang et al. (2014) found polycyclic aromatic hydrocarbons (PAHs), ammonia, cyanides and thiocyanates to be resistant to biological degradation. Ji et al. (2015a) reported that biological processes were the most cost-effective to treat pretreated coal gasification wastewater.

Interestingly, relatively scant published literature is available on the presence of hydantoins in coal gasification stripped gas liquor (CGSGL) wastewater. Hydantoins are non-volatile, highly polar heterocyclic compounds which are not removed by solvent extraction or ammonia-stripping (Turner et al., 1985). Pavlovich and Luthy (1988) reported that 5,5-dimethyl-hydantoin (DMH) was slightly more soluble in aqueous media than 5-ethyl-5-methyl-hydantoin (EMH) and both could form complexes with transition metals at a pH of 8.5. According to Turner et al. (1985), hydantoins were specific to slagging fixed-bed gasification due to the high hearth temperatures that promote cyanide formation. Cyanides combine with carbon dioxide, ammonia and ketones during the gas quenching process to form hydantoins. Ethylmethylhydantoin (EMH) is formed when the ketone is 2-butanone, and dimethylhydantoin (DMH) is formed when the ketone is acetone. Olson et al. (1985) reported that hydantoins were formed at a pH of 8.5 and were found in relatively high concentrations (2 000 mg/L for DMH and 500 mg/L for EMH) in CGSGL. Pavlovich and Luthy (1988) found DMH to be the major constituent of hydantoins identified in CGSGL from slagging fixed-bed gasification and that it accounted for most of the chemical oxygen demand (COD) fraction in CGSGL. According to Wernberg et al. (1984), DMH and EMH contributed up to 90% of the total COD.

2.3.2 Inorganic compounds and metals

The identification of inorganics, metals and salts is important from an environmental and a biological treatment perspective since certain substances cause a shift in microbial communities while others inhibit microbial growth. Iwase et al. (1979) reported the presence of sodium, potassium, calcium, barium and aluminium, while Luthy et al. (1980) observed the presence of low levels of heavy metals such as cadmium, chromium, copper, nickel and iron. Iron complexed with cyanide makes iron unavailable as an inhibitor (complexed cyanide is less

toxic) or as a biological nutrient. According to Luthy et al. (1980), the wastewater was deficient in magnesium, phosphorus and potassium. Potassium, magnesium, sodium, calcium, iron and chlorides are macronutrients required for membrane stabilisation. Excessive amounts can be inhibitory to microbial growth.

Micronutrients such as zinc, manganese, molybdenum, selenium, copper, cobalt, nickel, vanadium and tungsten have been reported to allow many enzymes to function properly. Calcium and phosphorus absorb and accumulate in the biofilm as insoluble compounds rendering the biofilm highly resistant to detachment. Sulphur is required for protein synthesis, phosphorus for nucleic acids and metabolic cofactors, and nitrogen for proteins, some sugars and nucleic acids. Aluminium binds to microbial cell membranes and potassium diffuses into the cell and neutralises the membrane potential (Rava et al., 2015).

2.3.3 Effluent discharge requirements for petrochemical refineries

The trend over the years has been to move away from the identification of specific organic compounds and to rather focus more on the quantification and reporting of phenols, ammonia-nitrogen, cyanides, thiocyanates, poly-aromatic hydrocarbons (PAHs) and chemical oxygen demand (COD) to meet specific discharge guidelines for CGSGL wastewater generated by petrochemical refineries. This has also led to the use of approved standardised methods for quantification.

The Minimal National Standard (MINAS) concentration limits for South African refineries are to be met at the outlet, discharging effluent (excluding discharge from sea-water cooling systems) to receiving environments (surface water bodies, marine systems or public sewers) (Mazema et al., 2008). In case of reuse of the effluent directly for irrigation/horticulture purposes (within the premises of the refinery) and/or make-up water for cooling systems, the concentration limits will also apply at the outlet before reusing the effluent.

The MINAS guideline is not as comprehensive as that issued by the World Bank Group but is more stringent in terms of biological oxygen demand (BOD_5), suspended solids (SS), oil and grease, sulphides and less stringent on COD, benzene, phenols and total nitrogen. No limits are indicated for benzo(a)pyrene, copper, cyanides, hexavalent chromium, iron, mercury, nickel, vanadium and phosphorus (Mazema et al., 2008; World Bank Group, 2007) (Table 2.1).

Table 2.1: Proposed guidelines for discharge or reuse of petrochemical refinery effluent

Pollutant	Nigeria	European Union	India	MINAS for SA	World Bank Group
pH		6–9	6–8.5	6–9	6–9
BOD_5	10	2–50	15	15	30
COD	40	30–225		125	150
SS		2–80	20	20	30
Oil and grease	10	0.05–9.8	1.0	5.0	10
Benzene		<0.001–1		0.10	0.05
Benzo(a)pyrene					0.05
Chromium		0.1–0.5		2.0	0.50
Copper					0.50
Cyanide (free)					0.10
Cyanide (total)					1.0
Hexavalent chromium					0.05
Iron					3.0
Lead	0.05	0.2–0.3		0.10	0.10
Mercury					0.02
Nickel					0.50
Phenols	0.50	0.03–1	1	0.35	0.20
Sulphides		0.01–1		0.50	1.0
Temperature variation	3	10–35		<35	<3
Total nitrogen		1.5–100		15	10
Total phosphorus					2.0
Vanadium					1.0

[(a)]All units in mg/L except for temperature (^{0}C) and pH

Most conventional aerobic systems for coal gasification wastewater (CGWW) treatment are not efficient in reducing COD to meet discharge standards due to the presence of refractory compounds. Nitrification is also not effective since the typical aromatics in CGWW such as phenol, cresol, pyridines (Ji et al., 2015a), polynuclear aromatic hydrocarbons (PAHs), phenols and nitrogen heterocyclic compounds are inhibitory to *Nitrobacter* (Zhao et al., 2014).

2.4 Hybrid bioreactors for the treatment of coal gasification stripped gas liquor wastewater

Hybrid bioreactors have been shown to be the most effective and competitive alternatives for the treatment of high-strength coal gasification stripped gas liquor (CGSGL) wastewaters based on their high volumetric loading rate, high microbial biomass and long mean cell retention time (MCRT) for effective nitrification efficiency and stable effluent quality (Zhou et al., 2014). Biofilm processes have proven to be reliable for organic carbon and nitrogen removal (Li and Han, 2013) and these biological methods are simple, cheap and environmentally friendly operations since the organics are biologically converted to carbon dioxide (CO_2) and water (H_2O) (Ishak et al., 2012; Lim et al., 2013a).

2.4.1 Hybrid fixed-film bioreactors

Hybrid bioreactors incorporate suspended biomass (flocs) and attached biomass (biofilm) within the activated sludge process (Borkar et al., 2013). In such a system, the biofilm is grown on a fixed or movable carrier (media) inside the biological reactor. The combination of suspended growth and attached growth provides the system with different microbial communities and increases the biomass concentration and sludge ages, higher than those normally found in conventional activated sludge processes. Thus, the hybrid system combines the potential advantages of both suspended and attached bioreactors such as higher carbon and nitrogen removal (Kim et al., 2011; Li et al., 2012; Makowska et al., 2013). The attached biomass thus provides improved capacity without construction of new reactors (Sen and Randall, 2008; Li et al., 2012). The suspended biomass has a higher density than the attached biomass due to the higher amount of polyphosphate storage which can affect settleability (Kim et al., 2011; Li et al., 2012).

Hybrid bioreactors have many advantages and can be managed and optimised easily. They have shorter hydraulic retention times, can operate at temperatures of between 8 °C and 40 °C, have higher biomass concentrations, low food-to-mass (F/M) ratios, low solids loading on the settling tank, good settling properties, good resistance to hydraulic and organic shock loadings, growth of highly specialised biomass to achieve the desired treatment goals, and a continuous flow process eliminating the backwashing requirements.

This technology also allows for different tank geometries, and conventional activated sludge processes can easily be retrofitted giving high efficiency removal of organics and nitrogenous compounds, and retention of slow-growing and temperature-sensitive bacterial communities. However, the hybrid systems are more complex and are not analysed by conventional methods for activated sludge processes (Makowska et al., 2013; Shahot et al., 2014). Other disadvantages are the high cost of the biofilm carriers and its facilities, and the fact that increasing the volumetric load of biomass may lead to oxygen-supply limitations (Makowska et al., 2013). Hybrid bioreactors have been used to treat phenolic wastewaters (Sarkar and Mazumder, 2014) and the attached biomass had a greater activity in removing COD than the suspended biomass (Jing et al., 2009).

Borghei and Hosseini (2004) reported using a moving-bed biofilm reactor (MBBR) for the removal of phenolics and COD in wastewater and found that the MBBR was very stable against hydraulic and toxic shock loads and could handle phenolic wastes at concentrations of up to 220 mg/L of phenol; however, COD removal decreased as phenol concentration increased. Jeong and Chung (2006) used a fluidised biofilm process for the removal of COD, thiocyanate, cyanide and nitrogen from a coal processing wastewater. High removal efficiencies of 97%, 99%, 99% and 93% were obtained for COD, cyanide, thiocyanate and ammonia, respectively. Mazumder (2010) found removal efficiencies of 80% and 90% for COD and ammonia, respectively, from high-strength wastewater using a shaft-type aerobic hybrid bioreactor. Li et al. (2011) reported the removal of phenols, thiocyanate and ammonia-nitrogen from coal gasification wastewater using the MBBR and found that biofilm processes were reliable for the removal of organic carbon and nitrogen without some of the problems associated with conventional activated sludge processes since nitrifying bacteria in the biofilm would be more resistant to inhibitory/toxic constituents in the wastewater.

2.4.2 Biofilm carriers

A moving-bed biofilm reactor (MBBR) and an integrated fixed-film activated sludge (IFAS) bioreactor are compact biological wastewater treatment systems that use submerged high-surface-area movable/floating plastic carriers (media) in aerobic and/or anoxic zones (Sen and Randall, 2008; Boltz et al., 2009). The IFAS process was introduced in the late 1990s as an evolution of the MBBR where activated sludge is recycled back to the bioreactor containing the carriers (Rosso et al., 2011).

The analysis of hybrid systems is very complicated due to the difficulty of conducting the biofilm analyses, and differentiation between suspended (heterotrophic biomass) and attached (nitrifying biomass) microbial activity (Albizuri et al., 2009). Describing a hybrid system using a steady state model based on Monod kinetics expressions often yields a set of algebraic equations having no explicit solution even for biofilm only (Sen and Randall, 2008). At present, hybrid bioreactors are designed and based on a recommended volume ratio of the biofilm carrier to the reactor, which is obtained from field experience or experimental results (Fouad and Bhargava, 2005). Ratcliffe et al. (2006) reported that the filling of carrier media may be decided for each case giving flexibility in the specific biofilm surface area. A carrier filling ratio of ≤70% allowed the plastic media to move freely (Abdul-Majeed, 2012) without dead or unused spaces in the reactor (Ratcliffe et al., 2006).

Minimal difference in performance was found between a 33% and 66% carrier filling rate; however, at a carrier filling rate of 70% the attached growth density was 5 to 13 times higher and responded more strongly to influent COD than that of activated sludge floc found in suspended activated sludge systems (Qiqi et al., 2012). Makowska et al. (2013) reported that a carrier filling rate of 70% achieved 91% to 94% removal of organic compounds and 73% to 85% removal of nitrogenous compounds from CGWW.

Biofilm carriers are found in a variety of shapes, sizes, geometries, material composition and treatment capabilities. Manufactured carriers of the fixed-bed cord type variety include hexagonal-cell-cord-looped and linear-looped-cord types, while carriers of the movable type include polyethylene-finned cylinders resembling wagon wheels and cuboid sponges. The carrier material must protect the biofilm from toxic and inhibitory effects and excessive shear forces (Boltz et al., 2009; Quan et al., 2012; El-Jafry et al., 2013).

The type of media selected should be such that the biofilm specific surface area does not decrease significantly as the thickness increases (Sen et al., 2007).

The attachment of biofilm depends mainly on the mechanisms of biofilm adhesion to solid surfaces and the correlation of adhesion to various characteristics of the carrier such as surface energy, hydrophobicity, surface roughness (Bolton et al., 2006), large surface area, strength, porosity and durability (Quan et al., 2012). The properties of an ideal carrier are summarised in Table 2.2.

Table 2.2: Properties of an ideal carrier material and the effect on biofilm attachment

Property	Effect
High adsorbent capacity	Binding of toxic and inhibitory substances, faster colonisation and thus faster start-up and performance
High active surface	Higher biofilm concentration in the reactor, lower degree of filling requirement and thus smaller volume of the reactor
High porosity	Protection of biofilm against adverse effects
Fast wetting	Good fluidisation and mass transfer efficiency as well as higher biological activity
Lower density	Lower energy consumption for mixing and circulation (floats easier)
Hydrophobic surface	Adherence of microorganisms to the carrier material and better process stability

Source: Christian (2014)

Biofilm thickness on the carriers depends on organic loading, as well as the shear forces imparted by the mixing and roll pattern, and temperature and oxygen concentration (Levstek and Plazl, 2009). Sloughing also depends on the type of microorganisms and rate of growth within the biofilm (Maas et al., 2007). The IFAS process needs to be operated at elevated dissolved oxygen (DO) concentration (>3 mg/L as O_2) to initiate and increase nitrification activity (Devi and Setty, 2014) in the attached and suspended biomass (DiMassimo and Bundgaard, 2011) and to prevent kinetic limitations associated with DO diffusional gradients through the biofilm (Rosso et al., 2011). A relatively thin (<50 µm) (Torresi et al., 2016) and evenly distributed biofilm results in higher activity of the biomass and full diffusion of substrates into the biofilm (Makowska et al., 2013). Levstek and Plazl (2009) reported that from a mathematical point of view, the biofilm in an AnoxKaldnes™ K1 carrier is assumed to be planar and homogeneous. Boltz and Daigger (2010) reported that high-turbulence bulk liquid hydrodynamics promotes thin and stable biofilms, i.e. steady detachment and not uncontrolled sloughing.

Biofilm increases the mass of the carriers which increases the intensity of mixing required and roll pattern required to keep the carriers afloat (Sen et al., 2007). Sloughing can take place off the outermost biofilm layer and/or breakage of biofilm off the innermost layer. The air flow

required will increase with the soluble biodegradable COD concentration due to the increase in the rate of COD uptake and the need to maintain a higher shear force to achieve a thin biofilm. The carriers are held in suspension within the reactor using aeration and/or mechanical mixing energy. The carriers can disperse the bubbles released from the bubble aeration diffuser and thus have a large impact on the volumetric oxygen mass transfer coefficient by affecting the bubble size and gas-liquid interfacial area. Therefore, it is important that the system is not oxygen-limited or over-designed. Ideally, the reactor should have a maximum oxygen mass transfer rate at an efficient mixing and a minimum energy input (Jing et al., 2009).

2.4.3 Microbial degradation of organic compounds in hybrid bioreactors

Several processes have been used for the removal of phenolic compounds, with biological treatments being preferred to physicochemical treatments. Physicochemical treatments include solvent extraction, ion exchange, absorption and chemical oxidation. These treatments often lead to the production of toxic intermediates and the costs involved are high (Shah et al., 2012; Lim et al., 2013). Biological treatments have been proven to be more cost-effective, practical and reliable as they lead to a lower possibility of by-product formation. They are green processes using microorganisms found in the environment and organics are degraded to CO_2 and H_2O (Silva et al., 2013; Lim et al., 2013; Nakhli et al., 2014).

Aerobic biological methods are preferred to anaerobic methods for the treatment of phenol in wastewaters. Aerobic microorganisms are more efficient for degrading phenolic compounds because they grow faster than anaerobes (Pradhan et al., 2012) and use phenolics as their sole source of carbon and energy (Pishgar et al., 2012). The rate and extent of degradation depend on the temperature and pH (Marrot et al., 2006). Higher temperatures result in higher production of metabolites. The pH affects the charge of the phenol thus affecting the electrostatic attraction to the biomass and will also affect the metabolic pathway for phenol degradation (Chakraborty et al., 2010). Most microorganisms cannot tolerate pH values of below 4.0 or above 9.0, since acids and bases are in the undissociated form and can penetrate cells more easily due to the absence of an electrostatic force across the cell membrane (Shah et al., 2012).

Aromatic structures with a hydrophilic substituent, particularly phenols which resemble phospholipids, act as membrane-active agents which increase the permeability of the

cytoplasmic membrane and cause leakage of the cytoplasmic material (Jiang et al., 2002; Rigo and Alegre, 2004). Phenols induce changes in the fatty acid composition (saturated versus unsaturated ratio) of the cell membrane thus affecting the permeability. A concentration-dependent efflux of potassium ions occurs with addition of phenols. The ability of microorganisms to tolerate the presence of phenolic compounds has been correlated with membrane fluidity. In the presence of sub-lethal concentrations of phenol, *Pseudomonas* can convert *cis*-unsaturated fatty acids to *trans*-fatty acids, thus reducing membrane fluidity due to steric differences and resulting in increased tolerance against toxic compounds (O'Sullivan, 1998).

Organic compounds in coal gasification and coking wastewater, such as CGSGL, can be degraded aerobically by fungal species such as *Candida* and bacterial species such as *Acinetobacter, Alcaligenes, Burkholderia* (Agarry and Solomon, 2008; Shah et al., 2012), *Micrococcus*, *Bacillus* (Hamza et al., 2009), *Rhodococcu*s (Barrios-Martinez et al., 2006), *Rhodoplanes* (Ma et al., 2015), *Arthrobacter*, *Stenotrophomonas* and *Ochrobactrum* (Pozo et al., 2002) with *Pseudomonas* species dominating the biological treatment systems (Jame et al., 2010). *Rhodococcus* and *Pseudomonas* can utilise aliphatic and aromatic hydrocarbons as carbon source and are the most active bacteria in coal gasification wastewaters (Meng et al., 2015). These bacteria produce biosurfactants to degrade phenols and aromatics and they have pathways for the degradation of aromatic hydrocarbons that are not easily transformed by other microorganisms. *Burkholderia* and *Pseudomonas* produce enzymes to access hydantoins and hydantoin-like molecules as metabolic substrates (Dürr et al., 2006). *Pseudomonas* has been reported to degrade complex aromatics such as pyrocatechol, alpha-naphthol, hydroquinone, naphthalene, isoquinoline and indole (Nawawi et al., 2014), while *Rhodococcus* spp. and *Burkholderia* spp. degrade C_5-C_{16} alkanes, fatty acids, alkylbenzenes and cycloalkanes (Das and Chandran, 2011).

Some denitrifying bacteria, such as *Thauera, Diaphorobacter* and *Ochrobactrum,* have been reported to degrade aromatic and non-aromatic compounds (Basha et al., 2010), as follows: (i) *Thauera* (Cydzik-Kwiatkowska and Zielinska, 2016) are commonly found in coking wastewater bioreactors and can degrade hydrocarbons, phenols, methyl phenols, quinolinone, indole (Jia et al., 2016), polyphenols, toluene and halobenzoate (Silva et al., 2010); (ii) *Diaphorobacter* (Székely, 2008) display simultaneous nitrification and denitrification of ammonia-nitrogen to nitrogen gas (Khardenavis et al., 2007) and can degrade phenols,

pyridines and pyrenes found in coking wastewater (Meng et al., 2015); (iii) *Ochrobactrum* are denitrifiers and sulphide oxidisers (Mahmood et al., 2009) which utilise sulphides and thiosulphates as substrates to reduce nitrite. *Ochrobactrum* can also adsorb metals, degrade aromatic hydrocarbons (Bhattacharya et al., 2008) and can form granules (Cydzik-Kwiatkowska and Zielinska, 2016); and (iv) *Xanthobacter* (Gomez et al., 2005) can degrade cyclohexane (Van der Werf et al., 2001).

The rate of substrate consumption in petrochemical refinery wastewater can be divided into fast and moderate based on the Michaelis-Menten kinetics. At a high substrate concentration, every site on the microorganism is saturated with the substrate and the rate of reaction is constant. As the substrate concentration decreases only a few sites of the microorganisms are covered with the substrate making the substrate reduction rate proportional to the substrate concentration (Hamza et al., 2009).

2.4.4 Degradation pathways of aromatic compounds

Aromatics are reduced compounds, thus, by increasing the oxidation state of the aromatic ring the compounds are made more susceptible to degradation enabling microorganisms to use these compounds as a sole source of carbon and energy (Phale et al., 2007). The first step in the oxidative degradation of aromatic compounds is the hydroxylation of aromatic organics into dihydroxylated intermediates catalysed by monooxygenases or hydroxylating dioxygenases. The reaction, catalysed by hydroxylating dioxygenases, requires the transfer of two electrons from NAD(P)H; these electrons are consecutively transferred to the terminal oxygenase through electron carriers such as ferredoxin and/or reductase. Hydroxylation results in the formation of catechol, protocatechuic acid, hydroxyquinol, or gentisic acid which are substrates for ring-cleaving dioxygenases. The ring-cleaving dioxygenases couple O_2 bond cleavage with ring fission of hydroxylated derivatives either between the two hydroxyl groups (*ortho* cleavage) or next to one (*meta* cleavage) to yield either acetyl-CoA and succinyl-CoA or pyruvic acid and acetaldehyde or pyruvic acid and fumarate that are readily metabolised by almost all microorganisms (Guzik et al., 2013).

The *ortho*-pathway is chromosomally encoded (Ambujom, 2001). The intradiol dioxygenases catalyse the intradiol cleavage of the aromatic ring at 1,2-position of catechol or its derivatives (protocatechuic acid, hydroxyquinol) with the incorporation of two atoms of molecular oxygen

into the substrate which leads to the production of *cis,cis*-muconic acid which is then subsequently transformed by muconate cycloisomerase to muconolactone. Muconolactone isomerase shifts the double bond to form 3-oxoadipate-enol-lactone, the first common intermediate of the catechol and protocatechuate or hydroxyquinol branch. The *meta*-pathway is plasmid encoded (Ambujom, 2001). The extradiol catechol and protocatechuate dioxygenases catalyse the ring fission between position C_2 and C_3 of the catechol ring and between C_2 and C_4 or C_4 and C_5 of the protocatechuate ring, respectively. Products of these reactions (2-hydroxymuconic semialdehyde or carboxy-2-hydroxymuconic semialdehyde) are transformed to pyruvic acid and oxaloacetic acid in the protocatechuate pathway (Guzik et al., 2013). The reactions are initiated by electrophilic attack (electron donating) of molecular oxygen on the hydrocarbon molecule and are deactivated in the presence of electron-withdrawing groups (EWGs).

Thus, the speed of the reaction is related to the type of group in the aromatic ring and enzyme activity (Guzik et al., 2013). Electron-withdrawing groups inhibit electrophilic attack by dioxygenases. Activating substituents favour electrophilic substitution about the *ortho* and *para* positions. Weakly deactivating groups direct electrophiles to attack the benzene molecule at the *ortho* and *para* positions, while strongly and moderately deactivating groups direct attacks to the *meta* position (Guzik et al., 2013) (Figure 2.4).

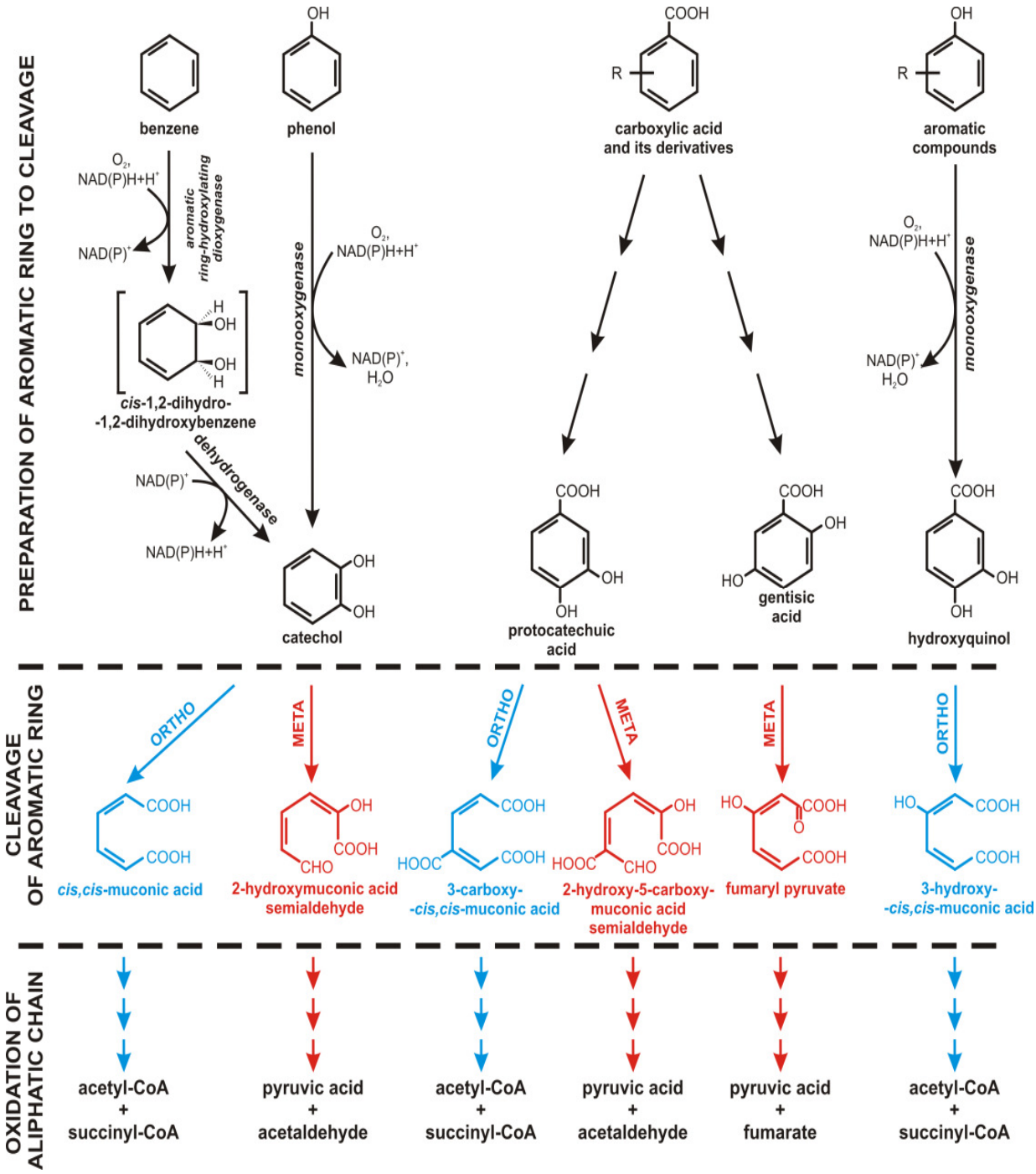

Figure 2.4: *Ortho* (intradiol) and *meta* (extradiol) pathways for the degradation of aromatic compounds (Guzik et al., 2013)

2.4.5 Degradation pathways of aliphatic compounds

The aerobic attack of aliphatics and cycloaliphatic hydrocarbons requires molecular oxygen. Oxidation of alkanes is classified as being terminal or subterminal (Figure 2.5).

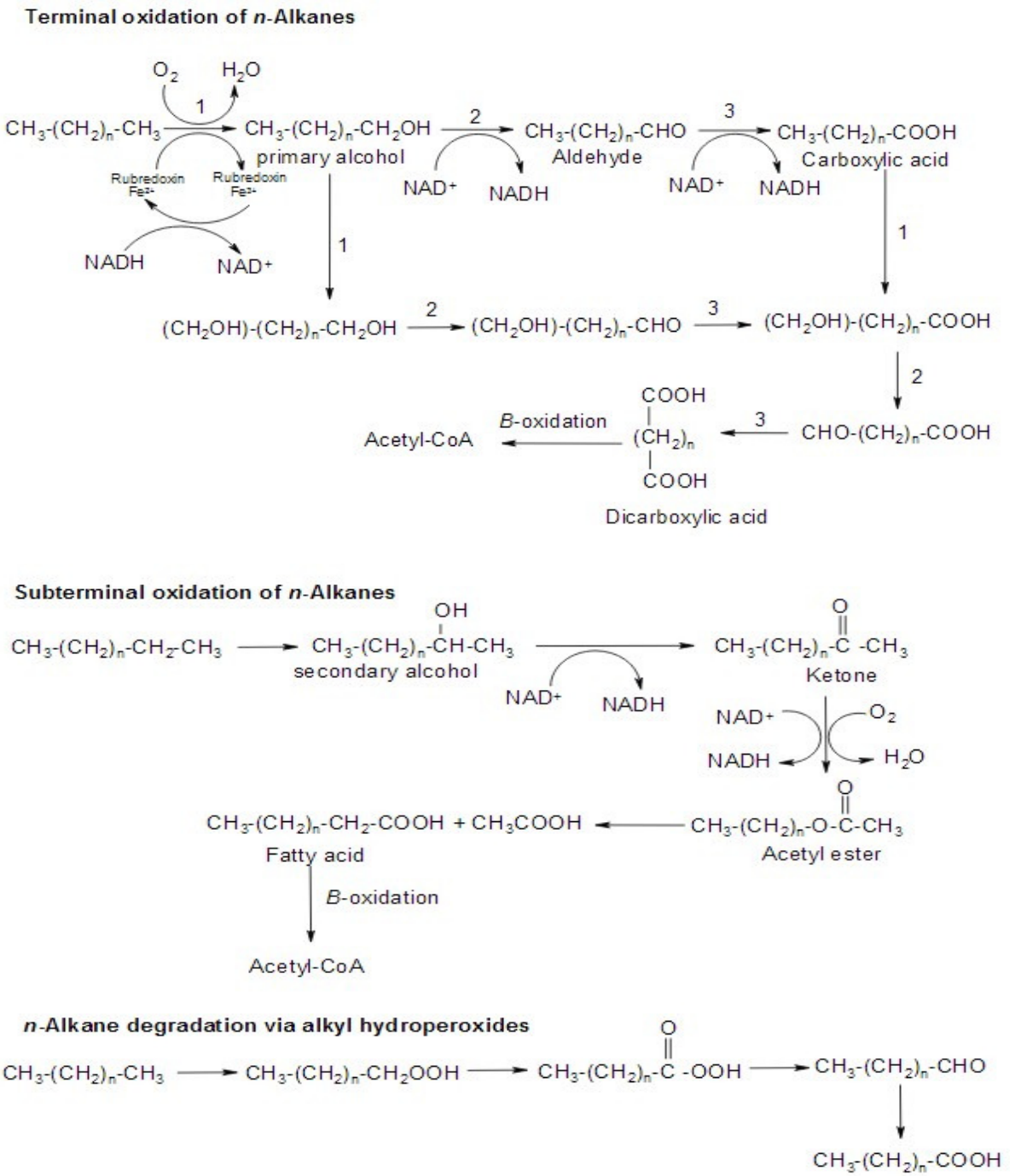

Figure 2.5: Peripheral aerobic pathways for n-alkane degradation with (1) alkane mono-oxygenase; (2) fatty alcohol dehydrogenase; and (3) fatty aldehyde dehydrogenase (Olajire and Essien, 2014)

The activation is catalysed either by substrate-specific terminal oxygenases (monooxygenases, non-heme iron monooxygenases, dioxygenases) or subterminal oxidation (cytochrome P450) (Rohrbacher and St-Arnaud, 2016). The monoterminal oxidation is the main pathway which proceeds via the formation of the corresponding alcohol, aldehyde and fatty acid. Beta-

oxidation of the fatty acids results in the formation of acetyl-CoA. The n-alkanes with an uneven number of carbon atoms are degraded to propionyl-CoA which in turn is carboxylated to methylmalonyl-CoA and then to succinyl-CoA. Fatty acids of a physiological chain length may be directly incorporated into membrane lipids; most of the degradation products are introduced into the tricarboxylic acid cycle (Fritsche and Hofrichter, 2008) which are catabolised in the Krebs cycle and fully oxidised to CO_2 (Rohrbacher and St-Arnaud, 2016).

The subterminal oxidation occurs with the lower (C_3-C_6) and longer alkanes with the formation of a secondary alcohol and subsequent ketone. Unsaturated alkenes are oxidised at the saturated end of the carbon chains. A minor pathway has been shown to proceed via an epoxide which is converted to a fatty acid. Branching reduces the rate of biodegradation. Methyl side groups do not drastically decrease biodegradability, whereas complex branching chains, such as the tertiary butyl group, hinder the action of degradative enzymes. Cyclic alkanes are relatively resistant to microbial attack due to the absence of an exposed methyl group. In general, alkyl side-chains of cycloalkanes facilitate biodegradation. Aliphatic hydrocarbons become less water soluble with increasing chain length of C_{12} and above. Two mechanisms are involved in the uptake of lipophilic substrates: (1) the attachment of the microbial cells at the oil droplet; and (2) the production of biosurfactants. Biosurfactants are molecules consisting of a hydrophilic and a hydrophobic moiety. Biosurfactants act as emulsifying agents by decreasing the surface tension and forming micelles. The micro-droplets may be encapsulated in the hydrophobic microbial cell surface. The products of hydrocarbon degradation are introduced into the central tricarboxylic acid cycle (Fritsche and Hofrichter, 2008). Aliphatic hydrocarbons are not very reactive since they do not have functional groups making them non-polar and slightly water soluble. Activation of these compounds makes them more water soluble and available for microbial degradation.

2.4.6 Microbial degradation of nitrogenous compounds in hybrid bioreactors

Although nitrifying bacteria use ammonia as an electron source for energy, nitrification can be inhibited by ammonia itself at concentrations above 350 mg/L. The inhibitory effect is due to free ammonia and not ammonia itself (Lui et al., 2005). Free ammonia diffuses through the cell membrane into the cell and changes the inner pH, neutralising the membrane potential thus leading to cell death (Jaroszynski et al., 2011). Thus, 350 mg/L of total ammonia contains 9.0 mg/L of free ammonia at pH 7.5 and 30 ºC. The threshold for free ammonia for ammonia

oxidisers (*Nitrosomonas)* is lower than for nitrite oxidisers (*Nitrobacter*). Wagner et al. (2002) reported that ammonia-oxidising bacteria out-number nitrite-oxidising bacteria in activated sludge systems. It has been reported that phenol concentrations above 200 mg/L inhibit nitrification (Marrot et al., 2006; Kim et al., 2008). Nitrification is also inhibited by o-cresol, phenolics and toluene (Jemaat et al., 2014). Inhibition of nitrification during a toxic shock will not take place immediately but over a period of several weeks (Björnsdotter, 2005). Nitrification can take place by heterotrophic bacterial species such as *Thiosphaera*, *Alcaligenes*, *Pseudomonas*, *Diaphorobacter and Bacillus.* According to Devi and Setty (2014), recent studies have shown that most heterotrophic-nitrifying bacteria are capable of aerobic denitrification, including *Alcaligenes*, *Pseudomonas*, *Microvirgula*, *Acinetobacter* and *Rhodococcus* species.

Thiocyanate is a major nitrogen compound found in CGSGL. It accounts for 15% of the total COD in the coke wastewater (Huang et al., 2013). It is inhibitory at concentrations higher than 200 mg/L. Degradation of thiocyanate by nitrifiers will result in an increase in total nitrogen (200 mg/L thiocyanate = 48 mg/L as N). Thiocyanates can be degraded by heterotrophic bacteria such as *Pseudomonas*, *Bacillus* and *Acinetobacter* species. Ammonium-nitrogen produced from the thiocyanate can be used as a nitrogen source by *Pseudomonas* and *Arthrobacter* species and the reduced sulphur used as a source of sulphur and not as an energy source (Sorokin et al., 2001). Heterotrophic bacteria convert the thiocyanate to CO_2 and ammonia via cyanate enzymatically, while the sulphur is hydrolysed to sulphide which is further oxidised to tetrathionate via the formation of thiosulphate (Patil, 2013). Thiocyanate-degrading bacteria (*Thiobacillus thioparus*) compete with nitrifiers for the inorganic carbon and nitrogen source and essential nutrients. In the absence of substantial nitrification, the effluent concentrations of ammonia will be greater than the influent concentration due to the biodegradation of thiocyanates (Kim et al., 2011).

Thiocyanate can be used as a nitrogen source by the bacterial consortium in a bioreactor in the presence of an external carbon supply to achieve a C/N ratio of 10 (Geets et al., 2006; De Brito, 2009). The bacterial consortium ceases to grow when the thiocyanate is supplied as the sole source of carbon since the C/N ratio is 0.5. Biodegradation of thiocyanate will occur after the biodegradation of ammonium. The degradation rate of thiocyanate will be much faster when the biomass is immobilised on an inert material in a bioreactor, as this would increase the amount of biomass in the bioreactor. The optimum pH and temperature for maximum

biodegradation of thiocyanate was found to be at pH 7.0 (range between 6.0 and 9.0) at 30 ºC (Patil, 2013). Thiocyanate degradation was reduced by 10% in the presence of cations/metal ions such as nickel, copper and zinc; decreased by 30% to 45% in the presence of lead and cadmium; and decreased by more than 80% in the presence of iron and chromium due to the strong iron-thiocyanate and chromium-thiocyanate complexes. Anions such as sulphate, chlorides and cyanides at relatively low concentrations did not affect the degradation of thiocyanate (Patil, 2013).

Huang et al. (2013) reported three thiocyanate-oxidising heterotrophic bacterial strains (*Burkholderia*, *Chryseobacterium* and *Ralstonia*) isolated from coke wastewater which were able to degrade thiocyanate as the sole carbon source with ammonium-nitrogen and sulphates produced as the end-products. Continuous increases in ammonia-nitrogen after complete degradation of thiocyanate was most likely due to endogenous decay of the cell mass. The sulphate concentration increased relatively slowly after the complete degradation of thiocyanate (sulphate-sulphur to thiocyanate-sulphur ratio should be 1 for complete sulphur to sulphate conversion). Thiocyanate nitrifiers are believed to be responsible for thiocyanate decomposition when the biodegradable carbon sources are consumed by heterotrophic bacteria. The highest decomposition rates for thiocyanate were observed between pH 6.5 and pH 8.5 at temperatures of between 30 ºC and 40 ºC. The optimum decomposition rate (7.2 mg/L.h) was achieved at pH 7.7 at 35 ºC. The biodegradation kinetics of thiocyanate was well fitted with the Andrew-Haldane model which demonstrated a distinct substrate concentration-inhibited growth pattern (Huang et al., 2013). *Pseudomonas* and *Arthrobacter* have been reported to use thiocyanates as a source of nitrogen and sulphur for growth (Katayama et al., 1992).

Free cyanide is expected to have the greatest influence on the nitrification of nitrogenous compounds in CGSGL. Cyanide is classified into free cyanide in the form of cyanide ion and complex cyanide combined with metals. Cyanides form weak complexes with copper, cadmium, lead, nickel and zinc and form strong complexes with iron and chromium (Patil, 2013). The complexed cyanide has very low toxicity to nitrifiers; however, the free cyanide has very high toxicity. Free cyanides at concentrations higher than 0.11 mg/L have been reported to inhibit nitrification, and levels above 0.5 mg/L produced excessive foam, decreased the microbial activity in the aeration basin and negatively affected settling of the sludge in the clarifier (Kim and Kim, 2003; Merlo et al., 2011).

Nitrite-oxidising bacteria (*Nitrospira* spp. and *Nitrobacter* spp.) are more sensitive to cyanide toxicity than ammonia-oxidising bacteria (*Nitrosomonas europaea*) (Sharma and Philip, 2014). Phenol-degrading bacteria degrade phenols via the *meta*-cleavage pathway to yield intermediates (muconic acid and a-hydroxymuconic semialdehyde) which are then metabolised as a carbon source by cyanide-degrading bacteria (Wang and Loh, 1999) and the yeast *Cryptococcus humicolus* (Park et al., 2008). Perumal et al. (2013) reported that *Klebsiella*, *Moraxella*, *Serratia*, *Alcaligenes* and *Pseudomonas* could utilise cyanide as a source of carbon and nitrogen; these authors also observed that *Bacillus* species were tolerant to high levels of cyanide (7 000 mg/L) and could degrade cyanide to ammonia and nitrate. The optimum temperature for cyanide biodegradation was found to be between 25 ºC and 37 ºC and the optimum pH between 6.0 and 7.5. According to Chakraborty and Veeramani (2006), cyanide can be biologically degraded by *Bacillus*, *Pseudomonas* and *Klebsiella* species by suspended and fixed-film systems under aerobic and anaerobic conditions.

In hybrid bioreactors such as the integrated fixed-film activated sludge (IFAS) reactor, the attached biomass enhances the slow-growing nitrifying bacteria (autotrophs) which are required for the removal of nitrogen in wastewater treatment plants and responsible for ammonia and nitrite oxidation (Li and Han, 2013). Nitrification is accomplished through the combined activities of ammonia-oxidising bacteria which oxidise ammonia to nitrite and nitrite-oxidising bacteria which then oxidise nitrite to nitrate. Ammonia-oxidisers are more sensitive to recalcitrant compounds than nitrite-oxidising bacteria (Boon, 2002). Nitrifiers growing in the attached phase are retained in the system longer than the suspended phase, which provides them with longer solids retention time (SRT) since less are washed out from the aeration tank (Almstrand et al., 2013). Longer SRTs are essential for the growth of nitrifying (autotrophic) bacteria especially at lower temperatures (Kim et al., 2011; Wang et al., 2012). Nitrifying bacteria show stable metabolism in biofilms (Woznica et al., 2010) attached to plastic carriers (Almstrand et al., 2013).

Bioreactor operating parameters such as alkalinity, pH, oxygen and temperature will also affect nitrification. It is known that alkalinity is lost during nitrification; however, when alkalinity is higher than 2.5 equivalent HCO_3^-/mole of ammonia-nitrogen, then nitrification will not be limited due to low alkalinity. The optimum pH for nitrification is between pH 6.45 and pH 8.95. Nitrifying bacteria require nutrients such as an inorganic carbon source and phosphate. Trace elements such as magnesium, molybdenum, calcium, copper and iron are also required

for the growth and activity of nitrifying bacteria. An excess of oxygen is required for a well-functioning nitrification process. The optimum temperature for constant growth of nitrifiers is between 30 ºC and 35 ºC and decreases sharply at temperatures of above 35 ºC. Ammonia-oxidising bacteria have a higher growth rate than nitrite-oxidising bacteria at higher temperatures (Boon, 2002; Björnsdotter, 2005).

2.4.7 Bioaugmentation of activated sludge systems

Bioaugmentation is the addition of selected microbial strains (indigenous or genetically modified) (Jianlong et al., 2002) with the desired degradative (catabolic) capacities to improve the catabolism (hydrolysis) of specific compounds such as refractory organics or overall COD (Herrero and Stuckey, 2015) from petrochemical wastewater (Zhao et al., 2007) and is an appropriate and promising alternative for treating CGWW (Fang et al., 2013; Herrero and Stuckey, 2015) to comply with industrial effluent discharge standards. Bioaugmentation is also an effective way of enhancing the removal rate (1.5 fold) of long-chain alkanes from coal gasification wastewater (Liu et al., 2013). Bioaugmentation can enhance the performance of both conventional activated sludge processes as well as hybrid fixed-film processes (Leu, 2009). Bioaugmentation is a feasible method to enhance biological treatment of refractory industrial wastewater (Bai et al., 2010).

The purpose of bioaugmentation is to minimise the lag phase (acclimation period) and increase the log phase (exponential growth) (Yelebe and Puyate, 2012; Lim et al., 2013). The objectives of bioaugmentation include: (i) accelerating the start-up of the reactor; (ii) protecting the existing microbial community from adverse effects (shock loads); (iii) increasing the overall organic removal rate; (iv) compensating for organic or hydraulic overloading; (v) increasing the removal of refractory organics (Mohan et al., 2009; Herrero and Stuckey, 2015); (vi) improving flocculation and settling in the clarifier (Schauer-Gimenez et al., 2010); and (vii) stabilising the microbial community (Jiuan et al., 2011).

Many industries are faced with difficult operating conditions and stringent discharge permits which challenge the capability of the wastewater treatment plant. Under these conditions bioaugmentation can be a cost-effective, short-term, or medium-term solution to maintain effluent compliance until system changes and/or plant upgrades can be implemented. In other cases, bioaugmentation can be a long-term, cost-effective solution because of the lack of capital

funds and the expense of system upgrades which often requires an expansion of the biological treatment system, including the costly installation of additional aeration (oxygen generation) capacity (Fuller, 2014).

Bioaugmentation can increase diversity and activity of a population by adding specialised microorganisms with enzymatic systems that allow degradation of previously non-biodegradable organics or by adding microorganisms which have a higher metabolic rate. An increase in bacterial diversity increases the gene pool that complements the existing one and helps further degradation of pollutants in refinery wastewater (Domde et al., 2007). The major factor affecting the survival of exogenous microorganisms is their ability to flocculate. Flocculated microorganisms will have a longer residence time in the bioreactor. Dispersed microorganisms are more susceptible to wash-out due to poor settling (non-steady state). This means that more bioaugmentation products need to be added which increases treatment costs (Mulcahy, 1993).

Leu (2009) reported that at higher bioaugmentation levels (1% to 2% of reactor biomass) a large fraction of the added biomass decays, thus reducing the benefits of bioaugmentation. Immobilisation of a mixed population of microorganisms, predominantly bacteria, on or within inert supports has the following advantages: (i) increased reactor biomass concentration; (ii) strong capacity to handle shock loadings; (iii) low excess sludge production (Guo et al., 2008); (iv) biodegradation of organics, nitrification, denitrification, sulphur reduction and phosphorus accumulation; and (v) helps to prevent microorganisms being washed out of the activated sludge process (Soljan et al., 2001).

The ability of microorganisms to compete effectively with the exogenous population determines their persistence and proliferation in the system. Other factors influencing the survival of added microorganisms include resistance to starvation, motility, nutrients (substrate and co-factors), growth inhibitors and physical factors such as oxygen concentration, temperature and pH (Mulcahy, 1993).

Commercial bioaugmentation products consist of patented blends of several selected strains of bacteria (Dueholm et al., 2014a; 2014b) and fungi (Tatarko, 2008; 2010). The microorganisms (single or mixed cultures) are isolated from nature and are not genetically modified (bioengineered) in any way (Simon et al., 2004). The microbes are grown or fermented under

controlled conditions in a manufacturing facility. The pure cultures of microbes are concentrated into a paste, reconstituted, and placed on an inert carrier such as bran, oatmeal, rye or cornhusks. These carrier materials are often sterilised to reduce the natural background contamination with unwanted microbes (Herrero and Stuckey, 2015).

The reconstituted mixture undergoes a stabilisation procedure, usually freeze-drying. This process kills about 90% of the microbes, thus only 1.0% to 10% of the microbes can be recovered after freeze-drying (Whiteman, 2010). The final products can contain wetting agents, buffers and nutrients (Stephenson and Stephenson, 1992; Abeysinghe et al., 2002). The products are sold in a variety of forms, with dried microorganisms on a carrier and liquid products being the two most common. The typical concentrations of bacteria used are in the billions per gram of dry product and somewhat less in the liquid products (Norman and Tramble, 2011; Fuller, 2014).

According to Chavan and Mukherji (2008), algae can facilitate spontaneous flocculation of bacteria to improve the quality of the treated effluent by indirectly providing surfaces for the adherence of hydrocarbon-degrading microorganisms, thus preventing them from being washed out. Zhang et al. (2009) reported the use of a cheap source of diatomite to increase the biomass and the settling rate of sludge when treating CGSGL for the removal of COD and total phenols. The diatomite-activated sludge system indicated that the diatomite was also acting as adsorbent for organics and as a carrier for the microorganisms in the bioreactor. Bioaugmentation is a feasible option for the treatment of coke wastewaters (Park et al., 2008), CGSGL (Fang et al., 2013) and petrochemical wastewater for the removal of aromatics, phenols, nitrogenous compounds and hydrocarbons (Liu et al., 2013). Jianlong et al. (2002) indicated that achieving a COD of less than 200 mg/L for coke plant wastewater was possible with bioaugmentation.

Acclimation of commercial products can reduce required treatment dosages and increase the speed of response of bioaugmentation (Norman and Tramble, 2011). Bioaugmentation is an efficient and cost-effective method for the treatment of aromatics (Yong and Zhong, 2013).

2.4.8 Benefits of bioaugmentation

Bioaugmentation provides the following key benefits for municipal and industrial wastewater treatment:

- improves floc formation and settling
- increases rates of waste assimilation and versatility in substrate uptake
- decreases sludge solids yield due to a more efficient breakdown of the colloidal material
- allows rapid recovery of metabolic functions after a hydraulic or toxic shock
- increases stability and tolerance to varying growth conditions
- reduces operating and energy costs
- provides greener technology
- converts larger organic molecules to smaller organic molecules for easier assimilation
- meets discharge limits with existing facilities while minimising expenditure by reducing or eliminating surcharges and fines (Bhattacharya et al., 2008)
- improves nitrification (Parker and Wanner, 2007)

Microorganisms selected for bioaugmentation should meet the following criteria (Herrero and Stuckey, 2015):

- be catabolically able to degrade contaminants in the presence of other potentially inhibitory pollutants
- be persistent and competitive after introduction into the bio-system
- be compatible with the indigenous microbial communities

2.4.9 Bioaugmentation dosages

The selection of the type and quantity of a bioaugmentation product required to boost treatment performance depends on the existing conditions of the process, causes of poor treatment, effect of the bioaugmentation product on the indigenous population and the toxicity of the influent (Abeysinghe et al., 2002). The bioaugmentation philosophies for aerobic biological treatment systems differ among manufacturers. Generally, Company 1 recommends dosages based on flow rates and COD loading of the effluent stream to the biological treatment system, Company

2 recommends dosages based on the type of aerobic biological system and flow rates, and Company 3 recommends dosages between 2 mg/L and 10 mg/L. The dosage regimes differ between start-up, maintenance, upset recovery and post-recovery. Manufacturers' recommendations may differ due to different fermentation processes and bacterial strains used (Whiteman, 2010).

2.4.10 Bioaugmentation failures

Stephenson and Stephenson (1992) reported the following as reasons for the failure of bioaugmentation:

- substrate concentration may be too low to support growth
- system may contain inhibitory substances or be operating under inhibitory conditions such as temperature
- competition with other microorganisms causing growth inhibition
- inoculant may use other organic substances in the system rather than the target pollutant
- number of microorganisms may be too low to effect significant change
- supplements not available to initiate breakdown rapidly enough without a period of acclimatisation
- poor biofilm formation

2.4.11 Quorum sensing

Quorum sensing (QS) plays an important role in the colonisation of the bioaugmented population within the indigenous population (Zhang and Li, 2016). Quorum sensing is a coordinated regulation of gene expression in response to fluctuations in cell-population density. In this process, bacteria produce signalling molecules called auto-inducers (AIs), intracellularly and then release them to the surrounding environment. The concentration of AIs in the bioreactor will increase as the bacterial population increases. When the population reaches a threshold level, the cognate receptors will bind to the AIs and trigger the downstream gene expression that controls a broad range of bacterial activities such as biofilm formation (Diaz de Rienzo et al., 2016), production of extracellular polymeric substance (EPS) (Frederik et al., 2011) and production of exoenzymes (Tan et al., 2015).

Quorum sensing enables bacteria to survive and adapt very quickly to a continuously changing environment (Feng et al., 2013). The N-acyl homoserine lactone (AHL)-mediated QS system is one of the most well-characterised bacterial communication systems and is present in 7% to 10% of Proteobacteria (α-, β- and γ-Proteobacteria), Bacteroidetes and Actinobacteria) (Chong et al., 2012; Kimura, 2014). Thus, communication among bacteria of different species or between organisms from different domains is possible (Tan et al., 2015). Quorum sensing in Gram-negative bacteria is assumed to be mediated by N-acyl homoserine lactone molecules, while Gram-positive bacteria make use of signalling peptides, such as competence-stimulating peptide (CSP). An accumulation of CSP induces autolysis releasing chromosomal DNA into the environment. Subsequent uptake of DNA by neighbouring cells is thought to promote horizontal gene transfer.

2.4.12 Horizontal gene transfer involved in bioaugmentation

Horizontal gene transfer is an important mechanism for microorganisms to rapidly adapt to changing environments. The ability of the microorganisms to transfer catabolic genes to the indigenous population may be of equal or greater importance than the survival of the microorganism itself. The degradative genes need to spread within the indigenous population, leading to *in situ* genetic modification of the existing indigenous microbial community itself (Bathe et al., 2005). The survival of the donor strain will thus no longer be needed once the catabolic genes have been transferred and expressed in the indigenous bacteria (Top et al., 2002). Catabolic genes can be directly inherited by future bacterial generations without reproduction. The catabolic genes can be disseminated by plasmids to phylogenetically diverse bacteria (Mohan et al., 2009).

The three main mechanisms of gene transfer are:

- Transformation - gene transfer resulting from the uptake of free extracellular DNA from the environment. This is the most general and non-species-specific type of gene transfer system (Heuer and Smalla, 2007; OECD, 2010).
- Conjugation - genetic material is transferred from one bacterium to another by cell-to-cell contact. This transfer is less efficient in dispersed biomass and more efficient with high cell densities of microorganisms such as activated sludge flocs and bacteria found in biofilms

(OECD, 2010; Semrany et al., 2012). Either double-stranded DNA or single-stranded DNA molecules are transported from donor to recipient bacterial cells. The transfer of double-stranded DNA is found only in *Actinobacillus* spp., while single-stranded DNA transfer is ubiquitous in bacteria and Archaea (Koraimann and Wagner, 2014).

- Transduction - transfer of genetic material between bacteria mediated by bacteriophages (Wasilkowski et al., 2012).

The coal gasification wastewater treatment process has become one of the key factors which restrict the development of coal chemical industry. A number of modifications to the Lurgi process have been reported by Yang et al. (2006), Gai et al. (2008), Feng et al. (2009), Yu et al. (2010), Gai et al. (2016) and Cui et al. (2017). These modifications include retrofitting the coal gasification process, simultaneous removal of ammonia and hydrogen sulphide using a single stripper, stripping of ammonia before the extraction of phenol, using methyl isobutyl ketone (MIBK) instead of diisopropyl ether (DIPE) to recover phenols, etc.

This wastewater has been regarded as one of the most difficult to treat due to high concentrations of complex inorganic and organic compounds, oils, fatty acids, hydrogen sulphide, carbon dioxide, phenols and ammonia which cause serious environmental problems. The performance of most of the known pretreatment techniques is inadequate for the removal of these compounds which hampers the function of the subsequent biological treatment processes, thus leading to wastewater not meeting legislative discharge requirements. Thus, many Lurgi coal gasification plants are facing a risk of suspended operation if the relevant effluent discharge requirements are not met.

CHAPTER 3
MATERIALS AND METHODS

3.1 Chemicals, reagents and gases

All chemicals, reagents and gases (Table 3.1) were supplied by Buckman Africa, South Africa. The pilot plant used in this study was made available by Sasol (Pty) Ltd, South Africa. All reagents and consumables for the polymerase chain reaction (PCR) sequencing studies were supplied by the University of Pretoria, South Africa.

Table 3.1: List of chemicals, reagents and gases used in the study

Chemicals, reagents and gases	Manufacturer/distributor
Ammonium dihydrogen phosphate (99%)	Merck (Pty) Ltd, South Africa
Argon (99.999%)	Air Liquide (Pty) Ltd, South Africa
Calcium chloride hydrate (≥99%)	Sigma-Aldrich, South Africa
Dichloromethane (99.9% BDH HiPerSolv)	Merck (Pty) Ltd, South Africa
Ethanol (≥99.5%, AR grade)	Merck (Pty) Ltd, South Africa
Glutaraldehyde solution (50%, AR grade)	Merck (Pty) Ltd, South Africa
Helium (99.999%)	Air Liquide (Pty) Ltd, South Africa
Hexamethyldisilazane (≥99%)	Sigma-Aldrich, South Africa
Hydrochloric acid (34%, AR grade)	Merck (Pty) Ltd, South Africa
Iron sulphate heptahydrate (≥99%)	Merck (Pty) Ltd, South Africa
Magnesium sulphate heptahydrate (99%)	Merck (Pty) Ltd, South Africa
Manganese sulphate hydrate (99%)	Merck (Pty) Ltd, South Africa
Nitric acid (70%, AR grade)	Merck (Pty) Ltd, South Africa
Phenol (99.5%)	Saarchem (Pty) Ltd, South Africa
Potassium dihydrogen phosphate (99.5%)	Saarchem (Pty) Ltd, South Africa
Potassium phosphate monobasic (≥99%)	Sigma-Aldrich, South Africa
Sodium cacodylate buffer (0.1M)	Sigma-Aldrich, South Africa
Sodium chloride (≥99%)	Sigma-Aldrich, South Africa
Sodium hydroxide (≥97%)	Merck (Pty) Ltd, South Africa
Sodium nitrate (≥99%)	Sigma-Aldrich, South Africa
Sodium nitrite (≥99%)	Sigma-Aldrich, South Africa
Sodium sulphate anhydrous (≥97%)	Sigma-Aldrich, South Africa
Sulphuric acid (98%)	Merck (Pty) Ltd, South Africa

All chemicals, except sodium sulphate, were used without further purification. Sodium sulphate was dried for a minimum of 24 h at 103 °C ± 2 °C and stored in a desiccator prior to

use. All chemicals and reagents were prepared using ultra-pure (Type 1) water from a Millipore Direct-Q® 5 purification system (Merck Millipore, South Africa).

3.2 Pilot plant reactor design and operating parameters

3.2.1 Pilot plant reactor design

The main components of the stainless steel pilot plant hybrid fixed-film bioreactor (H-FFBR) (1.8 m long x 1.05 m high x 0.65 m wide) with three aeration compartments in series, designated as Zone 1, Zone 2, and Zone 3, containing acclimatised fixed and suspended biomass, and a clarifier (0.5 m diameter, 0.238 m^2 surface area, 1.43 m side water depth) (Figure 3.1). The bioreactor was acclimatised to the feed over a period of time such that the reactor was subjected to at least three complete bacterial sludge ages. The volume in each zone was approximately 0.250 m^3, 0.150 m^3 and 0.600 m^3 for Zone 1, Zone 2 and Zone 3, respectively.

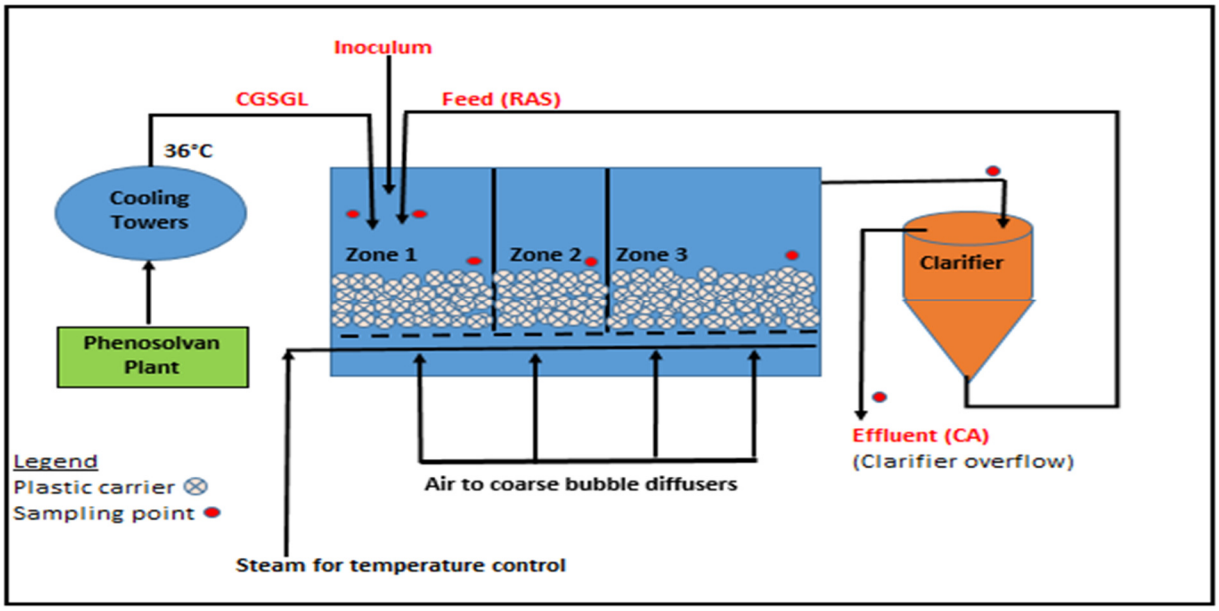

Figure 3.1: Configuration of the pilot plant hybrid fixed-film bioreactor used in the study

The AnoxKaldnes™ K1 carrier (Veolia Water Technologies, Sweden) was used in this study. This carrier is shaped as a small cylinder with a cross on the inside of the cylinder with longitudinal fins on the outside. It is approximately 10 mm in diameter and 7 mm long with a

protected surface area of 500 m^2/m^3, density of 0.92 g/cm^3 to 0.96 g/cm^3 and 95% porosity (Ratcliffe et al., 2006; Levstek and Plazl, 2009; Ibrahim et al., 2012).

The biofilm carrier filling fraction (based on volume) for the aeration zones was approximately 70% for Zone 1, 50% for Zone 2 and 30% for Zone 3. A 70% filling of biofilm carrier media corresponded to an effective biofilm growth area equal to 350 m^2/m^3, 50% fill equal to 250 m^2/m^3 and a 30% fill equal to 150 m^2/m^3 (Ratcliffe et al., 2006; Aygun et al., 2008). Each aeration zone was linked to a data-collection-system (DCS) and parameters such as temperature, dissolved oxygen (DO), recycling rate, feed rate, desludging rate, hydraulic retention time (HRT), pH and sludge retention time (SRT) were controlled and optimised automatically.

3.2.2 Reactor operating parameters

The reactor operating parameters and conditions were based on simulating real plant conditions (Table 3.2). Addition of nitrogen and phosphorus was not required since sufficient levels were present in the feed stream.

Table 3.2: Reactor operating parameters over the study period

Operating parameters	
Reactor volume (m^3)	1.30
CGSGL (L/h)	30
Recycle flow (L/h)	60
Feed: Recycle ratio	1:2
Clarifier upflow (m/h)	<0.3
Temperature (°C)	36 ± 1
pH	7.5 ± 1
DO (mg/L)	5 ± 1
F/M (kg COD/kg MLSS.d)	< 0.45 of the biodegradable COD fraction
HRT (h)	33
SRT (d)	18

3.3 Collection and preservation of reactor samples

Composite samples of the influent and effluent were collected over a 24-hour period at a rate of 50 mL/h into 2 000 mL sample bottles with polypropylene caps and liners. The composite samples were collected daily between 09:00 and 10:00 from the pilot plant. Grab samples (± 500 mL) of the biofilm carriers were taken twice weekly from each aeration zone using sterile Whirl-Pak® sampling bags (Guth SA, South Africa). The respective samples were packed in a cooler box with sufficient ice to cool samples (6 ºC ± 2 ºC) and transported within 4 hours to the laboratory. Sampling and analyses were scheduled as per Table 3.3.

Table 3.3: Sampling and analysis schedule over the study period

Analysis	Unit	Frequency of testing
Ammonia-nitrogen[(b)]	mg/L as NH_3-N	Monday, Wednesday, Friday
Carbonaceous biochemical oxygen demand ($CBOD_5$)[(a)]	mg/L as O_2	Wednesday
Biomass oxygen uptake rates (OUR)[(a,c)]	mg O_2/L.h	Monday
Biomass weight[(b)]	g TSS/m^2	Monday, Wednesday
Biomass thickness[(b)]	µm	Monday, Wednesday
Chemical oxygen demand (COD)[(b)]	mg/L as O_2	Daily
Conductivity[(b)]	µS/cm	Daily
Cyanide free [(a,c)]	mg/L as CN	Wednesday
Dissolved oxygen (DO)[(b,c)]	mg/L as O_2	Daily
EDX[(a)]	% Weight	Monday
FT-IR[(a)]	cm^{-1}	Monday, Wednesday
GC/MS[(a)]	µg/L	Monday, Wednesday
M-alkalinity[(b)]	mg/L	Monday, Wednesday, Friday
Metals[(a)]	mg/L	Monday
Nitrate-nitrogen[(b)]	mg/L as NO_3-N	Monday, Wednesday, Friday
Nitrite-nitrogen[(b)]	mg/L as NO_2-N	Monday, Wednesday, Friday
Orthophosphates[(b)]	mg/L as P	Monday, Wednesday, Friday
pH[(b,c)]		Daily
Phenols[(b)]	mg/L	Daily
SEM[(a)]	kV	Monday
Sulphates[(a)]	mg/L as SO_4	Monday
Sulphides[(a,c)]	mg/L as S^{2-}	Monday
Suspended solids[(b)]	mg/L	Daily
Temperature[(b,c)]	ºC	Daily
Total Kjeldahl Nitrogen (TKN)[(a)]	mg/L as N	Monday, Wednesday, Friday

[(a)] Performed before the inoculation period, baseline data (Week 1 to Week 12)

[(b)] Performed throughout the study period (Week 1 to Week 65)

[(c)] Performed immediately on-site

All samples were refrigerated at 6 ºC ± 2 ºC upon receipt in the laboratory and analysed within 24 h after sampling, where possible. If not, the samples were preserved as per standard methods (APHA, 2012).

3.4 Analytical methods and equipment

All instrumentation and methods used in this study were calibrated and validated according to the ISO/IEC 17025:2005 technical requirements, respectively.

3.4.1 Determination of metals

Samples for the analysis of soluble metals (sodium, calcium, iron, silica, potassium, copper, zinc, lead, vanadium, manganese, chromium, cobalt, nickel, aluminium, molybdenum and magnesium) were filtered through 0.45 µm membrane filters (Merck Millipore, South Africa) and analysed by inductively coupled plasma - optical emission spectrometry (ICP-OES) (Agilent Technologies, USA). The ICP-OES was operated and controlled using the installed Agilent ICP Expert II software (Agilent Technologies, USA). ICP-OES operating parameters are indicated in Table 3.4.

Table 3.4: ICP-OES operating parameters

Operating parameters	
Power	1.5 kW
Plasma gas flow rate	15 L/min
Auxiliary gas flow rate	1.5 L/min
Spray chamber type	Glass cyclonic
Torch	Quartz, Axial
Nebuliser type	Glass concentric
Nebuliser flow rate	0.65 L/min
Pump speed	15 r/min
Replicate read time	5 s
Number of replicates	3
Sample uptake delay time	30 s
Stabilisation time	15 s
Rinse time	10 s
Fast pump	On

The ICP-OES stock solutions were prepared using Titrisol® ICP single-element standards (1 000 mg/L) (Merck Millipore, South Africa). Secondary standard solutions were prepared from the stock solutions using diluted nitric acid (5%).

3.4.2 Determination of chemical and physical parameters

Except for suspended solids and oxygen uptake rates (OUR), all samples were pre-filtered through a 0.45 µm membrane filter (Merck Millipore, South Africa).

(a) Suspended solids (SS) were determined gravimetrically by filtering 100 mL sample aliquots through Whatman® glass microfibre GF/C filter paper (Merck (Pty) Ltd, South Africa) under vacuum suction using a vacuum pump (Boeco R-300, Germany) and drying in an oven (Labcon, South Africa) at 103 °C ± 2 °C for 1 h, and cooled in a desiccator for 1 h.

(b) Oxygen uptake rate (OUR), pH and conductivity were measured using a portable Hach® HQ40d multimeter fitted with a Hach® IntelliCAL™ LDO 101 luminescent probe, Hach® IntelliCAL™ LBOD 101 luminescent probe, Hach® IntelliCAL™ PHC201 gel-filled pH probe and a Hach® IntelliCAL™ CDC401 conductivity probe, respectively. All samples were analysed on site.

(c) Dichloromethane (DCM) extractions were performed by liquid-liquid separation according to the SANS 6051:2007 test method (SABS, 2007) where petroleum ether was substituted for DCM.

(d) Hach® Test Methods and analyses are presented in Table 3.5.

Table 3.5: Analyses using Hach® spectrophotometric test methods for wastewater

Analysis	Test method	Principle
Ammonia-nitrogen	10031	Ammonia compounds combine with chlorine to form monochloramine. Monochloramine reacts with salicylate to form 5-aminosalicylate. The 5-aminosalicylate is oxidised in the presence of a sodium nitroprusside catalyst to form a blue-coloured compound. The intensity of the colour is proportional to the ammonia-nitrogen concentration.
Biochemical oxygen demand (acclimatised carbonaceous BOD_5)	8043	BOD is a measurement of the oxygen requirements of municipal wastewater (sewage) and industrial wastewater. The test results are used to calculate the effect of waste discharges on the oxygen resources of the receiving waters. The BOD test measures the oxygen uptake for a specified effluent over a period of 5 days.
Chemical oxygen demand (COD)	8000	Dichromate ion oxidises organic material in the sample. This results in the change of chromium from the hexavalent (VI) state to the trivalent (III) state. The intensity of the colour is proportional to the COD concentration.
Cyanides (free)	8027	The pyridine-pyrazolone method gives an intense blue colour with free cyanide. The intensity of the colour is proportional to the cyanide concentration.
M-alkalinity	8203	Bromocresol green-methyl red indicator is added to the sample and titrated to a pH between 4.3 and 4.9 with sulphuric acid. The volume of titrant indicates the total (M) alkalinity (carbonate, bicarbonate and hydroxide) in the sample.
Sulphides	8131	Sulphides and acid-soluble metal sulphides react with N, N-dimethyl-p-phenylenediamine oxalate to form methylene blue. The intensity of the blue colour is proportional to the sulphide concentration.
Total Kjeldahl Nitrogen (TKN) (Nessler method)	8075	TKN refers to the combination of ammonia-nitrogen and organic nitrogen. Organically bound in the trinegative oxidation state, it is converted into ammonium salts by the action of sulphuric acid and hydrogen peroxide.

3.4.3 Determination of anions by ion chromatography

The following anions, i.e. chlorides, sulphates, nitrites, nitrates and phosphates were determined by ion chromatography based on the APHA Standard Method 4110B (APHA, 2012) and USEPA Method 300.0 (USEPA, 1983) (Table 3.6).

Stock anion standard solutions (1 000 mg/L) were prepared by weighing off the specified amount of salt, pre-dried to a constant weight at 103 °C ± 2 °C and made up to 1 000 mL with water (Table 3.7). Solutions were stored in plastic bottles and refrigerated at 6 ºC ± 2 °C. Solutions were stable for a month. Combined working standard solutions (high range and low range) were prepared daily. Samples were treated with pre-conditioned C_{18} Sep-Pak® cartridges (Merck Millipore, South Africa) to remove hydrophobic organic material and prevent fouling of the column.

Table 3.6: Ion chromatograph parameters used for analysis

Dionex™ DX-120 Ion Chromatograph	
Auto-sampler	AS 3500
Software	PeakNet™ Work station
Anion separator column	IonPac AS4A-SC, 4 x 250 mm
Eluent concentrate solution	0.18 M sodium carbonate/0.17 M sodium bicarbonate
Eluent	1.8 mM sodium carbonate/1.7 mM sodium bicarbonate
Run time	8 min
Flow rate	2.0 mL/min
Injection volume	50 µL
Detection	Suppressed conductivity, ASRS-ULTRA (4 mm) in recycle mode, 50 mA current
System back pressure	6 894.76 kPa
Background conductance	14 µS

Table 3.7: Compound mass used to prepare 1 L stock solutions (1 000 mg/L)

Anion	Compound	Mass (g)
Chloride	Sodium chloride	1.648
Nitrite	Sodium nitrate	1.499
Nitrate	Sodium nitrite	1.371
o-Phosphate	Potassium phosphate monobasic	1.433
Sulphate	Sodium sulphate	1.522

3.4.4 Identification of organic compounds by gas chromatography-mass spectrometry (GC-MS)

Dichloromethane (liquid-liquid) extractives were characterised using an Agilent 7890A gas chromatograph (Agilent Technologies, USA) equipped with an Agilent 5975C inert mass selective detector (MSD) (Agilent Technologies, USA) using an Agilent DB-5MS capillary column (Agilent Technologies, USA). The GC-MS operating parameters are indicated in Table 3.8.

Table 3.8: GC-MS operating parameters

GC conditions	
GC column	Agilent DB-5MS capillary column
Column dimensions	30 m x 0.3 mm ID with 0.25 µm film thickness
GC oven conditions	
Initial oven temperature	40 ℃ (1 min)
Ramp 1	8 ℃/min to 280 ℃ (0 min)
Ramp 2	5 ℃/min to 300 ℃ (1 min)
Carrier gas	Helium
Flow rate	1 mL/min
Split ratio	10:1 (direct injection)
MS conditions	
Transfer line temperature	280 ℃
Source temperature	230 ℃

Table 3.8 continued

MS conditions	
Ionisation mode	Electron Impact (EI^+)
Electron energy	69.9 eV
Mass scan	35–550 amu
Scan time	2.83 scans/s
Solvent delay	3.0 min
Electron multiplier voltage	1600 V
Mass spectral library (database)	NIST05

3.4.5 Determination of soluble phenols

Phenols (except those with para-substitutions) react with 4-aminoantipyrine (4-AAP) in the presence of potassium ferricyanide at a pH of 10 to form a stable reddish-brown coloured antipyrine dye. The intensity of the colour produced is a function of the concentration of phenolic material in the sample. Phenolic type wastewaters usually contain a variety of phenols; therefore, it is not possible to duplicate a mixture of phenols to be used as a standard. Thus, phenol was selected as a standard and any colour produced by the reaction of other phenolics was reported as phenol. This value will represent the minimum concentration of phenolic compounds present in the sample. Results were confirmed using phenol (99.5%) as a standard. Standard solutions were prepared in the intended range of 0.0 mg/L to 5.0 mg/L using water and Class A volumetric glassware. The range was extended by appropriate dilution of the sample aliquot. Hach® Phenol Model PL-1 test kit (Hach, USA) was purchased and supplied by Buckman Africa.

3.5 Mobilisation of the bioaugmentation inocula for laboratory test work

The selected bioaugmentation inocula (PA1, PA2 and PA3) were mobilised by hydrating the respective freeze-dried inoculum (20% w/v) using a mineral salt medium (Table 3.9 and Table 3.10) and stirring using a Heidolph RZR 2051 (Heidolph, Germany) over-head stirrer at 500 r/min for 60 min. The hydrated inoculum was then filtered through a 100 mesh screen to remove inert material. The bioaugmentation inoculum PA4 was used without hydration.

Table 3.9: Salt solution for mineral salt medium

Salt solution	Mass (g)/100 mL water
Magnesium sulphate heptahydrate ($MgSO_4.7H_2O$)	4.0
Sodium chloride (NaCl)	0.2
Iron sulphate heptahydrate ($FeSO_4.7H_2O$)	0.2
Manganese sulphate hydrate ($MnSO_4.H_2O$)	0.2
Calcium chloride hydrate ($CaCl_2.H_2O$)	0.2

Table 3.10: Mineral salt medium for exogenous inoculum mobilisation

Mineral salt solution	Mass (g)/1 000 mL water
Potassium dihydrogen phosphate (KH_2PO_4)	3.8
Dipotassium hydrogen phosphate (K_2HPO_4)	12.5
Di-ammonium hydrogen phosphate $(NH_4)_2HPO_4$	1.0
Salt solution (Table 3.9)	1.0 mL

The respective hydrated exogenous inocula were added daily directly into aeration Zone 1 of the H-FFBR. Each treatment programme ran for a period of 12 weeks to allow sufficient time for the exogenous microorganisms to acclimatise to the CGSGL wastewater and to achieve maximum growth rate and biological activity. The reactor was subjected to three sludge ages.

The microbial activity of the exogenous inocula was determined monthly during the inoculation phase of the study (9 months). The average heterotrophic plate count (HPC) for inocula PA1, PA2 and PA3 was 2.2 x 10^9 cfu/g, 3.0 x 10^9 cfu/g and 2.4 x 10^9 cfu/g, respectively. The *Pseudomonas* plate count for inocula PA1, PA2 and PA3 was 1.2 x 10^9 cfu/g, 4.0 x 10^9 cfu/g and 1.64 x 10^9 cfu/g, respectively. The average *Cocconeis* and *Nitzschia* cell count in inoculum PA4 was 3.2 x 10^3 cells/g and 2.2 x 10^3 cells/g, respectively. The mass of inoculum added to the reactor was based on the maximum oxygen uptake rate (OUR) since bacterial activity is not linearly related to the number of bacterial cells.

The bioaugmentation (inoculation) regime was as follows:

- Week 1 to 12: Pretreatment (steady-state baseline data)
- Week 13 to 24: PA1 (50 mg/L) and PA4 (20 mg/L)
- Week 25 to 36: PA1 (50 mg/L), PA2 (150 mg/L) and PA4 (20 mg/L)

- Week 37 to 48: PA1 (50 mg/L), PA2 (150 mg/L), PA3 (150 mg/L) and PA4 (20 mg/L)
- Week 49 to 65: Post-treatment

3.6 Phylogenetic analysis of the microbial communities

Samples of the feed, suspended biomass, biofilm and effluent taken from Week 2 to Week 5 of the study period were processed based on the procedures described by Albertsen et al. (2015). Metagenomic data generated for each individual sample were used for comparative studies of phylogenetic lineages between and within the respective samples (Lajeunesse, 2009; Li et al., 2012a).

(i) Removal of DNA from dead cells and extracellular DNA: Samples were spiked with extracted *E. coli* DNA relative to the suspended solids content of the samples. Each sample was divided into 2 mL aliquots and treated with propidium monoazide (Biotium, USA) and incubated in the dark for 10 min with occasional shaking. After incubation, the samples (on ice) were subjected to a strong visible light (650 W halogen light) for 10 min at a distance of 20 cm.

(ii) DNA extraction: Genomic DNA (gDNA) was extracted using the FastDNA™ spin kit for soil (MP Biomedicals, USA) according to the manufacturer's instructions. The purity of the extracted DNA was measured spectrophotometrically with a NanoDrop™1000 spectrophotometer at $Abs_{260/230nm}$ and $Abs_{260/280nm}$ (Thermo Fisher Scientific Inc., USA). The quality of the extracted DNA was evaluated with agarose gel electrophoresis using the TapeStation™ 2200 (Agilent Technologies, USA) and Genomic DNA ScreenTape™ system (Agilent Technologies, USA). The concentration of the gDNA was measured fluorometrically with a Quant-iT™ dsDNA High-Sensitivity assay kit (Molecular Probes, UK) on an Infinite® M1000 PRO (Tecan, Switzerland) microplate reader.

(iii) 16S rRNA amplicon sequencing: The V1 and V3 variable regions were amplified using Q5® Hot Start High-Fidelity 2X Master Mix (New England Biolabs (UK) Ltd). Amplicon library PCR was performed on all replicate extractions separately. The DNA primers used were 27F (5'-AGAGTTTGATCMTGGCTCAG-'3) and 518R (5'-ATTACCGCGGCTGCTGG-'3). Thermocycler settings for PCR amplification were as follows: (i) initial denaturation at 95 ºC

for 2 min; (ii) 30 cycles at 95 ºC for 20 s; (iii) 55 ºC for 30 s; (iv) 72 ºC for 30 s; and final elongation at 72 ºC for 5 min. All PCR reactions were run in duplicate and pooled. The amplicon libraries were purified using the Agencourt® Ampure® XP bead protocol (Beckman Coulter, USA). The library concentration was measured using the NEBNext® Library Quant assay kit for Illumina® (New England Biolabs (UK) Ltd). The quality was validated using the Agilent 2100 Bioanalyzer (Agilent Technologies, USA). The samples were pooled in equimolar concentrations and diluted to 4 nM based on the library concentrations and calculated amplicon sizes. The library pool was sequenced on a MiSeq™ (Illumina, USA) using the MiSeq™ Reagent kit v3, 600 cycles PE (Illumina, USA). The final pooled library was at 10 pM with 20% PhiX as control.

(iv) Metagenomics: Three replicate DNA extractions used for amplicon sequencing were selected for metagenome sequencing and prepared according to the Illumina® TruSeq® PCR free protocol (Illumina, USA). Paired-end sequencing was performed on the prepared libraries using 2 x 300 base pair MiSeq™ Reagent kits v3 (Illumina, USA). The reads were trimmed using CLC Genomics Workbench v.7.03 (CLC bio, Aarhus, Denmark) by requiring a QPhred score >30, a minimum length of >50 base pairs and removing any adaptors. The trimmed metagenome reads were mapped to the MiDAS database version 1.20 using the map reads to reference function in the CLC Main Genomics Workbench v.7.03 bioinformatics software (CLC bio, Aarhus, Denmark) requiring 95% similarity over the full read length and random assignments of reads.

(v) Metatranscriptomics: Three replicate samples were subjected to RNA extraction using the RiboPure™-Bacteria Kit (Thermo Fisher Scientific Inc., USA) according to the manufacturer's instructions. The purity of the extracted total RNA was evaluated using a NanoDrop™ 1000 spectrophotometer (Thermo Scientific Fisher Inc., USA). The quality was determined with the Agilent TapeStation™ 2200 (Agilent Technologies, USA) using the High Sensitivity ScreenTapes® (Agilent Technologies, USA) and the concentration was determined using the Qubit® RNA BR assay kit (Thermo Scientific Fisher Inc., USA). The extracted RNA was used for the library preparation using the TruSeq® stranded mRNA library preparation kit protocol (Illumina, USA) and sequenced using 2 x 75 base pair MiSeq™ Reagent kits v3 on an Illumina MiSeq™ (Illumina, USA). The reads were trimmed using the CLC Genomics Workbench v.7.03 bioinformatics software (CLC bio, Aarhus, Denmark) requiring a minimum Phred score of 20 and a minimum length of 75 base pairs. The trimmed metatranscriptome

reads were mapped to the MiDAS database version 1.20 using the map reads to reference function in CLC Genomics Workbench v.7.03 bioinformatics software (CLC bio, Aarhus, Denmark) requiring 95% similarity over the full read length and random assignments of reads.

3.7 DNA extraction and PCR analysis of the bioaugmentation inocula

Bacterial isolates were characterised by sequencing the 16S rRNA using the ZR Fungal/Bacterial DNA MiniPrep™ test kit (Zymo Research Corp, USA). The universal primers 16S-27F (5'-AGAGTTTGATCMTGGCTCAG-3') and 1492R (5' – CGGTTACCTTGTTACGATT-3') were used to amplify the 16S rRNA target region using DreamTaq™ DNA polymerase (Thermo Fischer Scientific, USA) and the primers were gel extracted using the Zymoclean™ Gel DNA Recovery Kit (Zymo Research, USA) and sequenced in the forward and reverse directions on the ABI PRISM 3500xl Genetic Analyzer (Applied Biosystems, USA). Amplification of DNA was performed using the following conditions: (i) initial denaturation at 95 ºC for 2 min; (ii) denaturation at 95 ºC for 30 s; (iii) annealing at 50 ºC for 30 s, and repeating steps (i) to (iii) for 45 cycles; and (iv) the reaction was terminated after the extension at 72 ºC for 10 min. The amplicons from each DNA sample, which were amplified in triplicate, were pooled and gel purified using 0.8% agarose gel. The PCR products were purified using the ZR-96 DNA Sequencing Clean-up Kit™ (Zymo Research Corp, USA) and the purified products were analysed using the CLC Main Genomics Workbench v.7.03 bioinformatics software (CLC bio, Aarhus, Denmark) followed by a nucleotide-nucleotide BLAST (BLASTn) (Altschul et al., 1990) similarity (>98%) genome search in the public NCBI GenBank database (http://blast.ncbi.nlm.nih.gov/Blast.cgi) to obtain an indication of the phylogenetic affiliation. All sequences were assigned to species level grouping.

The hydrated PA4 sample was prepared using the NEB® PCR cloning kit (New England Biolab (UK) Ltd) purchased from Inqaba Biotechnology, South Africa and supplied by the University of Pretoria, South Africa. The primers used were 18S_D512_F (5'-ATTCCAGCTCCAATAGCG-3') and 18S_D978_R (5'-GACTACGATGGTATCTAATC-3') based on the method of Zimmerman et al. (2011). The identification was achieved with data from reference and type strains, as well as environmental clones. Evolutionary genetic distances were derived from the sequence pair dissimilarities calculated using the Kimura-2-parameter (K80) model. The phylogenetic reconstructions were done using the Unweighted

Pair Group Method with Arithmetic Mean (UPGMA) algorithm, with bootstrap values calculated from 1 000 replicate runs using the CLC Main Genomics Workbench v.7.03 bioinformatics software (CLC bio, Aarhus, Denmark). Complete genomes producing significant alignments were used for the generation of phylogenetic trees.

3.7.1 Metagenomic sequencing data

All metagenomic sequencing data were deposited in the NCBI GenBank database under Bioproject: PRJNA 315566 and Biosample accession numbers: SAMN 04565875 to SAMN 04565882.

3.7.2 16S rRNA and 18S rRNA sequencing

A representative sequence from each sample cluster was BLASTed (Altschul et al., 1990) against an updated NCBI GenBank public database (http://blast.ncbi.nlm.nih.gov/Blast.cgi) to obtain an indication of the phylogenetic affiliation. All sequences were assigned to species level grouping at a cut-off similarity threshold of 0.05.

3.8 Analysis of attached and suspended biomass

3.8.1 Attached biomass weight

Attached biomass (biofilm) was determined by grabbing approximately 200 randomly selected plastic carriers from the respective aeration zones. Carriers were rinsed well, but gently, with water. The rinsed carriers were split into three portions, placed on watch-glasses and dried in a drying oven (Labcon, South Africa) at 103 ºC ± 2 ºC for 24 h, cooled in a desiccator for 1 h, and then weighed using a 4 decimal place analytical balance (Mettler, Germany). The carriers were then soaked in a 0.25 N NaOH solution for 24 h with intermittent shaking. The alkali wash was repeated after rinsing the carriers well with copious amounts of water. The second alkali wash was performed in an ultrasonic water-bath (Integral Systems, South Africa) for 90 min. The carriers were then rinsed well with copious amounts of water, placed on watch-glasses and dried for 24 h at 103 ºC ± 2 ºC, cooled in a desiccator for 1 h, and re-weighed (Equation (3.1).

$$\text{Biomass (mg/carrier)} = (B - A)/C \times 1000 \quad (3.1)$$

where:

B is the mass (g) of the carriers after rinsing and drying

A is the mass (g) of the carriers after second alkali wash and drying

C is the number of carriers

Biomass (mg/carrier) was converted to g TSS/m^2.

3.8.2 Attached and suspended biomass activity

The oxygen uptake rate (OUR) for each aeration zone was measured on-site at 36 ºC ± 1 ºC using a calibrated portable Hach® model HQ40d multimeter fitted with a Hach® LBOD 101 probe. The attached biomass activity was measured by filling a biochemical oxygen demand (BOD) sample bottle (300 mL) with 150 mL carrier media and 150 mL of activated sludge from the specific aeration zone. The suspended biomass activity was determined in the same manner except that no carriers were added to the BOD bottle. The dissolved oxygen (DO) was measured every 60 s for a period of 10 min. The respective OUR (mg O_2/L.h) was calculated using Microsoft Excel™ for Windows 7, where OUR is the slope (m) of a straight line ($y = mx + c$) obtained by plotting the DO concentration versus time (Qiqi et al., 2012).

3.8.3 Biofilm structure

Biofilm samples were fixed using 2.5% glutaraldehyde in 0.1 M sodium cacodylate buffer (pH 7.4) for 20 min and then exposed to an ethanol dehydration series of 50%, 60%, 70%, 80%, 90%, and 2 × 100% for 10 min at each concentration. This was followed by a chemical dehydration series of ethanol and hexamethyldisilazane (HMDS) at 50%, 60%, 70%, 80%, 90%, and 2 × 100% HMDS for 5 min at each concentration.

The last HMDS change was allowed to evaporate overnight. The biofilm samples were mounted on aluminium stubs using adhesive carbon tape and then sputter coated with a very thin film of gold/palladium before imaging. Scanning electron microscopy (SEM) was performed with a Zeiss Ultraplus Field Emission Gun-Scanning Electron Microscope (FEG-SEM) (Zeiss, Germany) at an acceleration voltage of 10 kV. Images were digitally captured using the calibrated SmartSEM® software (Zeiss, Germany). The optical magnification range was 20-135X,

electron magnification range was 80-130000X and the maximum digital zoom was 12X. The energy dispersive X-ray spectroscopy (EDX) was performed using the AZtecEnergy software (Oxford Instruments, UK) linked to an Oxford detector (Oxford Instruments, UK) with an 80 mm^2 detection window. Imaging was performed using an in-lens detector for surface structure and an SE2 (Everhart-Thornley) detector for topography (Zeiss, Germany).

3.8.4 Fourier transform infrared (FT-IR) spectroscopy

An Agilent Cary 670 Fourier Transform Infrared (FT-IR) spectrophotometer (Agilent Technologies, USA) was used to identify the functional groups in the dichloromethane extractives in the mid-IR wavelength range (4 000 cm^{-1} to 400 cm^{-1}). About 50 µL of the extracted sample was placed on a NaCl crystal window to form a thin film. The spectra for the respective samples were read after evaporation of the solvent under vacuum at room temperature.

3.9. Artificial intelligence model development

3.9.1 Model topology development

The artificial neural network (ANN) with multi-layer perceptron (MLP) was structured for this study. The artificial neural network topology adopted for the H-FFBR consisted of 1 input layer of 10 neurons, 1 hidden layer comprising 14 neurons and 1 output layer of 14 neurons (10-14-14) (Figure 3.2). A logistic sigmoid transfer function was employed for the hidden layer. This hidden layer served two purposes; addition of weighted inputs as well as the linked bias and shift input data to a non-linear form as shown in Equation (3.2) and Equation (3.3) (Rorke et al., 2017). Microsoft™ Visual basic v.6.0 was used for the ANN object.

$$sum = \sum_{i}^{n} = 1^{xiwi} + \theta \quad (3.2)$$

where:

w_i ($i = 1, n$) are the connection weights

θ is the bias

x_i is the input variable

$$f(sum) = \frac{1}{(1+\exp(-sum))} \quad (3.3)$$

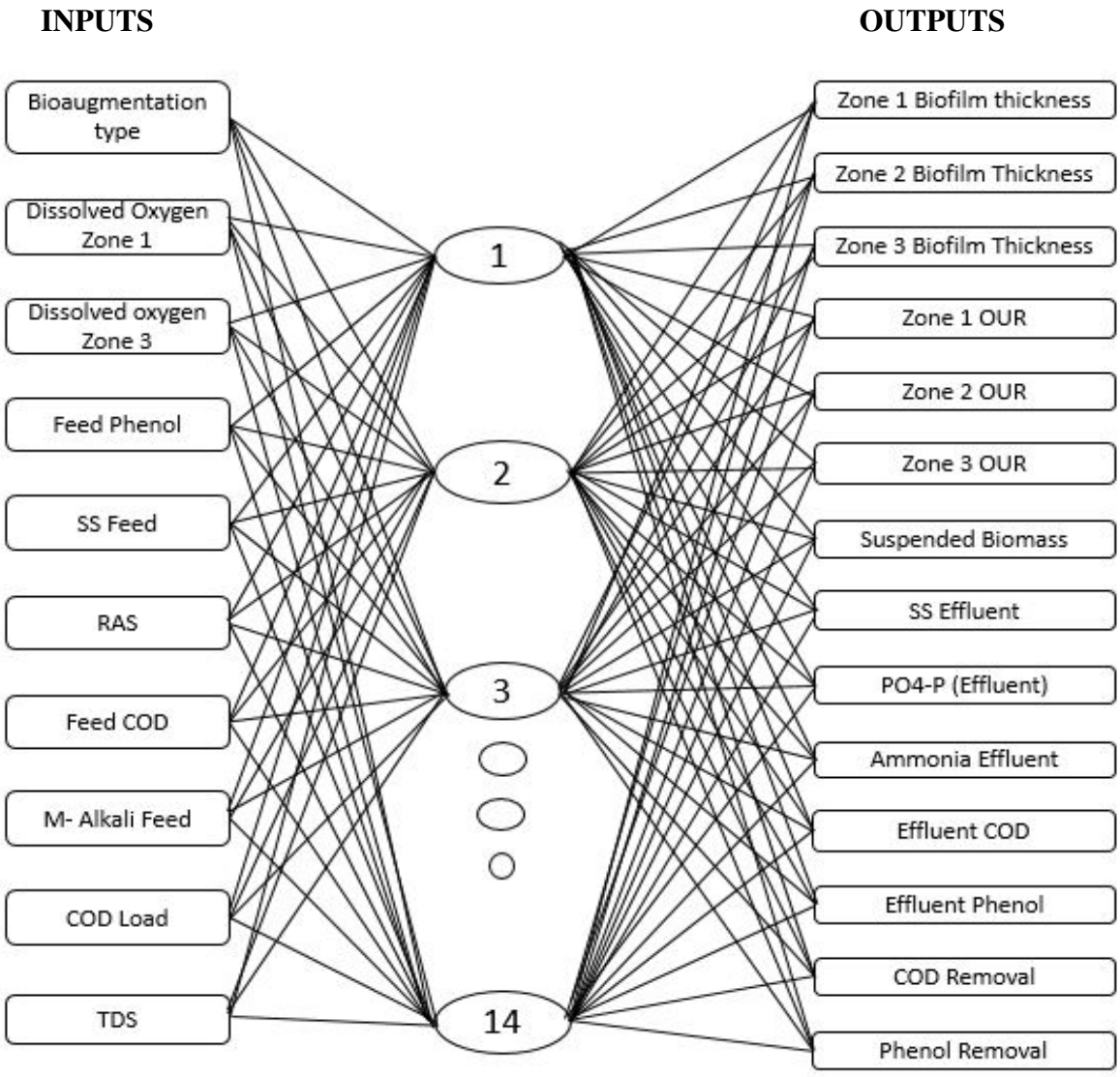

Figure 3.2: Artificial neural network (feed forward back-propagation) topology adopted for the H-FFBR

3.9.2 Selection of input variables

Ten H-FFBR input variables were selected, as follows: bioaugmentation type (BT); dissolved oxygen zone 1; dissolved oxygen Zone 3; feed phenol; suspended solids (SS) feed; return activated sludge (RAS); feed COD; M-alkalinity feed; COD load; and total dissolved solids (TDS). Fourteen H-FFBR output variables were selected: Zone 1 biofilm thickness; Zone 2 biofilm thickness; Zone 3 biofilm thickness; Zone 1 OUR; Zone 2 OUR; Zone 3 OUR; suspended biomass (MLSS); SS effluent; o-PO_4 as P effluent; ammonia-N; effluent COD; effluent phenol; COD removal; and phenol removal. The experimental data obtained in this study were used for the model development.

The input data streams for the bioaugmentation regimes were coded as follows:

0 = Pretreatment (baseline data) with no bioaugmentation
2 = PA1 (50 mg/L) and PA4 (20 mg/L) bioaugmentation
3 = PA1 (50 mg/L), PA2 (150 mg/L) and PA4 (20 mg/L) bioaugmentation
4 = PA1 (50 mg/L), PA2 (150 mg/L), PA3 (150 mg/L) and PA4 (20 mg/L) bioaugmentation
1 = Post-treatment; no bioaugmentation

Experimental data were normalised according to Equation (3.4):

$$\text{Normalised } (e_i) = \frac{e_{i-E_{min}}}{E_{max}-E_{min}} \quad (3.4)$$

where:

e_i is the normalised data
E_{min} denotes the minimum value
E_{max} denotes the maximum value

3.9.3 ANN training and validation

The artificial neural network (ANN) was trained using a back-propagation algorithm (Figure 3.3) with the goal of achieving a minimum net error on the validation data set while preventing overtraining or memorisation (Rorke et al., 2017).

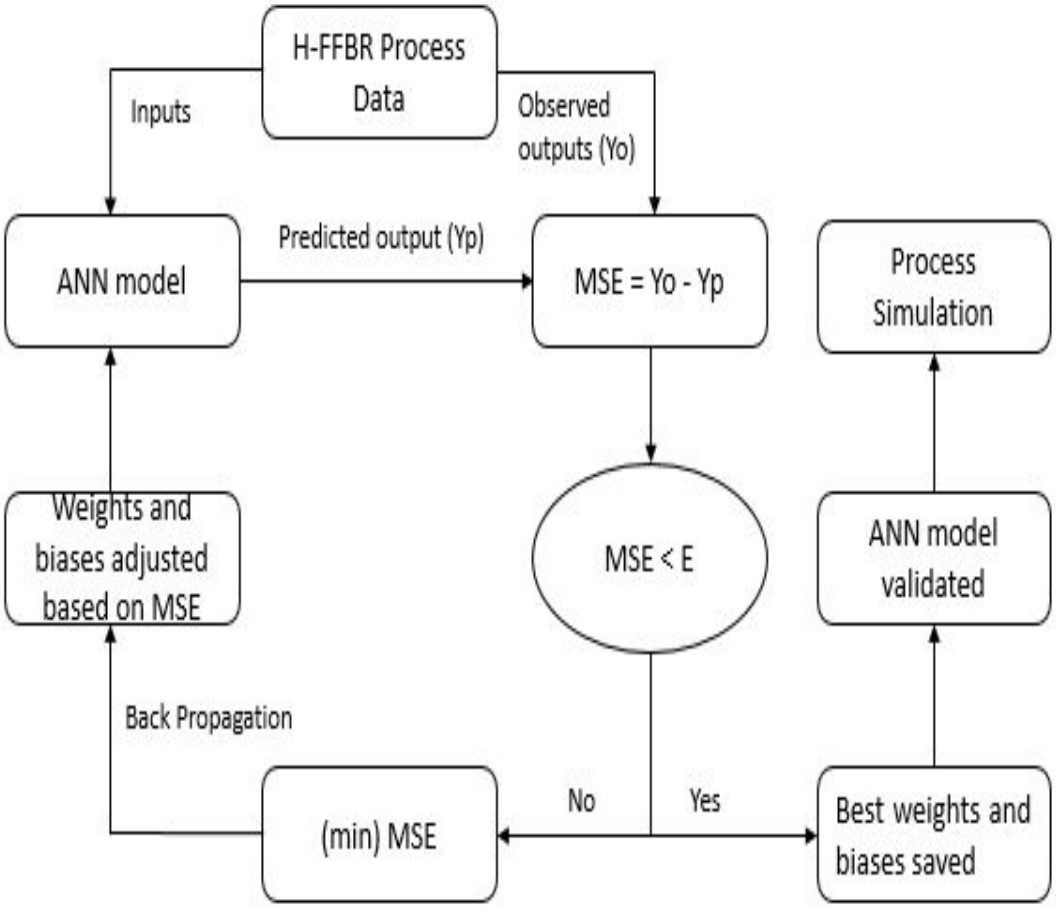

Figure 3.3: Back-propagation training algorithm used for the ANN training model (MSE = mean square error; E = error; *Yo* = observed experimental values; *Yp* = model predicted values) (Rorke et al., 2017)

The experimental data sets were randomly divided into two sets: (i) 75% of the data were used for training; and (ii) 25% of the data were used for the validation and testing process. A net error value on the validation data set of 0.018 was achieved after 3 700 training epochs. The accuracy of the developed model was assessed on 14 novel process conditions (validation data set). With this data set, the regression analyses on predicted and observed process outputs, and the coefficients of determination (R^2), were calculated for each model output.

The learning patterns were randomly selected during the learning process. The root mean square error (RMSE) between predicted and observed values for the cross-validating data was calculated according to Equation (3.5) (Desai et al., 2008; Sewsynker and Kana, 2016). The lower the RMSE, the more accurate the prediction model.

$$RMSE = \sqrt{\frac{\sum_{i}^{N}\sum_{n-1}^{N}(y^{i}n - \hat{y}^{i}n)^{2}}{NM}} \quad (3.5)$$

where:

N refers to the number of patterns used in the training

M denotes the number of output nodes

i denotes the index of the input system (vector)

$y^{i}n$ denotes the actual output

$\hat{y}^{i}n$ denotes the predicted output

3.9.4 Sensitivity analysis and knowledge discovery

Mathematical equations illustrating the various functional relationships between the various process inputs and outputs from the developed model were derived using curve fitting (CurveExpert Professional v.2.4.0).

The process models developed in this study have been deposited into the Repository of Experimental Data & Intelligent Models [REDIM] with accession number PRNQ000775 (http://www.redim.org.za/?search=PRNQ000775).

3.10 Statistical analysis

Statistical analysis was performed using Minitab® 17 and Microsoft™ Excel.

CHAPTER 4
METAGENOMIC STUDY OF THE MICROBIAL COMMUNITY IN THE H-FFBR

4.1 Microbial community and diversity by Illumina high-throughput sequencing

The microbial community determines the metabolic pathways for the removal of chemical oxygen demand (COD), phenol, and ammonia-nitrogen from coal gasification stripped gas liquor (CGSGL) wastewater. This study reveals the microbial communities between and within the samples (biofilm, suspended biomass, effluent and feed) taken across the hybrid fixed-film bioreactor (H-FFBR) using culture-independent Illumina high-throughput sequencing. Knowledge of the indigenous microbial community and diversity is essential in order to select inoculum strains to facilitate enhanced biodegradation of the organic compounds present in the CGSGL wastewater.

4.1.1 Microbial community and diversity at high taxonomic levels

The results revealed that bacteria (97.9%-99.8%, average 98.9%) and Archaea (0.2%-2.1%, average 1.15%) were the dominant taxa for the biofilm, suspended biomass (SB), effluent (CA) and feed (RAS). In addition to the taxa level, the bacterial community diversity was also analysed at the phylum level.

The results revealed that Proteobacteria was the most abundant phylum in the H-FFBR. The proportions of Proteobacteria in the samples ranged between 50% and 95%. The other dominant phyla were Firmicutes (0.57%-17%, average 8.78%), Actinobacteria (0.28%-3.74%, average 2.01%) and Bacteroidetes (0.18%-5.16%, average 2.67%).

The less dominant phyla Deinococcus-Thermus (0.5%), Acidobacteria (0.22%) and Chloroflexi (2.5%) were only found in the feed and Planctomycetes (2.1%) in the suspended biomass. The proportion of unidentified (uncultured bacteria) phyla across the H-FFBR ranged between 12% and 25% thus indicating the possibility of novel bacteria in the treatment of the CGSGL wastewater.

4.1.2 Microbial community and diversity at low taxonomic levels

The dominant classes revealed in the Proteobacteria phylum were α-Proteobacteria, β-Proteobacteria and γ-Proteobacteria with α-Proteobacteria dominant in the effluent (59%) and suspended biomass (34%), β-Proteobacteria dominant in the biofilm (43%) and the feed (28%) and γ-Proteobacteria dominant in the effluent (18%). The class δ-Proteobacteria was not detected in the above-mentioned samples.

The uncultured classes in the Proteobacteria phylum were as follows:

- Feed: 7% to 12% α-Proteobacteria, 0.7% to 1.1% β-Proteobacteria and 0% to 1.2% γ-Proteobacteria
- Biofilm: 0.8% to 5.8% β-Proteobacteria
- Suspended biomass: 1% to 2% α-Proteobacteria, 0.3% to 3% β-Proteobacteria
- Effluent: 0% to 3.7% γ-Proteobacteria

The dominant orders revealed were Burkholderiales (3%-16%, average 18.5%), Rhizobiales (1%-29%, average 15%), Pseudomonadales (3%-12%, average 7.5%) and the less dominant orders were Clostridiales (17%) in the feed, Rhodocyclales (2%) and Xanthomonadales (4%) in the biofilm, Bacteroidales (4%) and Xanthomonadales (5%) in the suspended biomass and Rhodospirillales (8%) in the effluent. The absence of the order Nitrosomondales and the presence of the order Rhizobiales in all the above samples indicates the absence of autotrophic ammonia-oxidising bacteria (*Nitrosomona*s and *Nitrosospira*) and the presence of autotrophic nitrifying bacteria (*Nitrobacter* and *Nitrospira*), respectively. Both species are required for autotrophic nitrification/denitrification to take place since ammonia oxidation is regarded as the rate-limiting step in autotrophic nitrification (Ma et al., 2015).

Except for the absence of δ-Proteobacteria and Nitrosomondales, the phyla, classes and orders were similar to those reported in coking wastewater (Felfoldi et al., 2010), desalination plants (Sanchez et al., 2013), sea sediment (Zhang et al., 2014), river sludge (Liu et al., 2015), steel industry wastewaters (Ma et al., 2015) and industrial wastewater treatment plants (Cydzik-Kwiatkowska and Zielinska, 2016). However, the abundance and diversity differed due to the varying physical, chemical and organic compositions of the respective effluents.

4.1.3 Core microbial genera and species of the indigenous microbial community

The closest match for the four most abundant identifiable species (16S rRNA, homology >99%) in the samples taken across the H-FFBR (feed, biofilm, suspended biomass and effluent) is revealed in Table 4.1 in order of decreasing abundance.

Table 4.1: Core genera and species across the H-FFBR

Feed (RAS)[(a)]	Biofilm[(a)]	Suspended biomass[(a)]	Effluent[(a)]
Pseudomonas aeruginosa (AF440523.1) (6-8%; average 7.5%)	*Thauera butanivorans* (NR_040797.1) (5-10%; average 6.9%)	*Ochrobactrum anthropi* (AB120120.1) (2-4%; average 2.2%)	*Rhodoplanes cryptolactis* (AB087718.1) (1-8%; average 2.8%)
Rhodoplanes cryptolactis (AB087718.11) (2-5%; average 4.5%)	*Pseudaminobacter salicyclatoxidans* (NR_028710.1) (3-5%; average 3.6%)	*Thauera butanivorans* (NR_040797.1) (1-4%; average 1.7%)	*Pseudomonas putida* (AE015451.1) (0.3-5%; 1.2%)
Xanthobacter polyaromaticivorans (AB106864.1) (1-3%; average 1.3%)	*Pseudomonas aeruginosa* (AF440523.1) (1-3%; average 2.3%)	*Pseudomonas aeruginosa* (AF440523.1) (1-3%; average 1.6%)	*Pseudomonas aeruginosa* (AF440523.1) (0-4%; average 0.9%)
Diaphorobacter nitroreducens (AB076856.1) (0.6-2%; average 1.5%)	*Diaphorobacter nitroreducens* (AB076856.1) (1-2%; average 1.6%)	*Ancylobacter polymorphus* (NR_04279.1) (0.6-2%; average 1.2%)	*Diaphorobacter nitroreducens* (AB076856.1) (0-3%; average 0.5%)

Samples (16) taken from Week 2 to Week 5 of the study period

The most abundant bacterial genera and species in the feed, biofilm, suspended biomass (SB) and effluent (CA) were *Pseudomonas aeruginosa, Thauera butanivorans*, *Ochrobactrum anthropi* and *Rhodoplanes cryptolactis*, respectively. The least abundant species were *Diaphorobacter nitroreducens* in the feed, biomass and effluent and *Ancylobacter*

polymorphus in the suspended biomass. The bacteria belonging to α-Proteobacteria (*Pseudaminobacter, Ancylobacter, Xanthobacter* and *Rhodoplanes*) are sensitive to temperature shifts (Cydzik-Kwiatkowska and Zielinska, 2016). The bacteria belonging to the β-Proteobacteria (*Thauera*, *Diaphorobacter* and *Ochrobactrum*) have slow degradation rates, whereas γ-Proteobacteria (*Pseudomonas*) have higher degradation rates in coal gasification wastewaters (Felfoldi et al., 2010). The class β-Proteobacteria, commonly found in coal gasification wastewater, are heterotrophic denitrifying bacteria converting nitrates to nitrogen gas and are also capable of degrading a range of aromatic and aliphatic organic compounds (Basha et al., 2010; Cydzik-Kwiatkowska and Zielinska, 2016) as follows: (i) *Thauera* degrade hydrocarbons, phenols, methyl phenols, quinolinone, indole (Jia et al., 2016), polyphenols, toluene and halobenzoate (Silva et al., 2010); (ii) *Diaphorobacter* (Székely, 2008) display simultaneous nitrification and denitrification of ammonia-nitrogen to nitrogen gas (Khardenavis et al., 2007) and can also degrade phenols, pyridines and pyrenes found in coking wastewater (Meng et al., 2015); (iii) *Ochrobactrum* are both denitrifiers and sulphide oxidisers (Mahmood et al., 2009) which utilise sulphides and thiosulphates as substrates to reduce nitrite. *Ochrobactrum* can also adsorb metals, degrade aromatic hydrocarbons (Bhattacharya et al., 2008) and form granules (Cydzik-Kwiatkowska and Zielinska, 2016); and (iv) *Xanthobacter* (Gomez et al., 2005) can degrade cyclohexane (Van der Werf et al., 2001).

The results revealed (Table 4.1) that up to 45% of the total microbial community washed out in the effluent were *Pseudomonas* (γ-Proteobacteria) resulting in the higher abundance of the slow degraders (β-Proteobacteria) returning to the H-FFBR. *Ochrobactrum* form flocs/granules which explains their abundance in the suspended biomass. Flocculated cells have longer residence times but lower substrate assimilation times due to intra-floc diffusive transport limitations (Hull and Kapuscinski, 1987). *Pseudomonas* do not form flocs and settle slowly in the clarifier and are thus easily washed out (Székely, 2008). However, they have higher assimilation rates than flocculated cells (Hull and Kapuscinski, 1987). The rate of substrate consumption in petrochemical refinery wastewater can be divided into fast and moderate based on the Michaelis-Menten kinetics. At a high substrate concentration, every site on the microorganism is saturated with the substrate and the rate of reaction is constant. As the substrate concentration decreases, only a few sites of the microorganisms are covered with the substrate, making the substrate reduction rate proportional to the substrate concentration (Hamza et al., 2009).

4.2 Measurement of community diversity across the H-FFBR

Alpha diversity evaluates the richness and evenness within the same microbial community. Shannon entropy (H_α) increases as the number of phyla increases and as the distribution becomes even (abundance and richness). Simpson's index (D) indicates phyla dominance and reflects the probability that two individuals randomly selected from a sample belong to the same phylum. The index varies between 0 and 1 and the index increases as the diversity decreases. The Chao 1 richness estimator coverage (C) is a non-parametric estimator that calculates the rare operational taxonomic units (OTUs) present in the sample and indicates the number of phyla in the microbial population (Lemos et al., 2011; Garrido et al., 2014).

Beta diversity is a visual interpretation of the distance (dissimilarity) between two or more microbial communities. Principal coordinates analysis (PCoA), a multivariate statistical technique, is used to reveal the dissimilarities between the microbial communities by finding clusters that reflect the dissimilarities of the microbial communities. PERMANOVA statistical analysis using the unique fraction metric (UniFrac) was used to determine the significance of these dissimilarities.

4.2.1 Alpha diversity

The results revealed that the feed (RAS) had the highest richness and evenness ($H_\alpha = 5.8$), the suspended biomass (SB) had the highest species dominance ($D = 0.71$) and the biofilm had the highest richness ($C = 550$) within the microbial community (Table 4.2).

Table 4.2: Diversity within the samples taken across the H-FFBR

Sample	Shannon entropy (H_α)	Simpson's index (D)	Chao 1-biased corrected (C)
Effluent (CA)	4.3	0.73	480
Feed (RAS)	5.8	0.91	400
Suspended biomass (SB)	3.2	0.72	520
Biofilm	5.1	0.91	550

Ma et al. (2015) reported a lower H_{α} range (3.0 to 4.4) and higher richness range (C = 534 to 1 223) for communities in coking wastewaters from steel industries. However, the community richness and diversity for coal gasification and coking wastewaters are lower than those of municipal wastewater due to the presence of inhibitory organic compounds (Ma et al., 2015).

4.2.2 Principal coordinates analysis (PCoA) of beta diversity

The PCoA analysis reveals phylogenetic dissimilarities between the feed (RAS) and effluent (CA) and dissimilarities between the biofilm and suspended biomass (SB). The coordinates PCo1, PCo2 and PCo3 explain 69%, 23% and 8% of the dissimilarities, respectively (Figure 4.1).

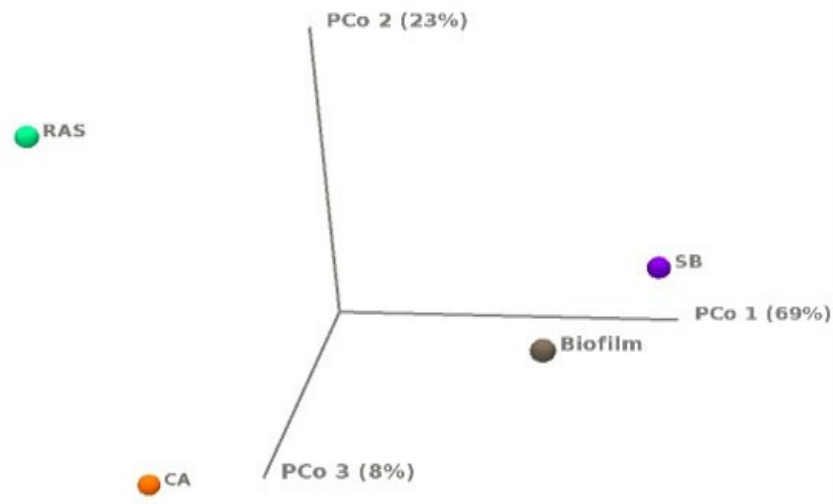

Figure 4.1: PCoA analysis indicating dissimilarities between samples taken across the H-FFBR

4.2.3 PERMANOVA statistical analysis using unique fraction metric (UniFrac)

The PERMANOVA weighted UniFrac diversity indicated a significant dissimilarity (pseudo-$F_{2.353;}$ $P_{0.0381}$) between the phylogenetic communities of the respective biomass samples taken across the H-FFBR. The pair-wise distance PERMANOVA weighted UniFrac (with Bonferroni correction) dissimilarity remained above 0.3 which reveals significant phylogenetic dissimilarities between the following pairs of samples:

- Suspended biomass (SB) and biofilm (pseudo-$F_{6.8508}$; $P_{0.3333}$)
- Suspended biomass (SB) and feed (RAS) (pseudo-$F_{13.603}$; $P_{0.3333}$)

- Biofilm and feed (RAS) (pseudo-$F_{15.868}$; $P_{0.3333}$)
- Biofilm and effluent (CA) (pseudo-$F_{1.6931}$; $P_{0.3333}$)
- Feed (RAS) and effluent (CA) (pseudo- $F_{0.7328}$; $P_{0.6666}$)

4.2.4 Effect of operating parameters on microbial community diversity

The biofilm (attached biomass) and suspended biomass (flocculated biomass) were subjected to higher aeration rates and temperatures than the effluent and feed. The age of the attached biomass (biofilm) was approximately 126 d (Toerien and Van Niekerk, 2013) which was far longer than the suspended biomass age of approximately 18 d. The effluent (dispersed cells) was not aerated and its temperature was 2 ºC lower than those of the biofilm and suspended biomass in the H-FFBR. The feed (settled flocculated biomass) was not aerated and its temperature was 3 ºC lower than those of the biofilm and suspended biomass in the H-FFBR and 1 ºC lower than that of the effluent. The feed consisted of flocculated sludge recycled from the bottom of the clarifier back to the H-FFBR. The presence of the order Clostridiales in the feed indicates the presence of anoxic zones in the sludge bed. A higher microbial diversity means that the organics present in the CGSGL wastewater can be degraded under a wider range of operating conditions. Microbial communities are constantly changing even when operating conditions and reactor performance are constant. The ammonia-oxidising bacteria (AOB) were out-competed by heterotrophic bacteria and ammonia-oxidising Archaea (AOA) in the high C/N environment of the H-FFBR. The Archaea were most abundant in the anoxic zones such as the feed (RAS). The class β-Proteobacteria was found to be the predominant microbial community in the H-FFBR. Thus, microbial communities from the class γ-Proteobacteria and class Actinobacteria were selected for bioaugmentation of the indigenous microbial community in the H-FFBR.

These findings reveal that dissolved oxygen, biofilm structure, biofilm thickness, temperature and chemical characteristics of the CGSGL wastewater impact the microbial community and diversity across the H-FFBR. The microbial communities and diversities between and within the samples taken across the H-FFBR (biofilm, suspended biomass, feed and effluent) were significantly dissimilar, thus indicating different phylogenetic lineages.

CHAPTER 5
PERFORMANCE OF THE H-FFBR IN REMOVING ORGANIC POLLUTANTS

5.1 Characterisation of the coal gasification stripped gas liquor

This study reveals the physical, chemical and organic characteristics of the real-time CGSGL wastewater fed continuously to the hybrid fixed-film bioreactor (H-FFBR) used in this study. The characterisation of this wastewater is a vital step in gaining an understanding of the effect this wastewater has on the acclimatised biomass when in contact with pollutants such as phenols, ammonia-nitrogen and organics contributing to the chemical oxygen demand (COD).

5.1.1 Identification of organic compounds in the feed and effluent by GC-MS

The organic compounds revealed by gas chromatography-mass spectrometry (GC-MS) "finger-printing" analyses (Table A-1 in Appendix A) were identified as hydantoins, benzoquinones, heterocyclic aromatic amines (acetylindole, benzimidazoles, indole, quinolinones), benzoic acid derivatives (benzamides), heterocyclic aromatic organics (furans, pyridines), aromatic isocyanates, unsaturated mono-carboxylic acids (C_1-C_{16}), aromatic carboxylic acids (benzoic acids), alkenes (olefins), saturated cyclic alkanones (cyclopentenones), and phenol. No semi-volatile organic carbons (SVOC) or polycyclic aromatic hydrocarbons (PAHs) were detected above the respective test method detection limits (Table A-2 in Appendix A), thus complying with MINAS requirements.

The composition of the feed has a direct effect on the removal of specific groups of organic compounds. Organics identified in the feed and not in the effluent are regarded as being available to the indigenous microbial population for degradation (Das and Chandran, 2011). No organics were detected above the method detection limit (25 µg/L) in the effluent when the following groups of compounds were detected in the feed:

(i) saturated carboxylic acids ($C_4H_8O_2$; $C_6H_{12}O_2$; $C_7H_{14}O_2$; $C_8H_{15}O_2$; $C_{16}H_{32}O_2$); unsaturated carboxylic acids ($C_4H_6O_2$; $C_5H_8O_2$); substituted unsaturated carboxylic acids ($C_6H_{10}O_2$); substituted benzoic acids ($C_8H_8O_2$; $C_9H_{10}O_2$; $C_{10}H_{12}O_2$; $C_{11}H_{14}O_2$), substituted cyclopentenones (C_6H_6O); quinolinols ($C_{10}H_7NO$; $C_{10}H_9NO$); acetylindoles ($C_{11}H_{11}NO$) and phenol (C_6H_6O)

(ii) phenol (C_6H_6O); aniline ($C_6H_5NH_2$); isoquinolinones (C_9H_7N); benzoquinones ($C_7H_6O_2$; $C_8H_8O_2$); benzenediol ($C_6H_6O_2$; $C_7H_8O_2$); indoles (C_9H_9N); benzamides (C_8H_9NO); phenyl-isocyanates (C_9H_9NO); substituted cyclopentenones (C_6H_8O; $C_7H_{10}O$; $C_{10}H_{10}O$); substituted cyclopentenones (C_6H_6O)

(iii) saturated short-chain carboxylic acids ($C_4H_8O_2$; $C_6H_{12}O_2$) and unsaturated long-chain carboxylic acids ($C_{16}H_{32}O_2$; $C_{18}H_{36}O_2$)

(iv) aniline ($C_6H_5NH_2$); phenol (C_6H_6O); benzimidazoles ($C_8H_8N_2$); isoquinolinols ($C_{10}H_7NO$; $C_{10}H_9NO$); quinolinones (C_9H_7N); substituted cyclopentenones (C_6H_6O); substituted cyclopentenones (C_6H_8O; $C_7H_{10}O$; $C_{10}H_{10}O$); benzamides (C_8H_9NO) and benzimidazoles ($C_8H_8N_2$)

(v) traces of long-chain hydrocarbons (>C_{15})

However, phenol (C_6H_6O), isoquinolinones (C_9H_7N) and saturated carboxylic acids ($C_4H_8O_2$; $C_6H_{12}O_2$; $C_7H_{14}O_2$; $C_8H_{15}O_2$; $C_{16}H_{32}O_2$) were detected in the effluent when phenol (C_6H_6O), isoquinolinones (C_9H_7N), substituted cyclopentenones (C_6H_6O), substituted benzoic acids ($C_8H_8O_2$) and phenylbutenones ($C_{10}H_{10}O$) were present in the feed. Thus, slower degradation of these compounds occurred when phenylbutenones (substituted aromatic alkenone) were present in the feed. Hydantoins ($C_5H_8N_2O_2$; $C_6H_{10}N_2O_2$) were only detected in the effluent when phenol (C_6H_6O), aniline (C_6H_5NH), substituted cyclopentenones (C_6H_6O), furans (C_6H_6O) and pyridines ($C_6H_7N_9$) were present in the feed.

The sourcing of calibration standards for all the organic compounds (>42) detected by GC-MS was not possible due to availability. Qualitative analysis, based on the relative percentage of the total peak area, was used to estimate the concentrations of phenols (100 mg/L to 150 mg/L), hydantoins (200 mg/L to 250 mg/L), carboxylic acids (150 mg/L to 250 mg/L), extractable hydrocarbons (10 mg/L to 30 mg/L) and nitrogen-containing organics (20 mg/L to 30 mg/L) in the feed. The concentrations of phenol (0.35 mg/L to 5 mg/L), carboxylic acids (<20 mg/L), hydantoins (50 mg/L to 70 mg/L), extractable hydrocarbons (10 mg/L to 30 mg/L) and nitrogen-containing organics (20 mg/L to 30 mg/L) were also estimated in the effluent. From these results it is clear that phenols, hydantoins and carboxylic acids were readily degraded by the indigenous microbial communities due to their lower molecular weight and simpler organic structure (lower oxidation state).

The GC-MS "finger-printing" of the composite biofilm sample revealed the sorption of trans-2-methyl-2-butenoic acid ($C_6H_{10}O_2$); 3-methyl-2-butenoic acid ($C_5H_{10}O_2$), 5-ethyl-5-methyl-hydantoin ($C_6H_{10}N_2O_2$); methyl-isobutyl-hydantoin ($C_8H_{14}N_2O_2$), hydantoin substitutions, long-chain hydrocarbons (>C_{15}) and n-hexadecanoic acid ($C_{16}H_{32}O_2$) to the biofilm. Methyl-isobutyl-hydantoin ($C_8H_{14}N_2O_2$), trans-2-methyl-2-butenoic acid ($C_6H_{10}O_2$) and 3-methyl-2-butenoic acid ($C_5H_{10}O_2$) were not detected in the feed or effluent. Thus, 5-ethyl-5-methyl-hydantoin ($C_6H_{10}N_2O_2$) and n-hexadecanoic acid ($C_{16}H_{32}O_2$) were present in the H-FFBR and the suspended biomass. The most abundant organics detected in the biofilm were 3-methyl-2-butenoic acid, followed by 5-ethyl-5-methyl-hydantoin, methyl-isobutyl-hydantoin, n-hexadecanoic acid, substituted hydantoins and traces of long-chain hydrocarbons.

5.1.2 Identification of organic compounds in the effluent by FT-IR

The Fourier transform infrared (FT-IR) absorption spectra of composite effluent samples revealed the presence of various functional groups which correlated with the organic compounds revealed by GC-MS. Absorption peaks were detected at the following wave numbers: 3 401 cm^{-1} (hydroxyl groups -OH); 3 244 cm^{-1} (hydrocarbon C-H); 3 000 cm^{-1} and 2 800 cm^{-1} (C-H stretch aliphatics); 2 926 cm^{-1} (C-H stretch); 2 200 cm^{-1} (cyanate and thiocyanate ions); 1 738 cm^{-1} (ester compounds); 1 716 cm^{-1} (carboxylic acid and ketones); 1 652 cm^{-1} (quinone or conjugated ketone); 1 313 cm^{-1} (aryl alkyl asymmetric groups); 1 264 cm^{-1} (aryl ether structure); 1 050 cm^{-1} (polysaccharide-like or polysaccharides); 800 cm^{-1} (hydrogen bending on an aromatic ring), 756 cm^{-1} (1,2 di-substitution aromatic ring), 651 cm^{-1} (C-O-S stretching); 590 cm^{-1} and 570 cm^{-1} (alkyl derivative stretching) and peaks in the region between 1 200 cm^{-1} and 500 cm^{-1} (combination of hydrocarbons and/or alcohols) (Zhao et al., 2013; Chandralal et al., 2014).

Ramasamy et al. (2014) reported that the extracellular polymeric substance (EPS) layer produced by *Ochrobactrum anthropi* indicated the presence of hydroxyl groups (-OH) at 3 401 cm^{-1}; C-H stretching at 2 926 cm^{-1}; C-H aliphatic stretching between 2 800 cm^{-1} and 3 000 cm^{-1}; and polysaccharide or polysaccharide-like substances at 1 050 cm^{-1}. The FT-IR results revealed the presence of various functional groups, including sulphur-containing groups, cyanates, and possible biomass wash-out which was not detected by the GC-MS analyses. *Ochrobactrum anthropi* are denitrifying and sulphur-oxidising bacteria present in the suspended biomass of the H-FFBR.

5.1.3 Chemical and physical composition of the effluent

The concentration of sulphides, free cyanide, phosphorus and pH of the CGSGL wastewater complied with the minimal national standard (MINAS) for South Africa and the World Bank Group guidelines (Mazema et al., 2008). However, the concentration of chemical oxygen demand (COD), phenol, suspended solids (SS) and ammonia-nitrogen (NH_3-N) did not comply (Table 5.1) with the MINAS standards. The COD, ammonia-nitrogen and phenol concentrations were higher than the Chinese specifications for COD (≤100 mg/L) and ammonia-nitrogen (≤16 mg/L) (Zhou et al., 2012) and the Indian minimum standards for phenol (≤0.5 mg/L) and ammonia-nitrogen (≤50 mg/L) (Kumar and Pal, 2014) for CGSGL wastewater and coking wastewater, respectively.

Free cyanide was not detected above the test method detection limit (0.1 mg/L); however, cyanates were detected by GC-MS and FT-IR, thus indicating the importance of testing samples using different techniques so that as many compounds as possible are identified to gain an understanding of the microbial mechanisms in a complex effluent such as CGSGL wastewater. The presence of cyanates and thiocyanates plays an important role in the removal of ammonium-nitrogen and phenol.

Table 5.1: Chemical and physical composition of the effluent

Analysis	Maximum	Minimum	Average	Standard deviation
Ammonia-nitrogen (mg/L as N)	512	172	285	64
Chemical oxygen demand (mg O_2/L)	977	400	692	186
Chlorides (mg/L as Cl)	158	19	48	13
Conductivity (µS/cm)	9 310	1 470	2 920	192
Cyanide (free) (mg/L as CN)	<0.1	<0.1	<0.1	<0.1
Nitrate-nitrogen (mg/L as NO_3-N)	7.91	4.04	5.41	0.78
Nitrite-nitrogen (mg/L as NO_2-N)	<0.2	<0.2	<0.2	<0.2
o-Phosphate (mg/L as P)	10.2	4.24	6.29	1.11
pH	7.68	7.21	7.50	0.11
Phenols (mg/L)	34	6	15	8.0
Sulphates (mg/L as SO_4)	516	68	443	130

Table 5.1 continued

Analysis	Maximum	Minimum	Average	Standard deviation
Sulphides (mg/L as S^{2-})	<0.50	<0.50	<0.50	<0.50
Suspended solids (mg/L)	460	44	160	140
Temperature (°C)	35.9	37.0	35.9	0.10
TKN (mg/L as N)	730	240	380	90
Total phosphorus (mg/L as P)[(a)]	3.32	1.38	2.05	0.36

[(a)] Determined by calculation: o-Phosphate (mg/L) x 0.3262

5.1.4 Metals in the effluent and effect of metals on biomass activity

The concentration of the heavy metals chromium, iron, copper, nickel, vanadium and lead in the effluent (Table 5.2) complied with the MINAS standard and the World Bank Group guidelines (Mazema et al., 2008). Microorganisms require certain trace metals (zinc, manganese, molybdenum, selenium, copper, cobalt, nickel, vanadium and tungsten) to achieve optimum growth by proper functioning of microbial enzyme systems (Todar, 2006).

Table 5.2: Soluble metals detected in the effluent

Analysis	Maximum	Minimum	Average	Standard deviation
Aluminium (mg/L as Al)	5.60	1.71	2.91	1.67
Calcium (mg/L as Ca)	9.37	0.14	2.84	0.05
Chromium (mg/L as Cr)	<0.001	<0.001	<0.001	<0.001
Cobalt (mg/L as Co)	<0.001	<0.001	<0.001	<0.001
Copper (mg/L as Cu)	<0.001	<0.001	<0.001	<0.001
Iron (mg/L as Fe)	3.62	0.11	0.68	0.12
Lead (mg/L as Pb)	<0.001	<0.001	<0.001	<0.001
Magnesium (mg/L as Mg)	8.28	0.25	1.34	0.38
Manganese (mg/L as Mn)	<0.001	<0.001	<0.001	<0.001
Nickel (mg/L as Ni)	<0.001	<0.001	<0.001	<0.001
Potassium (mg/L as K)	15.2	0.43	1.83	1.12
Silica (mg/L as SiO_2)	31.5	8.61	18.9	4.64
Sodium (mg/L as Na)	18.6	3.10	11.0	2.00
Vanadium (mg/L as V)	0.34	0.11	0.23	0.06
Zinc (mg/L as Zn)	3.14	0.10	0.75	1.34

Skepu (2000) reported that the presence of magnesium, manganese, cobalt and copper reduces the conversion of hydantoins to amino acids by the hydantoinase enzyme and Pozo et al. (2002) stated that the presence of calcium, sodium, cobalt, magnesium, zinc and iron increases the hydantoinase activity of *Ochrobactrum anthropi*. These bacteria were present in the suspended biomass.

According to Defiery and Reddy (2014), metals can increase or decrease the removal of phenols, i.e. magnesium, iron or calcium do not inhibit catechol 1,2-dioxygenase from *Pseudomonas aeruginosa* since they have mechanisms to counteract metal-induced stress such as sequestration, reduction and direct flux of the metal out of the cell. *Pseudomonas aeruginosa* was present in the H-FFBR. However, the production of catechol 1,2-dioxygenase by *Rhodococcus* spp. is inhibited by iron, copper and mercury.

5.2 Attached biomass and suspended biomass

The impact of the CGSGL wastewater characteristics on the acclimatised suspended biomass and fixed biomass (biofilm) properties, structure and activity is revealed in this section. Knowledge of the CGSGL wastewater characteristics is of significance since the microbial diversity plays an important role in the removal of COD, ammonia-nitrogen and phenols in the H-FFBR.

5.2.1 Attached biomass activity versus suspended biomass activity

The average values (22 samples per aeration zone) for the biofilm thickness were 51.45 ± 40.3 µm, 6.19 ± 3.09 µm and 6.61 ± 4.13 µm for the respective aeration zones (Table 5.3). The differences in biofilm thickness across the aeration zones were significant (p<0.001; α=0.05) (Figures B-1 and B-2 in Appendix B). The average values (13 samples per aeration zone) for the fixed biomass activity were 62.58 ± 15.56 (mg O_2/L.h), 33.80 ± 8.07 (mg O_2/L.h) and 33.71 ± 10.65 (mg O_2/L.h) for the respective aeration zones. The differences across the aeration zones were significant (p<0.001; α=0.05) (Figures B-3 and B-4 in Appendix B). The average values (13 samples per aeration zone) for the suspended biomass activity were 48.47 ± 14.98 (mg O_2/L.h), 37.48 ± 16.45 (mg O_2/L.h) and 37.48 ± 13.76 (mg O_2/L.h) for the respective aeration zones (Table 5.3). The differences across the aeration zones were not significant (p=0.116; α=0.05) (Figures B-5 and B-6 in Appendix B). The average values (60 samples per aeration

zone) for the DO were 3.91 ± 0.75 mg/L, 4.95 ± 0.48 mg/L and 4.86 ± 0.45 mg/L for the respective aeration zones (Table 5.3). The difference across the aeration zones was significant (p=0.001; α=0.05) (Figures B-7 and B-8 in Appendix B). The average values (60 samples per aeration zone) for pH were 7.42 ± 0.18, 7.50 ± 0.18 and 7.50 ± 0.15 for the respective zones. The difference across the aeration zones was not significant (p=0.250; α=0.05).

Table 5.3: Biomass thickness and biomass activity for each aeration zone in the reactor

Parameter	Biofilm thickness (µm)	OUR fixed film (mg O_2/L.h)	OUR suspended biomass (mg O_2/L.h)	DO (mg/L)
Zone 1 (70% carrier fill)				
Average	51.5	62.58	48.47	3.91
Maximum	213	76.88	68.56	5.54
Minimum	1.79	27.66	19.66	2.23
Std dev	40.3	15.63	14.98	0.75
Zone 2 (50% carrier fill)				
Average	6.19	33.80	37.08	4.95
Maximum	13.6	43.90	67.90	6.20
Minimum	0.46	18.32	14.70	3.60
Std dev	3.09	8.07	16.45	0.48
Zone 3 (30% carrier fill)				
Average	6.61	37.48	37.48	4.86
Maximum	24.0	51.46	59.64	6.03
Minimum	1.45	14.72	11.98	3.75
Std dev	4.13	10.65	13.76	0.45

The results revealed a relationship between the percentage carrier fill, biofilm thickness, biomass oxygen uptake rate (OUR) and dissolved oxygen (aeration). Higher aeration rates increase the mixing energy of the carrier (roll pattern), resulting in higher shear across the biofilm layer which influences the biofilm thickness, microbial population and growth rate. The mixing energy provided by the aeration is critical for sloughing off the biomass and the formation of a thin biofilm yielding higher kinetic rates due to a larger surface area for substrate

penetration. Thin biofilms (<50 µm; Torresi et al., 2016) increase the available surface area and reduce the variability of solids discharge due to sloughing (Goode, 2010).

5.2.2 Biofilm structure

Energy-dispersive X-ray (EDX) analyses of the respective biofilm layers revealed the presence of carbon, oxygen, sodium, aluminium, silicon, phosphorus, sulphur, chloride, potassium, calcium, nitrogen, copper and iron for all three aeration zones. The presence of aluminium, silicon, calcium and iron was highest in Zone 1; nitrogen, oxygen, sodium, magnesium, potassium and chlorides were highest in Zone 2; while carbon, phosphorus and copper were highest in Zone 3. The EDX analyses revealed that copper was the only metal bound to the biofilms in Zone 1 and Zone 3 (Table 5.4, Figure 5.1, Figure 5.2, Figure 5.3).

Table 5.4: List of elements identified in the respective biofilm layers

Element	Zone 1 (% by weight)	Zone 2 (% by weight)	Zone 3 (% by weight)
Carbon	67.74	66.22	68.38
Nitrogen	<0.1	0.88	0.62
Oxygen	24.66	25.70	25.01
Sodium	0.17	0.47	0.22
Magnesium	0.10	0.19	0.01
Aluminium	0.42	0.24	0.22
Silicon	0.41	0.10	0.22
Phosphorus	0.24	0.21	0.28
Sulphur	4.79	4.86	4.23
Chloride	0.10	0.37	0.16
Potassium	0.12	0.21	0.15
Calcium	0.36	0.22	0.22
Iron	0.85	0.55	0.40
Copper	0.13	0	0.20

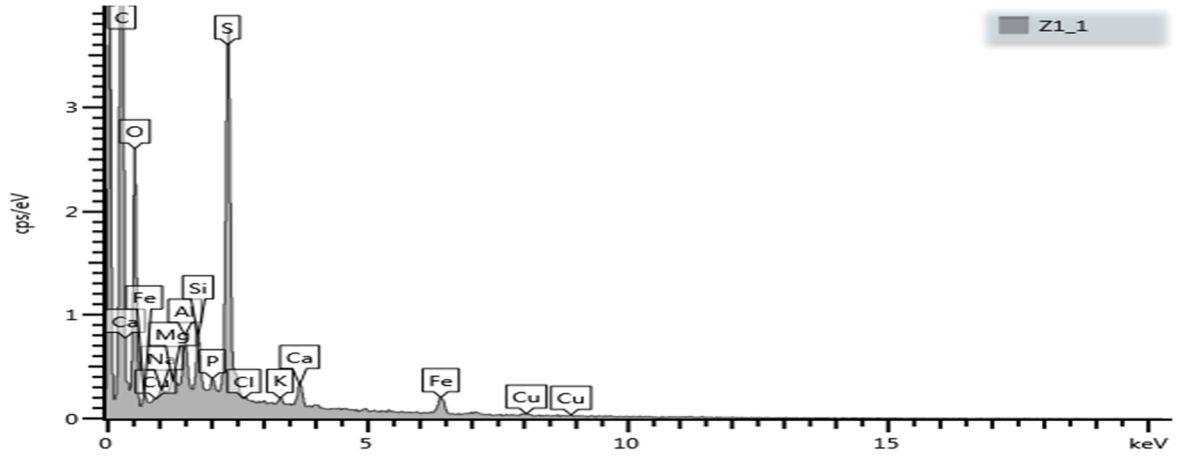

Figure 5.1: EDX of the fixed biofilm in aeration Zone 1 during the operation of the H-FFBR

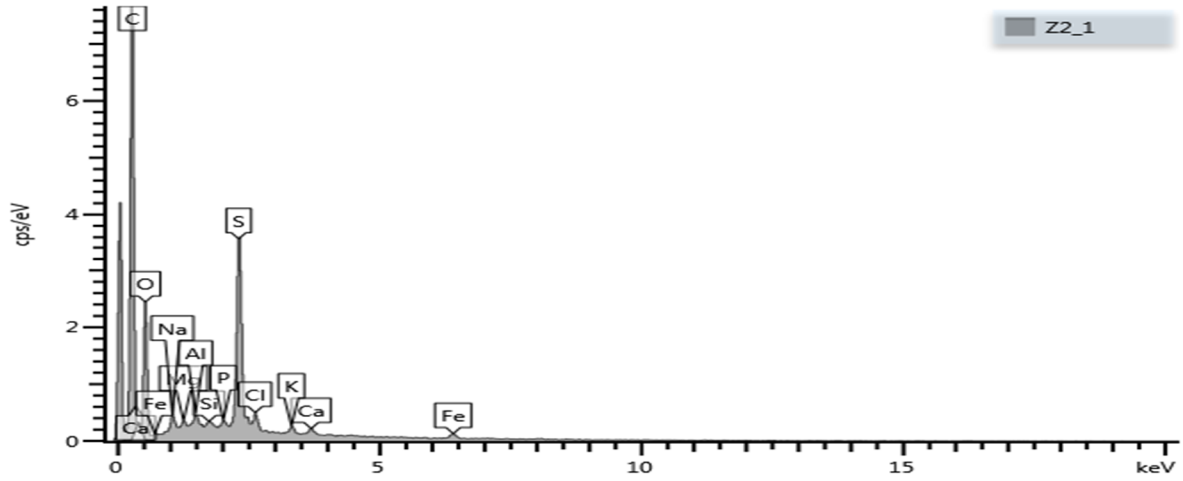

Figure 5.2: EDX of the fixed biofilm in aeration Zone 2 during the operation of the H-FFBR

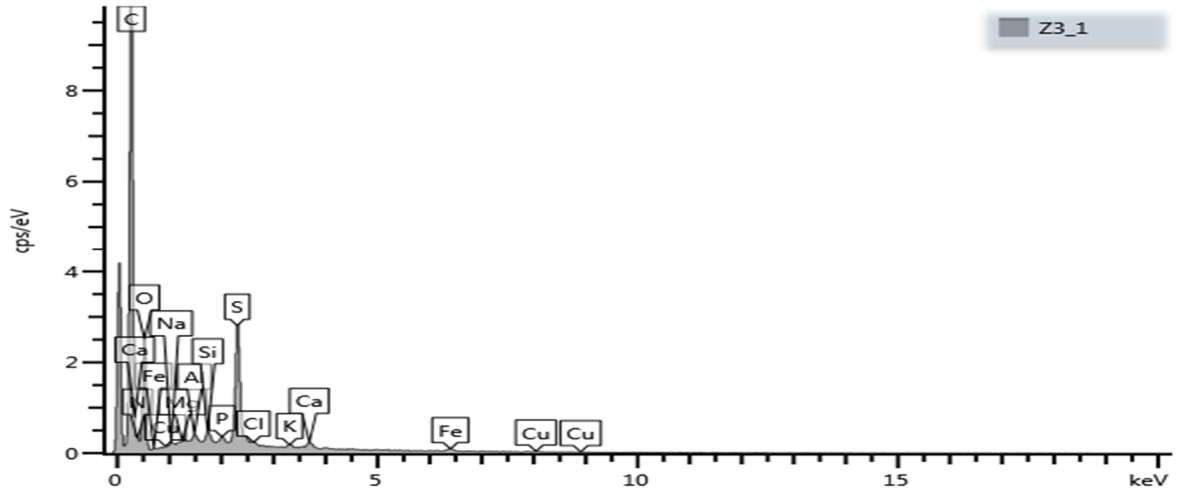

Figure 5.3: EDX of the fixed biofilm in aeration Zone 3 during the operation of the H-FFBR

The effect of metals on the biofilm structure is summarised as follows:

- Silicon and aluminium increase biomass resistance to toxic shocks and the presence of iron, sulphur and copper contribute to the aggregation of biomass (Annachhatre and Bhamidimarri, 1992).
- Potassium, magnesium, sodium and calcium are required for membrane stabilisation and are enzyme activators (Revanuru and Mishra, 2011).
- Potassium is also required for osmotic balance, sodium for cell integrity and transport across the membrane, iron for an energy source and heme-containing enzymes and proteins, cobalt for co-enzymes, manganese for transferring phosphate groups and molybdenum for nitrogenase (Hu et al., 2013).
- Calcium and phosphorus are absorbed by and accumulate in the biofilm as insoluble compounds, rendering the biofilm highly resistant to detachment by maintaining the intercellular polymer matrix structure (Goode, 2010).
- Sulphur is required for protein synthesis, phosphorus for nucleic acids and metabolic cofactors, and nitrogen for proteins, some sugars and nucleic acids (Todar, 2006; Rava and Chirwa, 2016).

Scanning electron microscopy (SEM) analyses of the biofilm from the respective aeration zones revealed the biofilm structure to be relatively uniform and dense for Zone 1 (Figure 5.4), ripple-like for Zone 2 (Figure 5.5) and porous for Zone 3 (Figure 5.6). Thus, the elements bound to the biofilm have an effect on the biofilm structure. This effect was also reported by Lembre et al. (2012) and Ward and King (2012).

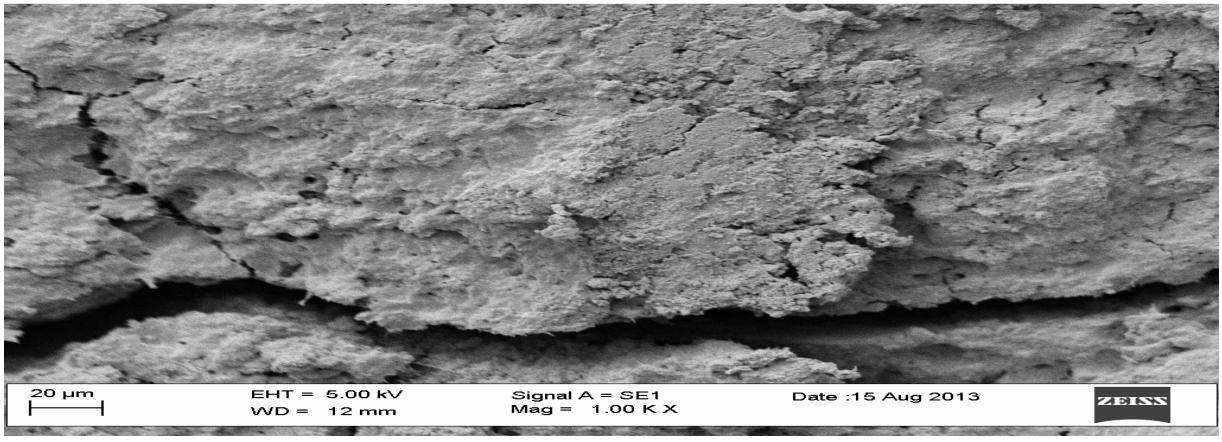

Figure 5.4: SEM image of the dense biofilm on the carriers taken from aeration Zone 1

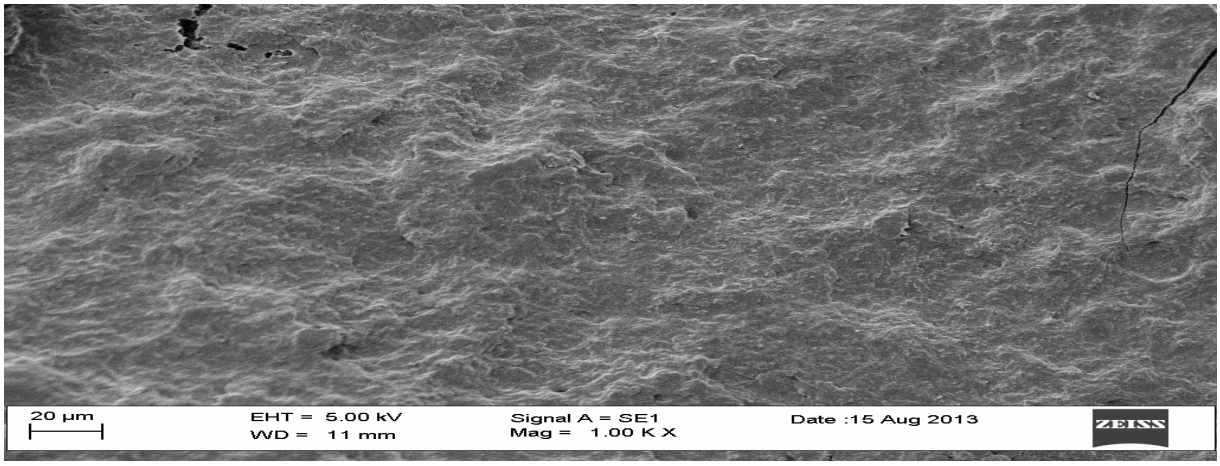

Figure 5.5: SEM image of the ripple-like biofilm on carriers taken from aeration Zone 2

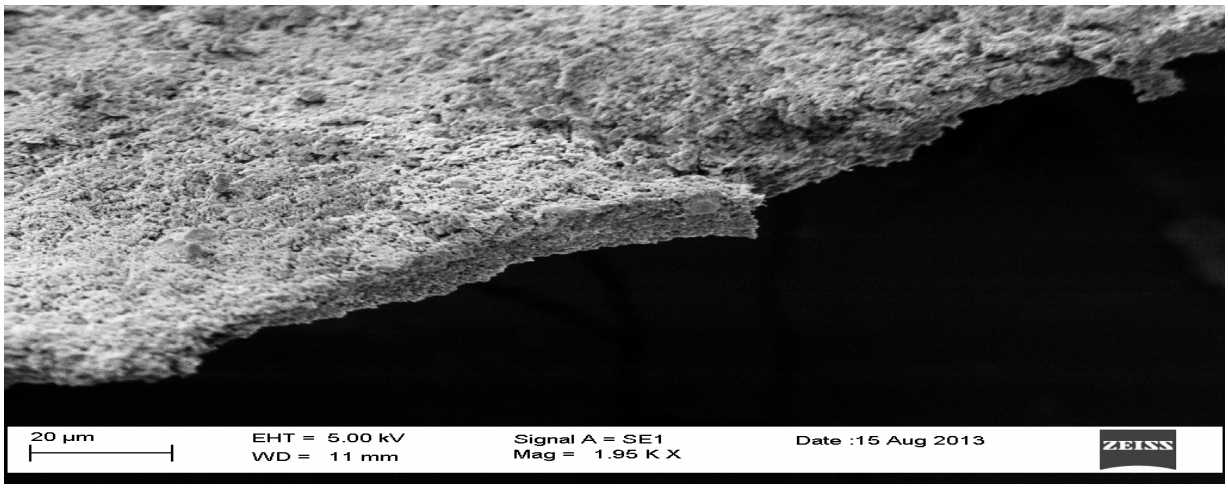

Figure 5.6: SEM image of the porous biofilm on carriers taken from aeration Zone 3

Bioreactor hydrodynamics and biofilm characteristics influence the performance of the H-FFBR. Thus, the control of the biofilm properties is important for a stable bioreactor performance since the biofilm controls the rate of mass transfer of nutrients and substrate to the microbial community.

5.3 Performance of the H-FFBR in removing pollutants

The performance of the H-FFBR was measured in terms of phenol, COD and ammonia-nitrogen removal. The H-FFBR was continuously fed real-time CGSGL wastewater directly from the plant. Thus, the acclimatised microbial communities were exposed to varying physical, chemical and organic characteristics of the wastewater.

5.3.1 Removal of phenols

The phenol concentration (Figure 5.7) of 60 feed samples ranged between 40 mg/L and 90 mg/L with an average of 70 ± 20 mg/L. The phenol concentration of 60 effluent samples ranged between 6 mg/L and 34 mg/L with an average of 15 ± 9 mg/L. The removal of phenols ranged between 62% and 93% with an average of 79%, thus 21% of the total phenols were soluble, but not readily degradable. The performance of the H-FFBR in terms of phenol removal was lower than 83% (pH 7.2; 30 ºC) and 95% (pH 6.8-7.5; 30 ºC) reported by Chakraborty et al. (2010) and Crutescu et al. (2008), respectively, when treating similar coal gasification wastewaters. The degradation of phenols is influenced by factors such as pH, temperature, biodegradation kinetics, microbial diversity and metabolic potential and nutrients.

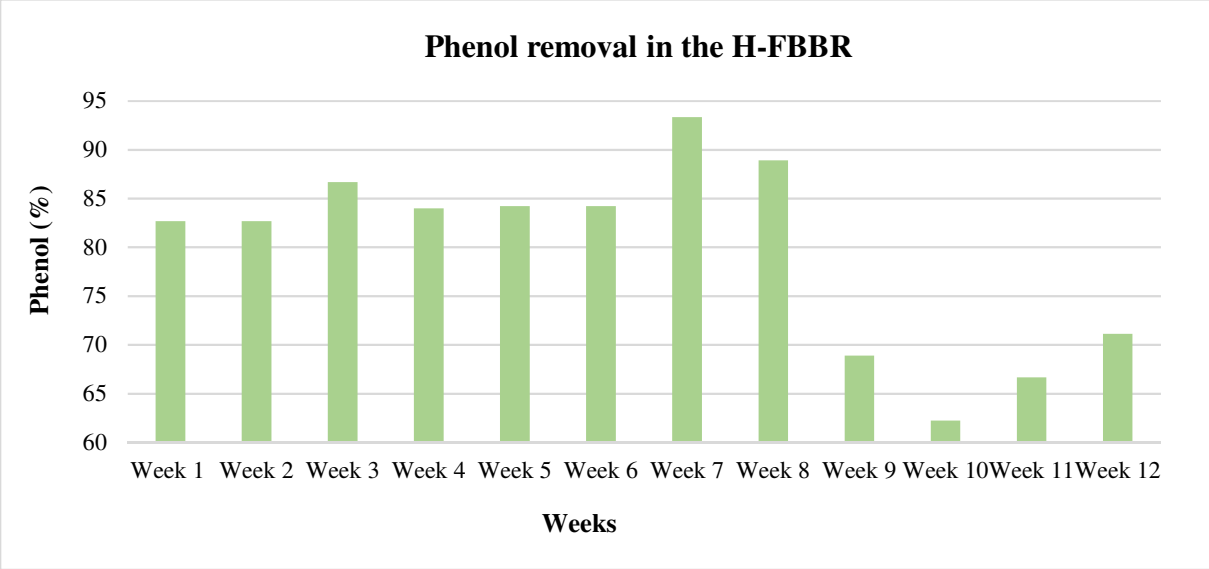

Figure 5.7: Removal of phenol in the H-FFBR without bioaugmentation (Week 1 to Week 12)

The degradation rate depends on the structure and the number of substituents on the aromatic nucleus and the positions of the methyl groups. The *para*-substituted phenols are more readily degradable than the *meta*- or the *ortho*-substituted phenols because they are weaker electron donors (lower oxidation state) (Adabju, 2013; Rava et al., 2015).

5.3.2 Removal of soluble COD

The COD concentration (Figure 5.8) of 60 feed samples ranged between 1 718 mg/L and 1 900 mg/L with an average of 1 710 ± 60 mg/L. The COD concentration of 60 effluent samples ranged between 400 mg/L and 977 mg/L with an average of 940 ± 70 mg/L. The removal of

COD ranged between 37% and 55% with an average of 45%, thus 55% of the COD was not readily degradable. The removal of COD was in the range (40% to 60%) reported by Galil et al. (1988) for coal gasification wastewater.

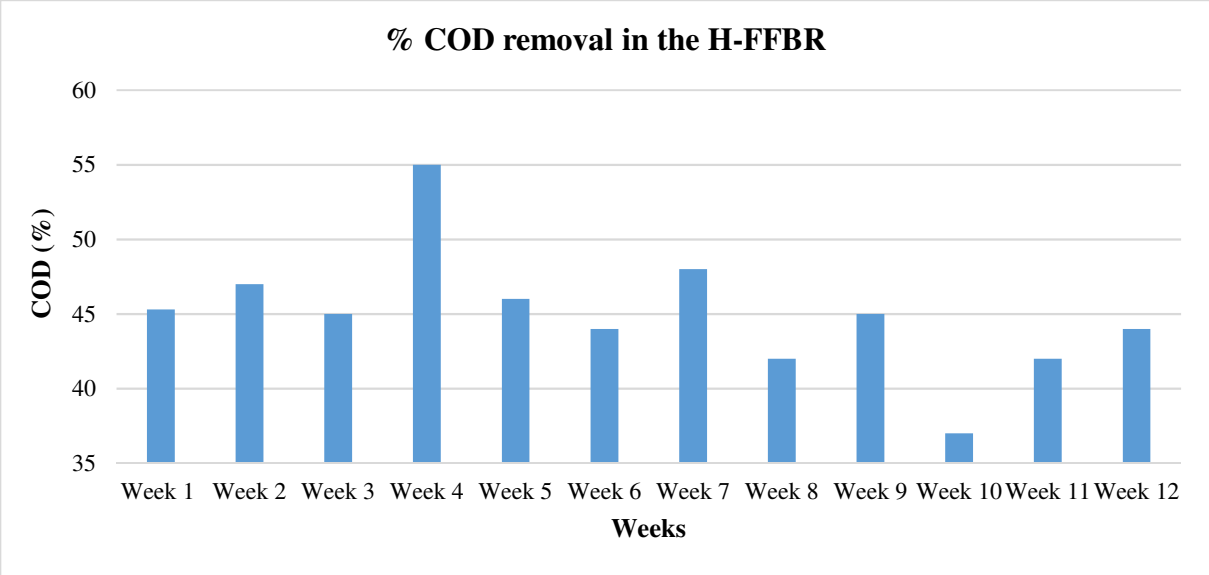

Figure 5.8: Removal of COD in the H-FFBR without bioaugmentation (Week 1 to Week 12)

The results also revealed (Table 5.5) that 60% of the feed COD was degraded in Zone 1, 27% of the COD not degraded in Zone 1 was degraded in Zone 2 and 30% of the COD not degraded in Zone 2 was degraded in Zone 3. Thus, the most biodegradable COD fraction was biodegraded in Zone 1. The biomass attached to the carriers in the respective aeration zones were higher than reported by Aygun et al. (2008), the ratio of attached biomass (98%) across the H-FFBR was higher than 90% reported by Makowaska et al. (2013) and 93% reported by Plattes et al. (2006) for the treatment of municipal wastewater in a H-FFBR. Toerien and van Niekerk (2013) reported the attached biomass age for the H-FFBR used in this study to be approximately 126 d which is in line with the biomass age (>100 d) reported by Makowska et al. (2013).

Table 5.5: COD removal performance profile across the H-FFBR

COD parameters	Zone 1	Zone 2	Zone 3	Average
Attached biomass (g TSS/m^2)	470	70	110	216
COD loading rate (g COD/m^2.d)	25	1.8	5.8	10.8
COD removal rate (g COD/m^2.d)	15 (60%)	0.5 (27%)	1.7 (30%)	5.73
COD removal rate (g COD/g TSS.d)	0.032	0.007	0.015	0.018

The characteristics of the CGSGL wastewater, microbial diversity, aeration rate, biofilm thickness, biofilm structure and carrier fill had an effect on the COD loading and removal rates in the respective aeration zones. The rate of COD removal decreased as the concentration of the biodegradable organics decreased in the H-FFBR (Zachopoulos and Hung, 1990) which is typical for microbial degradation of mixed substrates (Donaldson et al., 1987). A slower growing porous biofilm such as in Zone 3 has a higher specific activity than the biofilms in Zone 2 and Zone 3 (Wijeyekoon et al., 2004).

5.3.3 Removal of nitrogen

The removal of ammonia-nitrogen ranged between 2% and 46% with an average of 15% for 58% of the samples (26/45) and increased between 13% and 97% with an average of 24% for 42% of the samples (19/45) (Figure 5.9). The removal of nitrate-nitrogen ranged between 1% and 38% with an average of 15% for 55% of the samples (25/45) and increased between 16% and 69% with an average of 18% for 45% of the samples (20/45) (Figure 5.9).

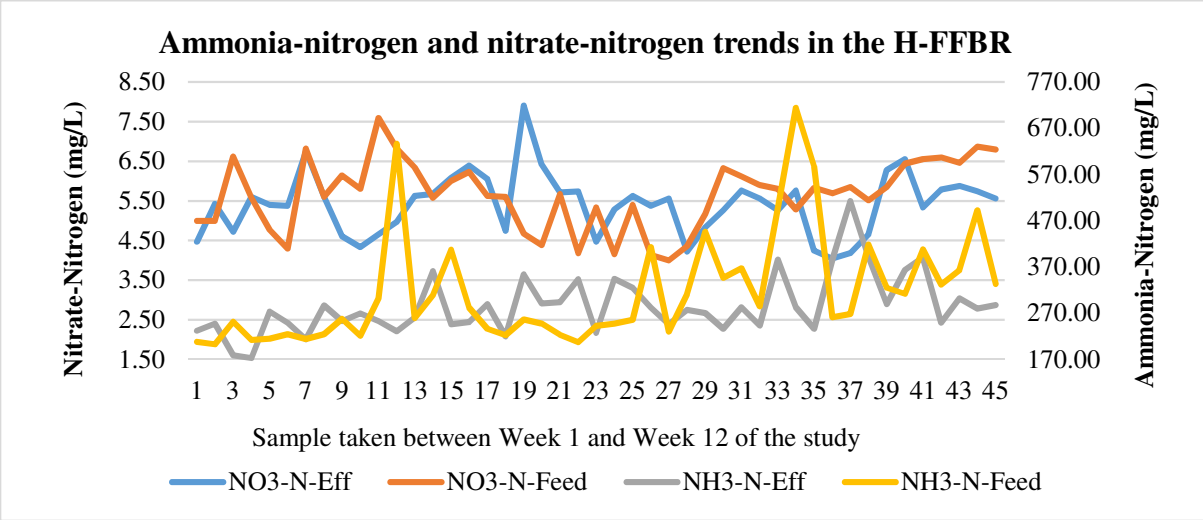

Figure 5.9: Ammonia-nitrogen and nitrate nitrogen trends for the feed and effluent samples

There was no significant difference between the feed and effluent ammonia-nitrogen (p=0.123; α=0.05) and between the feed and effluent nitrate nitrogen (p=0.151; α=0.05). Ammonia-nitrogen and nitrate-nitrogen spikes were observed in 26% of the effluent samples thus indicating aerobic degradation of organic nitrogenous compounds (Table A-1 in Appendix A) by members belonging to the genus *Pseudomonas* (Katayama et al., 1992). *Pseudomonas aeruginosa*, *Pseudomonas putida* and *Pseudomonas stutzeri* were present (culturable isolation

technique; 10^5-10^6 cfu/mL) in the H-FFBR biomass. Metagenomic (non-culturable isolation technique) studies also indicated the presence of numerous *Pseudomonas* species in the H-FFBR biomass. The TKN required for biological growth was 54 mg/L (Table 5.6).

Table: 5.6: Soluble nitrogen levels in the feed and effluent (Week 1 to Week 12)

Parameters	NO_3-N Feed (mg/L)	NO_3-N Effluent (mg/L)	NH_3-N Feed (mg/L)	NH_3-N Effluent (mg/L)	TKN Feed (mg/L)	TKN Effluent (mg/L)
Average	5.66	5.41	317	285	434	380
Maximum	7.59	7.91	714	512	971	730
Minimum	4.00	4.04	202	172	243	240
Std dev	0.87	0.78	110	64	85	90
No. samples	45	45	45	45	45	45

NO_2-N: <0.2 mg/L; TON = TKN – NH_3-N; TN = TKN+NO_3-N+ NO_2-N; TKN = NH_3-N+ TON

The relatively high organic substrate concentration (C/N ratio, >1.5) (Ji et al., 2015a) resulted in a competition between the fast-growing heterotrophs and the slower growing nitrifying bacteria for nutrients, thus influencing the microbial community diversity, biofilm composition, biofilm thickness and oxygen gradient in the biofilm. Ammonia-oxidising bacteria (*Nitrosomonas* spp.) and nitrite-oxidising bacteria (*Nitrobacter* spp.) are required for the nitrification process to take place (Ma et al., 2015). However, *Nitrosomonas* and *Nitrobacter* were not detected, by culturable and non-culturable isolation techniques, in the biomass. Oxidation of hydantoins occurs simultaneously during the nitrification process by the symbiotic relationship between *Nitrobacter* spp. and *Arthrobacter* spp. (Mazumder, 2010). Degradation of ammonia-nitrogen and hydantoins will result in an increase in nitrates and the degradation of nitrates will result in an increase in nitrites (Turner and Wernberg, 1985). No significant changes in nitrite, nitrates and ammonia-nitrogen levels were detected.

5.3.4 Nutrient uptake

The average (45 samples) ammonia-nitrogen concentration was 317 ± 110 mg/L and 285 ± 64 mg/L in the feed and effluent, respectively. A nutrient (BOD_5:N:P) ratio of 100:5:1 is used as a benchmark for nutrient addition in nutrient-limited wastewaters (Slade et al., 2011) and 100:15:3 to 120:10:1 for biodegradation of aromatic compounds (Bamforth and Singleton,

2005). The CGSGL wastewater ratio was 100:31:2 and the biodegradability (BOD_5/COD; >0.35) ratio was 0.56. Thus, nutrients were available and the wastewater was biodegradable (Sarkar and Mazumder, 2015). The average (36 samples) total phosphorus (TP) concentrations in the feed and effluent were 24.8 ± 4.32 mg/L and 2.04 ± 0.36 mg/L, respectively. Cells saturated with phosphorus have a higher tendency to flocculate and to adhere due to their increased hydrophobicity. Cells with lower phosphorus levels are more hydrophilic and have a lower tendency to flocculate and adhere (Annachhatre and Bhamidimarri, 1992). Thus, this will affect biofilm formation (adherence) and dispersion (adhesion) of suspended biomass.

The H-FFBR was not deficient in nutrients such as ammonia-nitrogen (NH_3-N) and total phosphorus (TP). Ammonia-oxidising bacteria (AOB) and nitrate-oxidising bacteria (NOB) were absent from the fixed biomass (biofilm), suspended biomass, effluent and feed samples due to competition for nutrients by the faster growing heterotrophic bacteria such as *Pseudomonas* spp. Toerien and van Niekerk (2013) reported the nitrogen content in the waste activated sludge (WAS), from the H-FFBR used in this study, to be 9.6% higher than typical values found in conventional wastewater treatment plants. The relatively high nitrogen concentration in the waste was most probably due to the low concentration of suspended solids and associated less biodegradable nitrogen compounds in the effluent returning to the reactor (RAS). Thus, improved settling in the clarifier will allow for greater removal of waste sludge thus reducing the return of particulate slowly biodegradable nitrogenous compounds (Rava et al., 2016).

CHAPTER 6
BIOAUGMENTATION OF THE H-FFBR FOR THE REMOVAL OF COD AND PHENOLS

6.1 Microbial community and degradation of organic compounds in the H-FFBR

The bacterial species to be used for bioaugmentation were selected from the γ-Proteobacteria (*Enterobacter* and *Pseudomonas*) and the Actinobacteria (*Rhodococcus*) class of bacteria based on the indigenous microbial community revealed in Chapter 4 and the composition of the CGSGL wastewater revealed in Chapter 5. A mixed microbial community increases the degradation rate of pollutants since the genetic information of more than one microorganism is required to degrade complex effluents (Tzirita, 2012) such as CGSGL wastewater. This study reveals the identity of the bioaugmented microbial communities to species level and their respective performance in the removal of COD and phenol to meet effluent discharge criteria.

6.2 Mixed microbial community across the H-FFBR during bioaugmentation

Culture-dependent techniques identified the presence of *Aeromonas hydrophila*, *Bacillus cereus*, *Burkholderia cepacia*, *Pseudomonas putida*, *Pseudomonas aeruginosa* and *Pseudomonas stutzeri* in the indigenous microbial community and *Bacillus amyloliquefaciens, Bacillus pumilus, Bacillus subtilis* and *Pseudomonas monteilii* in the bioaugmented microbial communities. Thus, the bioaugmented microbial community in the H-FFBR included algae, diatoms, Archaea and different classes of bacteria belonging to the α-Proteobacteria, β-Proteobacteria, γ-Proteobacteria and Actinobacteria.

All the above-mentioned bacteria are aerobic mesophilic Gram-negative except for *Bacillus* spp. (spore-forming) and *Rhodococcus* spp. (non-spore-forming) which are Gram-positive. *Pseudomonas putida*, *Bacillus pumilus* and *Bacillus subtilis* cleave the aromatic nucleus via the *meta*-pathway, while *Pseudomonas stutzeri, Actinobacillus* spp. and *Rhodococcus* spp. cleave the aromatic nucleus via the *ortho*-pathway. Ring fission via the *ortho*-pathway is plasmid encoded and slower than via the *meta*-pathway which is chromosomally encoded (Ambujom, 2001).

6.2.1 16S rRNA and 18S rRNA PCR sequencing of the bioaugmented microbial communities

Commercially formulated microbial products designed to degrade a wide range of aliphatic and aromatic compounds in aerobic biological wastewater treatment systems contain a range of non-pathogenic microorganisms including members of the genera *Aeromonas, Bacillus*, *Pseudomonas, Rhodococcus* (Mulcahy, 1993) and *Enterobacter* spp. (Hesnawi et al., 2014). The bacteria and seaweed in the respective bioaugmentation inocula used in this study were identified to species level.

6.2.2 Inoculum PA1

The complete genome sequencing producing significant alignments are presented in Table 6.1 and the phylogenetic tree in Figure 6.1. The bacterial BLAST nucleotides were >99% homologous to three strains of *Pseudomonas putida*, two strains of *Enterobacter cloacae*, one strain of *Enterobacter asburiae* and one strain of *Rhodococcus erythropolis*.

Table 6.1: Bacterial species and strains identified in the bioaugmentation inoculum PA1

Clone number	Predicted bacteria	GenBank number
1	*Pseudomonas putida* strain ppnb1	FJ545651.1
2	*Enterobacter cloacae* strain ECNIH 4	CP009850.1
3	*Enterobacter cloacae* strain SB 3013	GU191924.1
4, 5, 7	*Enterobacter asburiae* strain 35734	CP012162.1
6	*Rhodococcus erythropolis* strain BG43	CP011295.1
8, 9	*Pseudomonas putida* strain POXNO1	KC189961.1
10	*Pseudomonas putida*	JX514408.1

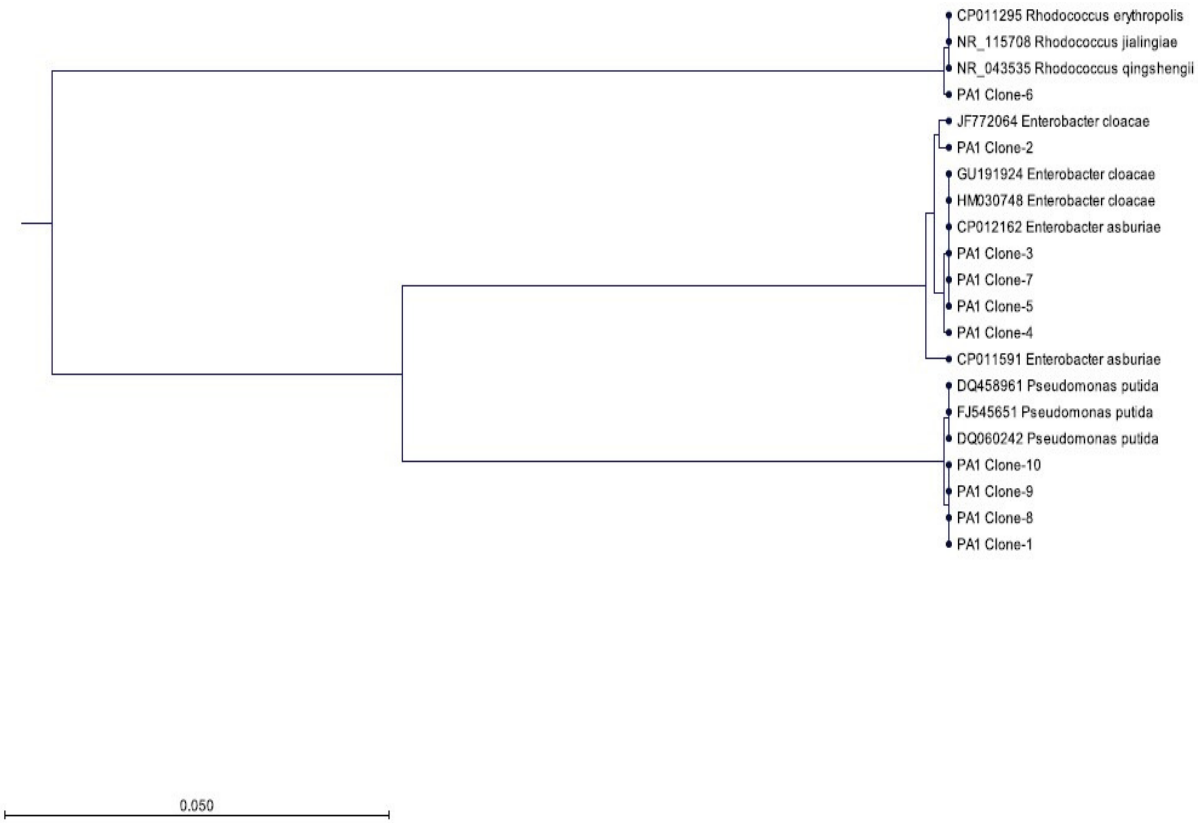

Figure 6.1: Phylogenetic tree for inoculum PA1. The scale bar (0.050) represents evolutionary distance.

6.2.3 Inoculum PA2

Complete genome sequencing producing significant alignments are presented in Table 6.2 and the phylogenetic tree in Figure 6.2. The bacterial BLAST nucleotides were >99% homologous to six different strains of *Pseudomonas putida.*

Table 6.2: Bacterial species and strains identified in the bioaugmentation inoculum PA2

Clone number	Predicted bacteria	GenBank number
1, 2, 4	*Pseudomonas putida* strain CDd-9	GU248219.1
3, 6, 10	*Pseudomonas putida* strain POXNO1	KC189961.1
5	*Pseudomonas putida*	CP010979.1
7	*Pseudomonas putida* strain L1-5	GU354317.1
8	*Pseudomonas putida* strain W619	CP000949.1
9	*Pseudomonas putida*	DQ060242.1

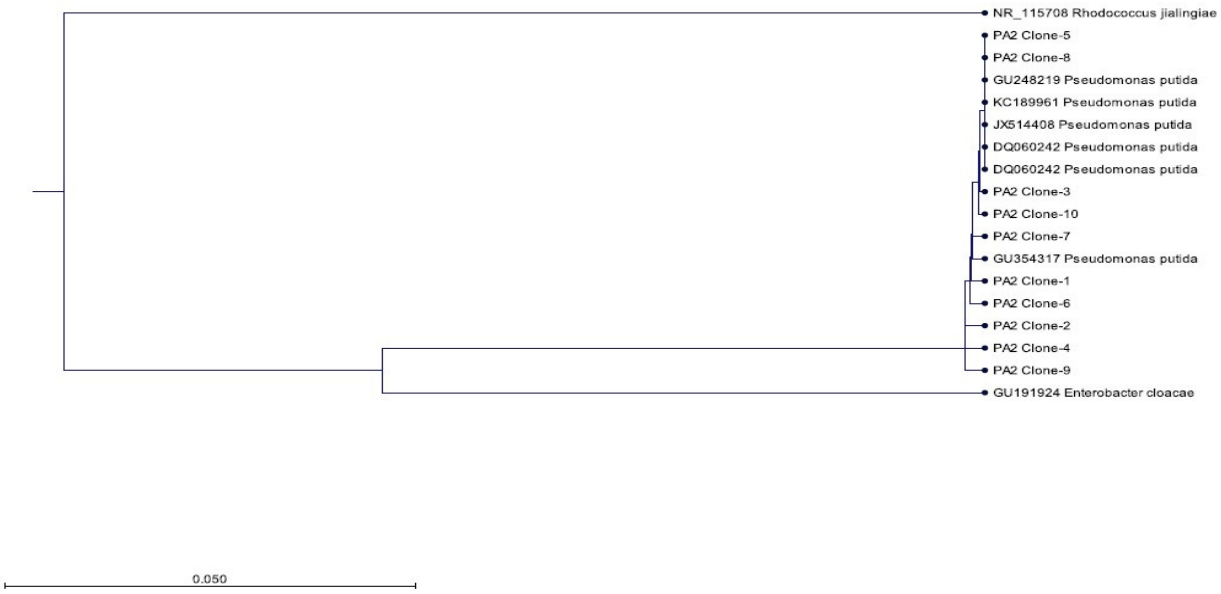

Figure 6.2: Phylogenetic tree for inoculum PA2. The scale bar (0.05) represents evolutionary distance.

6.2.4 Inoculum PA3

Complete genome sequencing producing significant alignments are presented in Table 6.3 and the phylogenetic tree in Figure 6.3. The bacterial BLAST nucleotides were >99% homologous to three strains of *Pseudomonas plecoglossicida*, five strains of *Pseudomonas putida*, one strain of *Enterobacter cloacae*, and one strain of *Rhodococcus qingshengii*.

Table 6.3: Bacterial species and strains identified in the bioaugmentation inoculum PA3

Clone number	Predicted bacteria	GenBank number
1	*Pseudomonas plecoglossicida*	AY972168.1
2, 6	*Pseudomonas putida* strain S6	HG421014.1
3	*Enterobacter cloacae* strain ECNH4	CP009850.1
4	*Pseudomonas plecoglossicida*	NR_024662.1
5	*Rhodococcus qingshengii*	KM873626.1
7	*Pseudomonas putida* strain CDd-9	GU248219.1
8	*Pseudomonas putida* strain POXNO1	KC189961.1
9	*Pseudomonas plecoglossicida* strain NyZ12	CP010359.1
10	*Pseudomonas putida*	KC93469.1

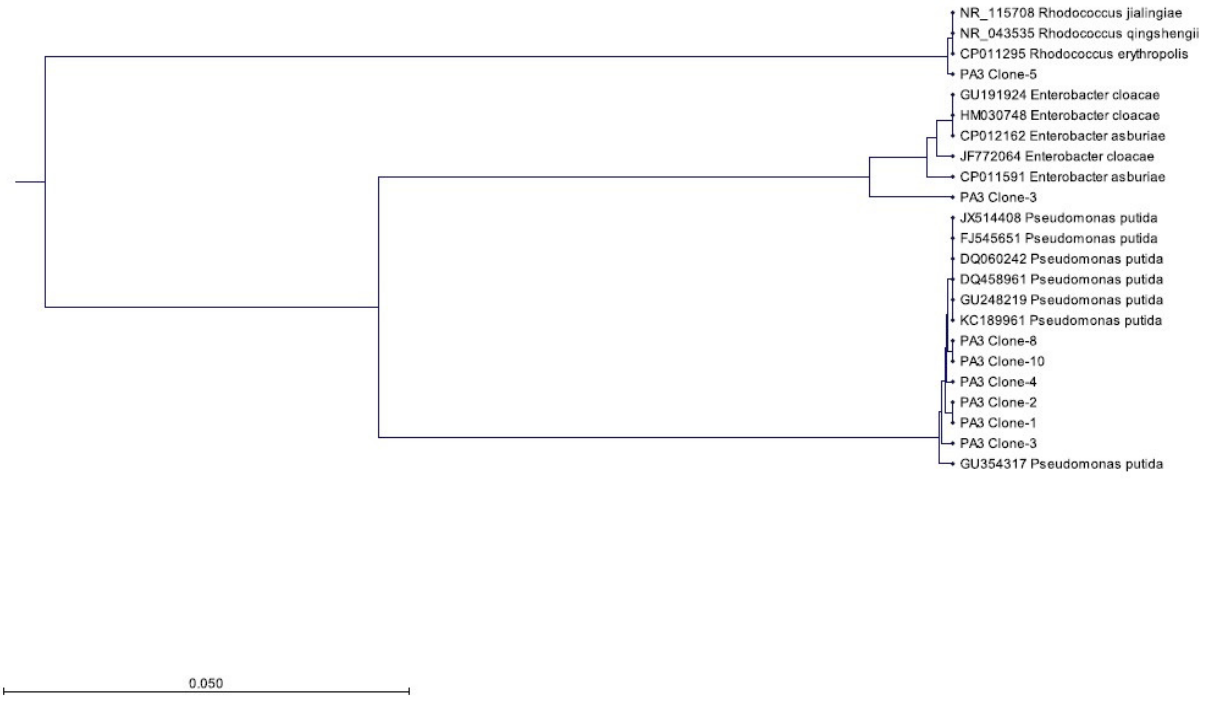

Figure 6.3: Phylogenetic tree for inoculum PA3. The scale bar (0.050) represents evolutionary distance.

6.2.5 Inoculum PA4

Complete genome sequencing producing significant alignments are presented in the phylogenetic tree (Figure C-1 in Appendix C). The BLAST nucleotides were >99% homologous to the seaweed *Silvetia siliquosa* (GQ433994). Microscopic observations of inoculum PA4 indicated the presence of the marine diatoms *Cocconeis* and *Nitzschia*. The hypothesis was that the diatoms and the seaweed (<50 µm particle size) would assist with the settling of suspended solids in the clarifier.

6.2.6 EDX analysis of the bioaugmentation inocula

The bacteria selected for the various bioaugmentation inocula were immobilised (adsorbed) on carrier material (so-called immobilised bioaugmentation). A cereal bran was used as carrier material; the carrier acts as a secondary carbon source, as it contains surfactants (Mulcahy, 1993) enzymes and specific nutrients and buffers to assist with the rapid growth of the respective bioaugmentation inocula in the H-FFBR (Tzirita, 2012). The inert material identified to be present in the respective bioaugmentation inocula PA1, PA2 and PA3 (Figures C-2, C-3

and C-4 in Appendix C) were carbon and oxygen which form part of the cereal bran carrier. All the bioaugmentation inocula contained potassium, aluminium and titanium. Phosphorus was only present in inocula PA2 and PA3. Inoculum PA4 (Figure C-5 in Appendix C) contained calcium, bromine, magnesium, iron, sodium and higher concentrations of oxygen and silicon due to the presence of the diatoms (SiO_2) (Table 6.4).

Table 6.4: Average EDX values of the elements identified in the bioaugmentation inocula

Element (% dry weight)	PA1	PA2	PA3	PA4
Carbon	39.36	66.9	60.25	0.74
Oxygen	54.98	23.26	38.03	40.51
Phosphorus	0	1.85	0.55	0
Potassium	5.66	4.32	1.22	3.26
Magnesium	0	0	0	2.76
Calcium	0	0	0	3.12
Iron	0	0	0	15.92
Bromine	0	0	0	5.39
Silicon	0	0	0	21.62
Sodium	0	0	0	2.07
Aluminium	3.25	2.69	2.34	3.55
Titanium	2.12	0.55	6.68	1.79

Samples were analysed in triplicate (N=3)

6.3 Removal of COD

The COD removal increased by 8% (45% to 53%) (Table 6.5, Figure 6.4) with the addition of inocula PA1 and PA4 which contained various strains of *Pseudomonas putida*, *Enterobacter* spp. and *Rhodococcus erythropolis*; increased by 13% (53% to 66%) with the addition of inocula PA2 and PA4 which included different strains of *Pseudomonas putida;* and increased by 7% (66% to 73%) with the addition of inocula PA3 and PA4 which included different strains of *Pseudomonas putida, Pseudomonas plecoglossicida* and *Rhodococcus qingshengii*. The increase in COD removal for each inoculum phase was significant ($p<0.001$; $\alpha=0.05$) when compared to the baseline value (Figures C-6 and C-7 in Appendix C). The combination of inocula PA1, PA2, PA3 and PA4 increased the removal of COD by a total of 28% of which

inocula PA2 and PA4 contributed 13%. The removal of organics more complex than phenol (COD_{phenol}/COD_{Total}) increased after each inoculation

Table 6.5: Soluble COD and phenol in the feed and effluent

Parameter	Pre-treatment[(a)]	PA1 and PA4[(a)]	PA1, PA2 and PA4[(a)]	PA1, PA2, PA3 and PA4[(a)]	Post-treatment[(a)]
Feed COD (mg/L)	1 710 ± 60	1 750 ± 20	1 690 ± 40	1 720 ± 70	1 750 ± 50
Effluent COD (mg/L)	940 ± 70	810 ± 80	570 ± 40	480 ± 40	870 ± 70
% COD removal	45 ± 4	53 ± 4	66 ± 5	73 ± 2	62 ± 12
Feed phenol (mg/L)	70 ± 20	75 ± 20	78 ± 15	73 ± 10	72 ±5
Effluent phenol (mg/L)	15 ± 9	14 ± 4	13 ± 8	14 ± 4	11 ± 2
% Phenols removal	79 ± 9	73 ± 7	77 ± 11	82 ± 5	78 ± 4
COD_{phenol}[(b)]/$COD_{Soluble}$	0.038	0.041	0.054	0.069	0.030

[(a)]Average value per treatment phase ± standard deviation (Week 1 to Week 65 of the study)

[(b)]COD_{phenol} = phenol (mg/L) x 2.38

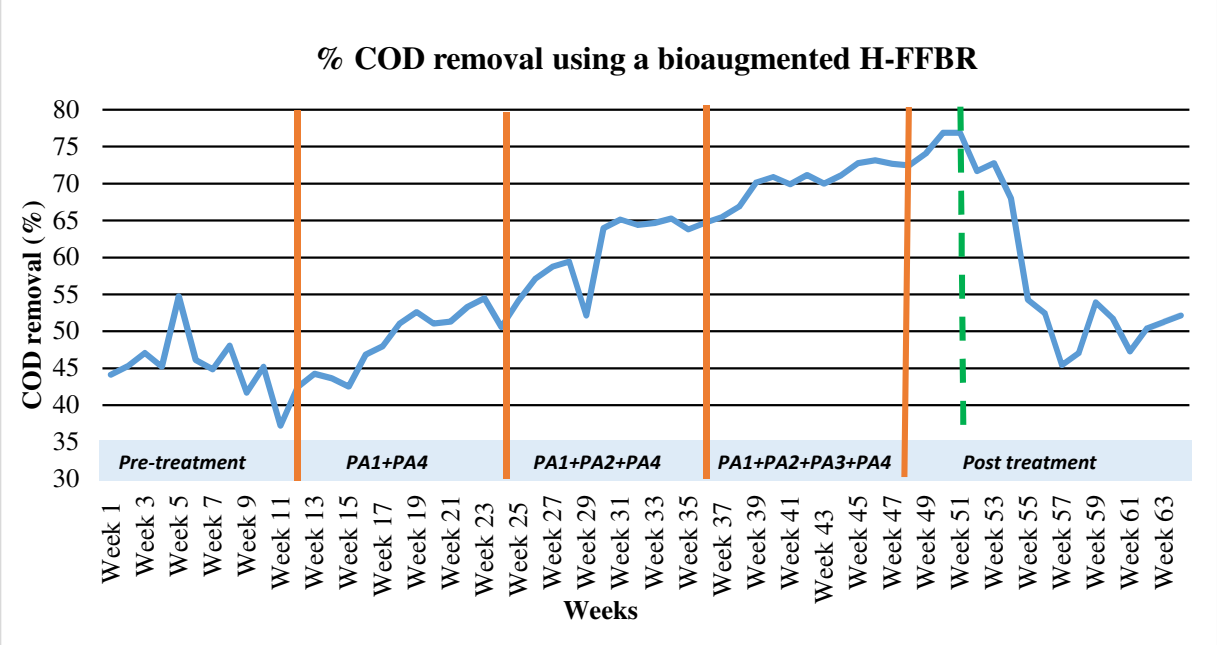

Figure 6.4: Comparison of COD removal from Week 1 to Week 65 of the study

The removal of COD increased by another 3% (73% to 76%) over a period of 2-3 weeks after the last inoculation made in Week 48 and then fluctuated between 45% and 53% after 15 weeks without bioaugmentation. This finding suggests that the transfer of catabolic plasmids between

the bacterial populations was dependent on the survival of donor plasmids which had a limited long-term impact (Mohan et al., 2009).

6.4 Removal of phenols

The removal of phenols decreased by 6% (79% to 73%) with the addition of inocula PA1 and PA4 which included strains of *Pseudomonas putida*, *Enterobacter* spp. and *Rhodococcus erythropolis*; increased by 4% (73% to 77%) with the addition of inocula PA2 and PA4 which included different strains of *Pseudomonas putida*; and increased by a further 5% (77% to 82%) with the addition of inocula PA3 and PA4 which included different strains of *Pseudomonas putida, Pseudomonas plecoglossicida* and *Rhodococcus qingshengii*. The decrease in the removal of phenol for each inoculum phase was significant (p<0.048; α=0.05) when compared to the baseline value. The increase in the effluent $COD_{phenol}/COD_{soluble}$ ratio indicated that organic compounds other than phenol were degraded by the mixed communities resulting in lower phenol removal. *Pseudomonas putida*, *Enterobacter* spp. and *Rhodococcus erythropolis* strains in PA1 significantly (p<0.001; α=0.05) decreased the removal of phenol.

6.5 Settling of suspended solids in the H-FFBR clarifier

The inoculation of PA4 did not initially improve settling of suspended solids in the clarifier as had been expected. The suspended solids in the effluent increased during the additions of inocula PA1 and PA4 and then decreased during the additions of inocula PA2 and PA3. As a separate study, the feed to the clarifier was collected and treated (6 mg/L) with a cationic polyacrylamide flocculant (5% mole charge and 10-15 x 10^6 Daltons). An increase in the settling of the suspended solids was observed, thus reducing the solids carry-over in the effluent by 70%. Decreasing the level of suspended solids in the effluent is important to meet discharge requirements. A benefit of using a flocculant is that previously dispersed cells will not be washed out but rather form part of the diverse flocculated microbial community in the H-FFBR.

The bioaugmentation of the H-FFBR with strains of bacteria selected from the γ-Proteobacteria and Actinobacteria class enhanced the removal of COD and phenol. Thus, a mixed microbial community with various metabolic activities and pathways is required for the removal of organics contributing to COD and phenols in the feed. The settling of the suspended solids in the clarifier was improved using a cationic polyacrylamide flocculant rather than seaweed and

diatoms. Improving the settling will allow greater retention of the dispersed biomass thus increasing the abundance of γ-Proteobacteria in the H-FFBR and reducing suspended solids carry-over to the effluent to comply with effluent discharge legislation.

CHAPTER 7
AN INTELLIGENT MODEL FOR THE PREDICTION OF COD AND PHENOL REMOVAL

7.1 Intelligent model development and knowledge discovery

This study reveals the development of an intelligent model based on artificial neural networks (ANNs) and non-linear mathematical curve-fitting to predict the removal of chemical oxygen demand (COD) and phenols from coal gasification stripped gas liquor (CGSGL) wastewater under novel hybrid fixed-film bioreactor (H-FFBR) operating conditions not previously used in model development.

7.1.1 Model validation

The validation was achieved by using the artificial neural network (ANN) model to predict the process output values of Zone 1 biofilm thickness, Zone 2 biofilm thickness, Zone 3 biofilm thickness, Zone 1 OUR, Zone 2 OUR, Zone 3 OUR, suspended biomass (MLSS), COD removal (%) and phenol removal (%) based on 14 process conditions not previously exposed to the model. The output values gave varied coefficients of determination (R^2) up to 0.96 (average 0.85).

A high coefficient of determination value (R^2>0.7) suggests a higher reproducibility and accuracy in the model prediction when subjected to the novel H-FFBR operating conditions (Whiteman and Kana, 2014; Rorke et al., 2017).

Thus, models with higher coefficient of determination (R^2>0.7) accounted for more than 70% variation in the observed data (Desai et al., 2008; Sewsynker and Kana, 2016). The only coefficients found to be below 0.7 were orthophosphate (R^2 = 0.06) and phenol removal efficiencies (%) (R^2 = 0.57). The removal of orthophosphates was not considered significant enough to be estimated using the developed ANN model (Figure 7.1).

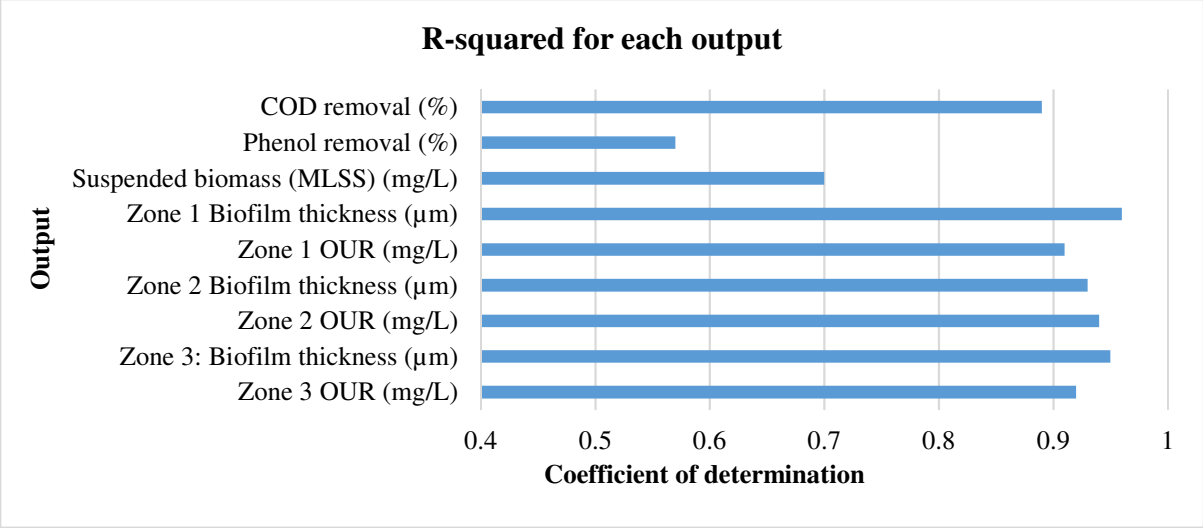

Figure 7.1: Comparative regression (R^2) values for each output using ANN (outliers excluded) (refer to Figures D-1 to D-9 in Appendix D for scatter plots)

7.1.2 Impact of input changes on process output

The sensitivity studies focused on the impact of process input variations on the H-FFBR process outputs. A high sensitivity to an input implies that the process output will be highly affected with little variation on the process input and vice versa (Rorke et al., 2017). The effects of varying input parameter values within the operational window of COD removal, phenol removal and biofilm thickness are illustrated in Table 7.1.

The sensitivity analyses revealed that the biofilm thickness in Zone 1, Zone 2 and Zone 3 increased during each bioaugmentation programme. The relationship between biofilm thickness and bioaugmentation programme was best fitted by a dose-response multistage-2 type equation for Zone 1 (Table 7.1a) and Zone 2 (Table 7.1b) and dose-response Hill-type equation for Zone 3 (Table 7.1c). The removal of COD increased by 5% (45%-50%) with bioaugmentation Programme 1, by a further 5% (50%-55%) with bioaugmentation Programme 2 and by a further 20% (55%-75%) with bioaugmentation Programme 3. The suspended biomass decreased from 870 mg/L to 630 mg/L during bioaugmentation Programme 1, decreased from 630 mg/L to 500 mg/L during bioaugmentation Programme 2 and decreased from 500 mg/L to below 200 mg/L during bioaugmentation Programme 3. The suspended biomass decreased as the attached biomass (biofilm thickness) increased. The relationship between biomass loss and bioaugmentation was best fitted by a dose-response Hill-type equation (Table 7.1d). The removal of phenol increased by 3% (64%-67%) during

bioaugmentation Programme 1 and bioaugmentation Programme 2 and increased by 8% (67%-78%) during bioaugmentation Programme 3. The direction and rate of COD and phenol removal as a function of bioaugmentation were best fitted by a dose-response Hill-type equation (Table 7.1e, Table 7.1f). Bioaugmentation increased microbial diversity, metabolic rate and enabled hydrolysis of biodegradable and less biodegradable compounds by diverse catabolic pathways (Mitra and Mukhopadhyay, 2016).

An increase in phenol (feed) concentration between the operational windows (OW) of 10 mg/L and 20 mg/L resulted in a slight decrease in phenol removal. The removal of phenol increased as the concentration of phenol in the feed increased from 20 mg/L to 85 mg/L. The phenol removal rate was highest when the phenol concentration in the feed ranged between 45 mg/L and 65 mg/L; however, the COD removal rate at this concentration remained constant at 50%. Phenol concentrations of between 60 mg/L and 85 mg/L in the feed increased the removal of phenol and decreased the removal of COD by 4.2% and 5%, respectively. The removal of phenol started to decrease as the phenol concentrations increased above 85 mg/L. The direction and rate of COD removal were best fitted by a rational model response-type equation (Table 7.1g) and the removal of phenol was best fitted by a dose-response Hill-type equation (Table 7.1h). This suggests that relatively high concentrations of phenol and organic intermediates generated in the CGSGL wastewater inhibit the activity of the mixed microbial community. With a decrease in phenol loading rate, the inhibitory effect decreases and therefore phenol is degraded (Fan, 1983). The same trend was reported by Nakhli et al. (2014) for the removal of phenol and COD from wastewater using a moving bed biofilm reactor (MBBR).

An increase in M-alkalinity (inorganic carbon source) between the OW of 100 mg/L to 600 mg/L resulted in a 9.5% (53.5%-44%) and 8.5% (72%-63.5%) decrease in COD and phenol efficiencies, respectively. The decrease in COD removal was linear between 280 mg/L and 460 mg/L, while the decrease in phenol removal was linear between 150 mg/L and 300 mg/L. The direction and rate of COD removal were best fitted by a Farazdaghi-Harris model response-type equation (Table 7.1i) and the removal of phenol was best fitted by a dose-response Hill-type equation (Table 7.1j). Mixed-species biofilms exposed to bicarbonate alkalinity (HCO_3^-) have been reported to trigger bacterial autolysis of subpopulations releasing DNA (eDNA) within the biofilm in a pH-independent manner. Biofilms containing eDNA have been associated with abundant carbonic anhydrases which can convert aqueous CO_2 to HCO_3^- (Rose and Bermudez, 2016). Enzymatic degradation of eDNA can weaken the biofilm structure and

release microbial cells from the surface (Jakubovics et al., 2013) thus reducing the removal of COD and phenol.

An increase in suspended biomass (RAS) between the OW of 500 mg/L to 1 500 mg/L resulted in a 6% (56%-50%) and 8% (72%-64%) decrease in COD and phenol removal efficiencies, respectively. However, the removal of phenol increased by 10% (64%-74%) when the suspended biomass was increased from 1 500 mg/L to 4 000 mg/L. The direction and rate of COD and phenol removal were best fitted by a rational model-type equation (Table 7.1k and Table 7.1l). The solids retention time (SRT) of the attached biomass (biofilm) was much longer (126 days) than that of the suspended biomass (18 days) in the H-FFBR. Increasing the suspended biomass concentration increased the phenol biodegradation capacity of the H-FFBR. Sarkar and Mazumder (2014) reported a similar trend when treating slowly biodegradable substances in a H-FFBR.

The COD removal efficiency increased by 13% (41%-54%) when the COD loading rate was increased from 2 kg/m^3.d to 4.5 kg/m^3.d. The phenol removal efficiency increased by 4.5% (63%-67.5%) when the COD loading rate was increased from 2 kg/m^3.d to 2.8 kg/m^3.d and then decreased by 2.5% (67.5%-65%) when the COD loading rate was increased from 2.8 kg/m^3.d to 3.8 kg/m^3.d. The phenol removal efficiency increased by 7% (64%-71%) when the COD loading was increased from 3.8 kg/m^3.d to 4.6 kg/m^3.d. The highest phenol removal rate was between 2 kg/m^3.d and 2.75 kg/m^3.d and the highest COD removal rate was between 2.5 g/m^3.d and 3.5 g/m^3.d. The direction and rate of COD removal were best fitted by a Morgan-Mercer-Flodin model response-type equation (Table 7.1m) and the removal of phenol was best fitted by a Farazdaghi-Harris-type equation (Table 7.1n). The increase in COD and phenol removal efficiency was due to the formation of a thicker biofilm layer on the carriers. The decrease in COD and phenol removal was due to the detachment of biomass from the carriers which follows a linear relationship with the organic loading rate (OLR) (Aygun et al., 2008).

The COD removal efficiency increased by 4.5% (47.5%-52%) and the removal of phenol decreased by 11% (70%-61%) when the total dissolved solids (TDS) concentration in the feed OW was increased from 500 mg/L to 3 500 mg/L. The direction and rate of COD and phenol removal were best fitted using a hyperbolic decline model response-type equation (Table 7.1o and Table 7.1p). An increase in TDS concentration decreases the solubility of phenolic compounds (Noubigh et al., 2007). The increase in COD removal efficiency is due to the ability

of the microbial community to metabolise aromatic compounds with low water solubilities. Some bacteria may facilitate the uptake of poorly soluble compounds by producing emulsifiers or may have hydrophobic cell surfaces that facilitate access and uptake of compounds (O'Sullivan, 1998).

The COD removal efficiency decreased by 4.5% (52.5%-48%) and the removal of phenol increased by 10% (62%-72%) when the COD concentration in the feed OW increased from 1 500 mg/L to 1 900 mg/L. The highest phenol removal rate occurred between 1 640 mg/L and 1 720 mg/L and the highest COD removal rate occurred between 1 590 mg/L and 1 740 mg/L. The direction and rate of COD and phenol removal were best fitted by a reciprocal quadratic model response-type equation (Table 7.1q and Table 7.1r). These results were found to be in line with the observed removal of COD and phenols in the H-FFBR inoculated with a mixed microbial community with different metabolic pathways and the less biodegradable intermediate products contributing to the COD. The microbial hydrolysis of the organic compounds results in the formation of biodegradable and less biodegradable intermediate compounds. Some compounds are not consumed as fast as they are produced, e.g. organic acids. The continuous change in feed composition and substrate availability triggers shifts in the microbial community composition and the cell growth rate (Mitra and Mukhopadhyay, 2016). The cell growth rate of the microbial communities assimilating biodegradable compounds follows the Monod growth rate kinetic model. The cell growth rate of microbial communities assimilating less biodegradable compounds follows the Haldane growth rate kinetic model (Mohanty, 2012).

The developed ANN revealed that COD removal (%) and phenol removal (%) exhibited high sensitivity to bioaugmentation Programme 3, M-alkalinity, TDS, suspended biomass (RAS), COD loading rate and phenol concentration in the feed. Significant non-linearities were observed between operating conditions (inputs) and the removal of COD (%) and phenol (%). The developed intelligent model gave R^2-values of up to 0.96 and an average R^2-value of 0.85, illustrating that it can accurately predict the removal of COD (%) and phenols (%) from the CGSGL wastewater in a bioaugmented H-FFBR. This knowledge will enhance the design of bioaugmentation programmes for the removal of COD and phenols to meet more stringent effluent discharge criteria.

Table 7.1: Model equations for the bioaugmented H-FFBR illustrating the direction and rate of change of outputs when input parameters were varied within their boundaries

Eq.	Process input/output pair	Model equation form	Equation type	Fitted model	R^2 value
(a)	BR: Zone 1 biofilm thickness	$y = \gamma + (1+\gamma)[1 - e^{-\beta_1 x - \beta_2 x^2}]$	DR-Multistage -2	$y = 1.84x10^1 + (1 - 1.84x10^1)[1 - e^{-2.30x10^{-1}x + 1.33x10^{-1}}]$	0.967
(b)	BR: Zone 2 biofilm thickness	$y = \gamma + (1+\gamma)[1 - e^{-\beta_1 x - \beta_2 x^2}]$	DR-Multistage -2	$y = 4.88 + (1 - 4.88)[1 - e^{-1.61x10^{-1}x + 7.09x10^{-2}}]$	0.989
(c)	BR: Zone 3 biofilm thickness	$y = \alpha + (\theta x^\eta / \kappa^\eta + x^\eta)$	DR-Hill	$y = 1.43x10^1 + (1.05x10^1 / 3.90^{1.04x10^1} + x^{1.04x10^1})$	0.997
(d)	BR: Suspended biomass	$y = \alpha + (\theta x^\eta / \kappa^\eta + x^\eta)$	DR–Hill	$y = 8.57x10^2 + (-3.62x10^5 x^{1.34} / 5.00x10^{2^{1.34}} + x^{1.34})$	0.999
(e)	BR: Phenol removal	$y = \alpha + (\theta x^\eta / \kappa^\eta + x^\eta)$	DR-Hill	$y = 6.48x10^1 + (1.50x10^1 x^{1.08x10^1} / 3.52^{1.08x10^1} + x^{1.08x10^1})$	0.998
(f)	BR: COD removal	$y = \alpha + (\theta x^\eta / \kappa^\eta + x^\eta)$	DR-Hill	$y = 4.79x10^1 + (3.69x10^1 x^{5.99} / 3.83^{5.99} + x^{5.99})$	0.981
(g)	Feed phenol: COD removal	$y = a + bx/1 + cx + dx^2$	Rational	$y = 8.61x10^5 + 1.16x10^6 x/1 + 2.29x10^4 x + 1.44x10^1 x^2$	0.931
(h)	Feed phenol: Phenol removal	$y = \alpha + (\theta x^\eta / \kappa^\eta + x^\eta)$	DR-Hill	$y = 6.26x10^1 + (4.50x^{5.27} / 5.36x10^{1^{5.27}} + x^{5.27})$	0.997

BR: Bioaugmentation regime, DR: Dose response

Table 7.1 continued

Eq.	Process input/output pair	Model equation form	Equation type	Fitted model	R^2 value
(i)	M-alkalinity: COD removal	$y = 1/(a + bx^c)$	Farazdaghi-Harris	$y = \frac{1}{1.86x10^{-2} + 2.54x10^{-8}x^{1.86}}$	0.999
(j)	M-alkalinity: Phenol removal	$y = \alpha + (\theta x^\eta/\kappa^\eta + x^\eta)$	DR-Hill	$y = 7.25x10^1 + (-9.30x^{3.16}/2.19x10^{2^{3.16}} + x^{3.16})$	0.998
(k)	RAS: Phenol removal	$y = a + bx/1 + cx + dx^2$	Rational	$y = 7.29x10^1 + 4.68x10^{-2}x/1 + 9.42x10^{-4}x - 8.22x10^{-8}x^2$	0.998
(l)	RAS: COD removal	$y = a + bx/1 + cx + dx^2$	Rational	$y = 5.60x10^1 + 8.93x10^{-2}x/1 + 1.84x10^{-3}x + 1.22x10^{-8}x^2$	0.999
(m)	COD load: COD removal	$y = ab + cx^d/b + x^d$	Morgan-Mercer-Flodin	$y = 4.09x10^1(2.41x10^5) + 5.38x10^1x^{1.08x10^1}/2.41x10^5 + x^{1.08x10^1}$	0.998
(n)	COD load: Phenol removal	$y = 1/(a + bx^c)$	Farazdaghi-Harris	$y = 1/(1.53x10^{-2} - 3.71x10^{-13}x^{1.43x10^1})$	0.623

DR: Dose response

Table 7.1 continued

Eq.	Process input/output pair	Model equation form	Equation type	Fitted model	R^2 value
(o)	TDS: Phenol removal	$y = q_0(1 + bx/a)^{(-1/b)}$	Hyperbolic decline	$y = 7.20x10^1(1 + 3.64x/1.57x10^4)^{(-1/3.64)}$	0.999
(p)	TDS: COD removal	$y = q_0(1 + bx/a)^{(-1/b)}$	Hyperbolic decline	$y = 4.73x10^1(1 + 1.81x/-4.07x10^4)^{(-1/1.81)}$	0.997
(q)	Feed COD: COD removal	$y = 1/(a + bx + cx^2)$	Reciprocal quadratic	$y = 1/(4.73x10^{-3} + 1.39x10^{-5}x - 2.84x10^{-9}x^2$	0.995
(r)	Feed COD: Phenol removal	$y = 1/(a + bx + cx^2)$	Reciprocal quadratic	$y = 1/(-4.95x10^{-3} + 2.99x10^{-5}x - 1.05x10^{-8}x^2$	0.988

Refer to Figures E-1 to E-18 in Appendix E for model response graphs.

CHAPTER 8
CONCLUSIONS AND RECOMMENDATIONS

The results obtained in this study have led to the following conclusions and recommendations.

8.1 Conclusions

- Real-time diluted coal gasification stripped gas liquor (CGSGL) wastewater can be treated in a hybrid fixed-film bioreactor (H-FFBR) bioaugmented with specific strains of *Pseudomonas putida*, *Pseudomonas plecoglossicida*, *Rhodococcus erythropolis*, *Rhodococcus qingshengii, Enterobacter cloacae, Enterobacter asburiae* and *Silvetia siliquosa.*
- A diverse microbial community decreased COD and phenol concentrations; however, ammonia-nitrogen was not decreased since no autotrophic ammonia-oxidising bacteria were present in the H-FFBR.
- The microbial community diversities in the biofilm, suspended biomass, feed and effluent samples were significantly dissimilar, thus indicating that microbial communities were affected by the different growth environments in the H-FFBR.
- Novel bacteria can play an important role in the treatment of the CGSGL wastewater; this was confirmed by the fact that uncultured bacteria were present across the H-FFBR.
- The developed intelligent model is a novel virtual tool for the prediction of COD and phenol removal from CGSGL wastewater treated under varying operating conditions in a bioaugmented H-FFBR.

8.2 Recommendations

- A combination of biological and chemical treatments such as the fixed-bed metal-oxide catalyst reactor should be investigated for increased removal of organic and nitrogenous compounds to meet discharge or reuse criteria. Preliminary tests using this technology revealed >99% removal of COD, phenol and ammonia-nitrogen.
- A low-charge cationic polyacrylamide flocculant can be used to improve the settling rate of the suspended solids in the clarifier and thus decrease the wash-out of bacterial cells and lower the cost of bioaugmentation.

- Studies on the Archaea population present in the biomass should be initiated to determine whether these species are ammonia-oxidisers to assist with the removal of ammonia-nitrogen and other organic compounds contributing to the effluent COD.

CHAPTER 9
REFERENCES

ABDUL-MAJEED M (2012) Wastewater treatment in Baghdad city using moving bed biofilm reactor (MBBR) technology. *Eng. Technol. J.* **30** (9) 1550-1560.

ABEYSINGHE DH, DE SILVA DGV, STAHL DA, RITTMANN BE (2002) The effectiveness of bioaugmentation in nitrifying systems stressed by a washout condition and cold temperature. *Water Environ. Res.* **74** (2) 187-199.

ADABJU S (2013) Specific moving bed biofilm reactor for removal of synthetic municipal wastewater. MSc dissertation, University of Technology, Sydney, Australia.

AGARRY SE and SOLOMON BO (2008) Kinetics of batch microbial degradation of phenols by indigenous binary mixed culture of *Pseudomonas aeruginosa* and *Pseudomonas fluorescence. Int. J. Environ. Sci. Technol.* **5** (2) 223-232.

ALBERTSEN M, KARST SM, ZIEGLER AS, KIRKEGAARD RH and NIELSEN PH (2015) Back to basics – the influence of DNA extraction and primer choice on phylogenetic analysis of activated sludge communities. *PLoS One* **1** (7) e0132783 (doi: 10.1371/journal.pone.0132783).

ALBIZURI J, VAN LOOSDRECHT MCM and LARREA L (2009) Extended mixed-culture biofilms (MCB) model to describe integrated fixed film/activated sludge (IFAS) process behaviour. *Water Sci. Technol.* **60** (12) 3233-3241.

ALMSTRAND R, LYDMARK P, LINDGREN PE, SÖRENSSON F and HERMANSSON M (2013) Dynamics of specific ammonia-oxidising bacterial communities and nitrification in response to controlled shifts in ammonium concentrations in wastewater. *Appl. Microbiol. Biotechnol.* **97** 2183-2191 (doi: 10.1007/s00253-012-4047-7).

ALTSCHUL SF, GISH W, MILLER W, MYERS EW and LIPMAN DJ (1990) Basic local alignment search tool. *J. Mol. Biol.* **215** (3) 403-410.

AMBUJOM S (2001) Studies on composition and stability of a large membered bacterial consortium degrading phenol. *Microbiol. Res*. **156** 293-301.

ANASTASI JL (1980) Sasol: South Africa's oil from coal story. EPA report 600/8/80-002. URL: http://www.fischer-tropsch.org/DOE/DOE_reports/600_8-80-002/epa-600_8-80-002.pdf (Accessed 2 January 2014).

ANNACHHATRE AP and BHAMIDIMARRI SMR (1992) Microbial attachment and growth in fixed-film reactors: Process startup considerations. *Biotech. Adv*. **10** 69-91.

APHA (2012) *Standard Methods for the Examination of Water and Wastewater*, 22nd edition. American Public Health Association/American Water Works Association/Water Environment Federation, Washington DC, USA (ISBN-13: 978-087553-0130).

AYGUN A, NAS B and BERKTAY A (2008) Influence of high organic loading rates on COD removal and sludge production in moving bed biofilm reactor. *Environ. Eng. Sci.* **25** (9) 1311–1316.

BAI Y, SUN Q, ZHAO C and WEN D (2010) Bioaugmentation treatment for coking wastewater containing pyridine and quinolone in a sequencing batch reactor. *Appl. Microbiol. Biotechnol.* **87** 1943-1951.

BAMFORTH SM and SINGLETON I (2005) Bioremediation of polycyclic aromatic hydrocarbons: current knowledge and future directions. *J. Chemical Technol. Biotechnol.* **80** 723–736 (doi: 10.1002/jctb.1276).

BARRIOS-MARTINEZ A, BARBOT E, MARROT B, MOULIN P and ROCHE N (2006) Degradation of synthetic phenol-containing wastewaters by MBR. *J. Membr. Sci.* **281** 288-296 (doi: 10.1016/j.memsci.2006.03.048).

BASHA KM, RAJENDRAN A and THANGAVELU V (2010) Recent advances in the biodegradation of phenol: A review. *Asian J. Exp. Biol. Sci.* **1** (2) 219-234.

BATHE S, SCHWARZENBECK N and HAUSER M (2005) Plasmid-mediated bioaugmentation of activated sludge bacteria in a sequencing batch moving bed reactor using pNB2. *Lett. Appl. Microbiol.* **41** (3):242-247.

BELOFF B LINES M and TANZIL D (Eds.) (2005) *Transforming Sustainability Strategy into Action: The Chemical Industry*. John Wiley and Sons Inc. (ISBN 978-0-471-64445-3).

BEYCHOK MR (1974) Coal gasification and the Phenosolvan process. In: *Proceedings of the American Chemical Society 168th Annual Meeting*, September 1974, Atlanta City, New Jersey, USA pp 85–93.

BHATTACHARYA AK, MANDAL SN and BHATTACHARYA B (2008) Bio-augmentation in textile mill wastewater management: A case study. *Res. J. Environ. Sci.* **2** (1) 32-39.

BJÖRNSDOTTER L (2005) Study of nitrification rates in a biofilm system. MSc dissertation, Chalmers University of Technology, Göteborg, Sweden.

BOLTON J, TUMMALA A, KAPADIA C, DANDAMUDI M and BELOVICH JM (2006) Procedure to quantify biofilm activity on carriers used in wastewater treatment systems. *J. Environ. Eng.* **132** (11) 1422-1430.

BOLTZ JP, JOHNSON BR, DAIGGER GT and SANDINO J (2009) Modeling integrated fixed-film activated sludge and moving-bed biofilm reactor systems 1: Mathematical treatment and model development. *Water Environ. Res.* **81** (6) 555–575.

BOLTZ JP and DAIGGER GT (2010) Uncertainty in bulk-liquid hydrodynamics and biofilm dynamics creates uncertainties in biofilm reactor design. *Water Sci. Technol.* **61** (2) 307-316.

BOON N (2002) Bioaugmentation of activated sludge reactors to enhance chloroaniline removal. PhD thesis, University of Ghent, Ghent, Belgium.

BORGHEI SM and HOSSEINI SH (2004) The treatment of phenolic wastewater using a moving bed biofilm reactor. *Process. Biochem.* **39** (10) 1177-1181.

BORKAR RP, GULHANE ML and KOTANGALE AJ (2013) Moving bed biofilm reactor – A new perspective in wastewater treatment. *IOSR – JESTFT* **6** (6) 15-21.

BRYANT CW, CAWEIN CC and KING PH (1988) Biological treatment of in situ coal gasification wastewater. *J. Environ. Eng.* **114** (2) 400–414.

CHAKRABORTY S, BHATTACHARYA T, PATEL TN and TIWARI KK (2010) Biodegradation of phenol by native microorganisms isolated from coke processing wastewater. *J. Environ. Biol.* **32** 293–296.

CHAKRABORTY S and VEERAMANI H (2006) Effect of HRT and recycle ratio of cyanide, phenol, thiocyanate and ammonia in an anaerobic-anoxic-aerobic continuous system. *Process. Biochem.* **41** 96-105.

CHAVAN A and MUKHERJI S (2008) Treatment of hydrocarbon-rich wastewater using oil degrading bacteria and phototrophic microorganisms in rotating biological contactor: Effect of N:P ratio. *J. Hazard. Mater.* **154** (1-3) 63-72.

CHANDRALAL N, MAHAPATRA D, SHOME D and DASGUPTA P (2014) Behaviour of low rank high moisture coal in small stock piles under controlled ambient conditions – A statistical approach. *AJIRFANS* **14** (236) 98-108.

CHONG G, KIMYON O, RICE SA, KJELLEBERG S and MANEFIELD M (2012) The presence and role of bacterial quorum sensing in activated sludge. *Microb. Biotechnol*. **5** (5) 621-633.

CHRISTIAN A (2014) High performance, highly adsorbent and porous PU carriers for MBBR/IFAS application. *Water Today, October 2014.* URL: http://www.slideshare.net/amitc2108/modified-pu-carriersforwastewatertreatment (Accessed 10 March 2015).

CRUTESCU R, FILIPESCU L and VASILESCU P (2008) Influence of operating parameters on degradation process of phenolic wastewaters. *U.P.B Bull. Series B* **70** (4) 13–28.

CUI P, MAI Z, YANG S and QIAN Y (2017) Integrated treatment processes for coal-gasification wastewater with high concentration of phenol and ammonia. *J. Clean. Prod*. **142** 2218-2226.

CYDZIK-KWIATKOWSKA A and ZIELINSKA M (2016) Bacterial communities in full-scale wastewater treatment systems. *World J. Microbiol. Biotechnol*. **32** (66) 1-8 (doi: 10.1007/s11274-016-2012-9).

DAS N and CHANDRAN P (2011) Microbial degradation of petroleum hydrocarbon contaminants: An overview. *Biotechnol. Res. Int.* (doi: 10.4061/2011/941810).

DE BRITO IRC (2009) Ecology of nitrification in oil refinery wastewater treatment systems. PhD thesis, Newcastle University, Newcastle upon Tyne, UK.

DEFIERY MEJA and REDDY G (2014) Influence of metal ions on phenol degradation by *Rhodococcus pyridinivorans* GM3. *Mesop. Environ. J.* **1** (1) 30-38.

DEPARTMENT OF WATER AFFAIRS AND FORESTRY (DWAF) (1996) South African Water Quality Guidelines Volume 7: Aquatic Ecosystems. Department of Water Affairs and Forestry, Pretoria, South Africa, Government Printer, Pretoria.

DESAI KM, SURVASE SA, SAUDAGAR PS, LELE SS and SINGHAL RS (2008) Comparison of artificial neural network (ANN) and response surface methodology (RSM) in fermentation media optimization: case study of fermentative production of scleroglucan. *Biochem. Eng. J*. **41** (3) 266-273.

DEVI PBNL and SETTY YP (2014) Biological nitrification of wastewater. *Int. J. Appl. Biol. Pharm.* **5** (4) 120-129.

DIAZ DE RIENZO MA, STEVENSON PS, MARCHANT R and BANAT IM (2016) Effect of biosurfactants of *Pseudomonas aeruginosa* and *Staphylococcus aureus* biofilms in a Bioflux channel. *Appl. Microbiol. Biotechnol*. (doi: 10.1007/s00253-016-7310-5).

DiMASSIMO RW and BUNDGAARD E (2011) Controlled aeration of integrated fixed-film activated sludge bioreactor systems for treatment of wastewater. United States Patent Number US2011/0284461 A1.

DOMDE P, KAPLEY A and PUROHIT HJ (2007) Impact of bioaugmentation with a consortium of bacteria on the remediation of wastewater-containing hydrocarbons. *Environ. Sci. Pollut. Res.* **14** (1) 7-11.

DONALDSON TL, LEE DD and SINGH SPN (1987) Treatment of coal gasification wastewaters: Final Report ORNL/TM-10241. Oak Ridge National Laboratory, Tennessee, USA.

DUEHOLM MS, ALBERTSEN M, D'IMPERIO S, TALE VP, LEWIS D, NIELSEN PH and NIELSEN JL (2014a) Complete genome sequences of *Pseudomonas monteilii* SB3078 and SB3101, two benzene, toluene-, and ethylbenzene-degrading bacteria used for bioaugmentation. *Genome Announc.* **2** (3) 1-2 e00524-14.

DUEHOLM MS, ALBERTSEN M, D'IMPERIO S, TALE VP, LEWIS D, NIELSEN PH and NIELSEN JL (2014b) Complete genome of *Rhodococcus pyridinivorans* SB3094, a methyl-ethyl-ketone-degrading bacterium used for bioaugmentation. *Genome Announc.* **2** (3) 1-2 e00525-14.

DÜRR R, VIELHAUER O, BURTON SG, COWAN DA and PUANL A (2006) Distribution of hydantoinase activity in bacterial isolates from geographically distinct environmental sources. *J. Mol. Catal. B: Enzym.* **39** 160–165.

EL-JAFRY MH, IBRAHIM WA and EL-ADAWY MS (2013) Enhanced COD and nutrient removal efficiency in integrated fixed film activated sludge (IFAS) process. In: *Proceedings of International Conference on Civil and Architecture Engineering (ICCAE 2013)*, 6-7 May 2013, Kuala Lumpur, Malaysia.

FAN LS (1983) Mechanisms of semi fluidized bed bioreactors for biological phenol degradation. Report Number 714438. Water Resources Center, Ohio State University, USA.

FANG F, HAN H, ZHAO Q, XU C and ZHANG L (2013) Bioaugmentation of biological contact oxidation reactor (BCOR) with phenol-degrading bacteria for coal gasification wastewater (CGW) treatment. *Bioresour. Technol.* **150** 314-320.

FANG F, HAN H, XU C, ZHAO Q and ZHANG L (2014) Degradation of phenolic compounds in coal gasification wastewater by biofilm reactor with isolated *Klebsiella* sp. *J. Harbin Inst. Technol.* **21** (3) 9-17.

FELFOLDI T, SZÉKELY AJ, GORAL R, BARKACS K, SCHEIRICH G, ANDRAS J, RACZ A and MARIALIGETI K (2010) Polyphasic bacterial community analysis of an aerobic activated sludge removing phenols and thiocyanate from coke plants. *Bioresour. Technol*. **101** 3405-3414.

FENG D, YU Z, CHEN Y and QIAN Y (2009) Novel single stripper with side-draw to remove ammonia and sour gas simultaneously for coal-gasification wastewater treatment and the industrial implication. *Ind. Eng. Chem. Res*. **48** 5816-5823.

FENG L, WU Z and YU X (2013) Quorum sensing in water and wastewater treatment biofilms. *J. Environ. Biol*. **34** 437-444.

FOUAD M and BHARGAVA R (2005) Mathematical model for the biofilm-activated sludge reactor. *J Environ. Eng.* **13**1 557-562.

FREDERIK MR, KUTTLER C, HENSE BA and EBERL HJ (2011) A mathematical model of quorum sensing regulated EPS production in biofilm communities. *Theor. Med. Model*. **8** (8) (doi: 10.1186/1742-4682-8-8).

FRITSCHE W and HOFRICHTER M (2008) Aerobic degradation by microorganisms (doi: 10.1002/9783527620999.ch6m) (Accessed 26 March 2016).

FULLER R (2014) Bioaugmentation. In: *Engineering Report*. Athlon Solutions, Geismar, Los Angeles, USA.
URL: http://waterfacts.net/Treatment/Activated_Sludge/Bioaugmentation/Bioaugmentation_Engineering_Report_December_2014.pdf (Accessed 6 February 2014).

GAI H, JIANG Y, QIAN Y and KRASLAWSKI A (2008) Conceptual design and retrofitting of the coal-gasification wastewater treatment process. *Chem. Eng. J.* **138** 84-94.

GAI H, SONG H, XIAO M, FENG Y, WE Y, ZHOU H and CHEN B (2016) Conceptual design of a modified phenol and ammonia recovery process for the treatment of coal gasification wastewater. *Chem. Eng. J.* **304** 621-628.

GALIL N, REBHUN M and BRAYER Y (1988) Disturbances and inhibition in biological treatment of wastewater from an integrated oil refinery. *Water Sci. Technol.* **20** (10) 21–29.

GARRIDO L, SANCHEZ O, FERRERA I, TOMAS N and MAS J (2014) Dynamics of microbial diversity profiles in waters of different qualities. Approximation to an ecological quality indicator. *Sci. Total Environ.* **468-469** 1154-1161.

GEETS J, BOON N and VERSTRAETE W (2006) Strategies of aerobic ammonia-oxidising bacteria for coping with nutrient and oxygen fluctuations. FEMS *Microbiol. Ecol.* **58** (1) 1-13.

GINSTER M and MATJIE RH (2005) Beneficial utilisation of Sasol coal gasification ash. In: *Proceedings of the 2005 World of Coal Ash (WOCA) Conference*, 11-15 April 2005, Lexington, Kentucky, USA. URL: http://www.flyash.info/2005/94gin.pdf (Accessed 26 March 2016).

GOMEZ MA, RODELAS B, SAEZ F, POZO C, MARTINEZ-TOLEDO MV, HONTORIA E and GONZALEZ-LOPEZ J (2005) Denitrifying activity of *Xanthobacter autotrophicus* strains isolated from a submerged fixed-film reactor. *Appl. Microbiol. Biotechnol.* **68** 680-685.

GOODE C (2010) Understanding biosolids dynamics in a moving bed biofilm reactor. PhD thesis, University of Toronto, Canada.

GUBUZA DM (2008) The use of stripped gas liquor (SGL) as process cooling water: Analysis of the effects of operational conditions on microbial community dynamics, fouling, scaling and corrosion. MSc dissertation, North-West University, Potchefstroom, South Africa.

GUO J, MA F, JIANG K and CUI D (2008) Bioaugmentation combined with biofilm process in the treatment of petrochemical wastewater at low temperatures. *J. Water Resource Prot.* **1** (1-65) 55-59.

GUZIK U, HUPERT-KOCUREK K and WOJCIESZYNSKA D (2013) Intradiol dioxygenases- The key enzymes in xenobiotics degradation. URL: http://dx.doi.org/10.5772/56205 (Accessed 26 March 2016).

HAMZA UD, MOHAMMED IA and IBRAHIM S (2009) Kinetics of biological reduction of chemical oxygen demand from petroleum refinery wastewater. *Research* **1** (2) 17-23.

HEUER H and SMALLA K (2007) Review article: Horizontal gene transfer between bacteria. *Environ. Biosafety Res*. **6** 3-13.

HERRERO M and STUCKEY DC (2015) Bioaugmentation and its application in wastewater treatment: A review. *Chemosphere* **140** 119-128.

HESNAWI R, DAHMANI K, AL-SWAYAH A, MOHAMED S and MOHAMMED SA (2014) Biodegradation of municipal wastewater with local and commercial bacteria. *Procedia Eng*. **70** 810-814

HIGMAN C and VAN DER BURGT M (2008) *Gasification.* Gulf Professional Publishing, Burlington, USA. 435 pp. (Permission granted under license 377465368525 for the publication of excerpts and figures in this thesis).

HUANG H, FENG C, PAN X, WU H, REN Y, WU C and WEI, **C** (2013) Thiocyanate oxidation by coculture from a coke wastewater treatment plant. *J. Biomater. Nanobiotechnol.* **4** 37-46.

HU XB, WANG Z, DING LL and REN HQ (2013) Characteristics of biofilm attaching to carriers in moving bed biofilm reactors used to treat vitamin C wastewater. Scanning **35** (5) 283-291.

HULL SJ and KAPUSCINSKI (1987) Efficacy of bioaugmentation products as predicted by a model of steady state flocculent cultures. In: *Proceedings of the 42nd Industrial Waste Conference,* 12-14 May 1987, Indiana, USA.

IBRAHIM HT, QIANG H, AL-REKABI WS and QIQI Y (2012) Improvements in biofilm processes for wastewater treatment. *Pak. J. Nutr.* **11** (8) 610-636.

ISHAK S, MALAJAHMAD A and ISA MH (2012) Refinery wastewater biological treatment: A short review. *J. Sci. Ind. Res.* **71** 251-256.

IWASE T, TERUO H and IGUCHI Y (1979) Method for treating gas liquor. United States Patent Number US 4132636.

JAKUBOVICS NS, SHIELDS RC, RAJARAJAN N and BURGESS JG (2013) Life after death: the critical role of extracellular DNA in microbial biofilms. *Lett. Appl. Microbiol.* **57** 467-475.

JIA S, HAN H ZHUANG H and HOU B (2016) The pollutants removal and bacterial community dynamics relationship within a full-scale British gas/Lurgi coal gasification wastewater treatment using a novel system. *Bioresour. Technol*. **200** 103-110.

JAME SA, ALAM AKMR, FAKHRUDDIN ANM and ALAM MK (2010) Degradation of phenol by mixed culture of locally isolated *Pseudomonas* species. *J. Bioremed. Biodegrad.* **1** (1) 1-4 (doi: 10.4172/2155-6199.1000102).

JAROSZYNSKI LW, CICEK N, SPARLING R and OLESZKIEWICZ JA (2011) Importance of the operating pH in maintaining the stability of anoxic ammonium oxidation (anammox) activity in moving bed biofilm reactors. *Bioresour. Technol.* **102** 7051-7056.

JEMAAT Z, SUAREX-OJEDA ME, PEREZ J and CARRERA J (2014) Partial nitritation and o-cresol removal with aerobic granular biomass in a continuous airlift reactor. *Water Res.* **48** 354-362.

JEONG Y and CHUNG JS (2006) Simultaneous removal of COD, thiocyanate, cyanide and nitrogen from coal process wastewater using fluidized biofilm process. *Process Biochem.* **41** 1141-1147.

JI Q, TABASSUM S, YU G, CHU C and ZHANG Z (2015) A high efficiency biological system for treatment of coal gasification wastewater-key depth technology research. *RSC Adv.* **50** (5) 40402-40413 (doi: 10.1039/C5RA04215A).

JI Q, TABASSUM S, YU G, CHU C and ZHANG Z (2015a) Determination of biological removal of recalcitrant organic contaminants in coal gasification waste water. *Environ. Technol*. URL: http:dx.doi.org/10.1080/09593330.2015.1049215 (Accessed 5 April 2016).

JIANG HL, TAY JH and TAY STL (2002) Aggregation of immobilised activated sludge cells into aerobically grown microbial granules for the aerobic biodegradation of phenol. *Lett. Appl. Microbiol.* **35** 439-445.

JIANLONG W, XIANGCHUN Q, LIBO W, YI Q and HEGEMANN W (2002) Bioaugmentation as a tool to enhance the removal of refractory compound in coke plant wastewater. *Process Biochem.* **38** 777-781.

JIN X, LI E, LU S, QUI Z and SUI Q (2013) Coking wastewater treatment for industrial reuse purpose: Combining biological processes with ultrafiltration, nanofiltration and reverse osmosis. *J. Environ. Sci.* **25** (8) 1565 to 1574.

JING JY, FENG J and LI WN (2009) Carrier effects on oxygen mass transfer behaviour in a moving bed biofilm reactor. *Asia-Pacific J. Chem. Eng*. **4** 618–623.

JIUAN L, ZHOU H, LIU Q, TAN Z and LI X (2011) Progress in bioaugmentation technology research for biological treatment of wastewaters. *Chinese J. Appl. Environ. Biol*. **17** (2) 273-279.

KAPUSTA K and STANCZYK K (2011) Pollution of water during underground coal gasification of hard coal and lignite. *Fuel* **90** 1927–1934.

KATAYAMA Y, NARAHARA Y, INOUE Y, AMANO F, KANAGAWA T and KURAISHI H (1992) A thiocyanate hydrolase of *Thiobacillus thioparus*: A novel enzyme catalysing the formation of carbonyl sulphide from thiocyanate. *J. Biol. Chem.* **267** (13) 9170-9175.

KHARDENAVIS AA, KAPLEY A and PUROHIT HJ (2007) Simultaneous nitrification and denitrification by diverse *Diaphorobacter* sp. *Appl. Microbiol. Biotechnol.* **77** (2) 403-409.

KIM S and KIM H (2003) Impact and threshold concentration of toxic materials in the stripped gas liquor on nitrification. *Korean J. Chem. Eng.* **20** (6) 1103-1110.

KIM YM, PARK D, LEE DS and PARK JM (2008) Inhibitory effects of toxic compounds on nitrification process for cokes wastewater treatment. *J. Hazard. Mater.* **152** 915-921.

KIM YM, CHO HU, LEE DS, PARK C, PARK D and PARK JM (2011) Response of nitrifying bacterial communities to the increased thiocyanate concentration in pre-denitrification process. *Bioresour. Technol.* **102** 913-922.

KIMURA N (2014) Metagenomics approaches to understanding phylogenetic diversity in quorum sensing. *Virulence* **5** (3) 433-442.

KORAIMANN G and WAGNER MA (2014) Social behaviour and decision making in bacterial conjugation. *Front. Cell. Infect. MI.* **4** (54) 1-7 (doi: 10.3389/fcimb.2014.00054).

KUMAR R and PAL P (2014) Membrane-integrated hybrid system for the effective treatment of ammoniacal wastewater of coke-making plant: a volume reduction approach. *Environ. Technol.* **35** (6) 2018-2027.

LAJEUNESSE MJ (2009) Meta-analysis and comparative phylogenetic method. *Am. Nat.* **174** (3) 369-381.

LEMBRE P, LORENTZ C and DI MARTINO P (2012) The complex world of polysaccharides. In Tech, Rijeka, Croatia, 371-392. ISBN: 978-953-51-0891-1.

LEMOS LN, FULTHORPE RR, TRIPLETT EW and ROESCH LFW (2011) Rethinking microbial diversity analysis in the high throughput sequencing era. *J. Microbiol. Methods* **86** 42-51.

LEU S (2009) Activated sludge process improvements: Benefits of bioaugmentation and improved monitoring. MSc dissertation, University of California, Berkeley, USA.

LEVSTEK M and PLAZL I (2009) Influence of carrier type on nitrification in the moving-bed biofilm process. *Water Sci. Technol.* **59** (5) 875-882.

LI H, HAN H, DU M and WANG W (2011) Removal of phenols, thiocyanate and ammonium from coal gasification wastewater using moving bed biofilm reactor. *Bioresour. Technol.* **102** 4667-4673.

LI C, LI XL, JI M and LIU J (2012) Performance and microbial characteristics of integrated fixed-film activated sludge systems treating industrial wastewater. *Water Sci. Technol.* **66** (2) 2785-2792.

LI W, FU L, NIU B, WU S and WOOLEY J (2012) Ultrafast clustering algorithms for metagenomic sequence analysis. *Brief. Bioinform.* **13** (6) 656-668

LI H and HAN H (2013) Effect of recycle ratio on performance of pre-nitrification moving bed biofilm reactors in treating coal gasification wastewater. *Desalin. Water Treat.* (doi:10.1080/19443994.2013.823353).

LIM J, SENG C, LIM P, NG S, TAN S and KEW S (2013) Response of low-strength phenol acclimated activated sludge to shock loading of high phenol concentrations. *Water SA* **39** (5) 695–700.

LIM J, TAN J and SENG C (2013a) Performance of phenol-acclimatised activated sludge in the presence of various phenolic compounds. *Appl. Water Sci.* **3** 515-525.

LIN Y, HE Y, KONG H, LIU B, LI Y and INAMON Y (2005) Isolation and characterization of heterotrophic nitrifying bacteria in MBR. *J. Environ. Sci.* **17** (4) 589-592.

LIU YS, HAN HJ and FANG F (2013) Application of bioaugmentation to improve the long-chain alkanes removal efficiency in coal gasification wastewater. *Fresenius Environ. Bull.* **22** (9) 2448-2455.

LIU S, SHEN L, LOU L, TIAN G, ZHENG P and HU B (2015) pH levels drive bacterial community structure in sediments of the Qiantang River as determined by 454 pyrosequencing. *Front. Microbiol.* **6** 285 (doi: 10.3389/fmicb.2015.00285).

LUI Y, TAY J, IVANOV V, MOY BY, YU L and TAY ST (2005) Influence of phenol on nitrification by microbial granules. *Process Biochem.* **40** 3285-3289.

LUTHY RG, ASCE AM, SEKEL DJ and TALLON J (1980) Biological treatment of synthetic fuel for wastewater. *J. Environ. Eng. Div.* **106** (EE3) 609–629.

MA Q, QU W, SHEN W, ZHANG Z, WANG J, LIU Z LI H and ZHOU J (2015) Bacterial community compositions of coking wastewater treatment plants in steel industry revealed by Illumina high through-put sequencing. *Bioresour Technol*. **179** 436-443.

MAAS CLA, PARKER WJ and LEGGE RL (2007) Detachment of solids and nitrifiers in IFAS systems. *WEFTEC* 1429-1449.

MAHMOOD Q, HU B, ZHENG P and AZIM MR (2009) Isolation of *Ochrobactrum* sp. QZ2 from sulphide and nitrite treatment system. *J. Hazard. Mater.* **165** 558-565.

MAKOWSKA M, SPYCHATA M and MAZUR R (2013) Removal of carbon and nitrogen compounds in hybrid bioreactors. URL: http://dx.doi.org/10.5772/53582 (Accessed 2 March 2014).

MARROT B, BARRIOS-MARTINEZ A, MOULIN P and ROCHE N (2006) Biodegradation of high phenol concentration by activated sludge in an immersed membrane bioreactor. *Biochem. Eng. J.* **30** 174–183.

MAZEMA HK, ALLY SH, KAMISH W and PETERSEN AM (2008) A pilot study into available upstream cleaner production technologies for the petroleum refining industry to meet

the requirements of the waste discharge system. WRC Report No. 1673/1/08, Water Research Commission, Pretoria, South Africa.

MAZUMDER D (2010) Simultaneous COD and ammonium nitrogen removal from a high-strength wastewater in a shaft-type aerobic hybrid reactor. *Int. J. Environ. Sci. Dev.* **1** (4) 327–332.

MEERHOLZ A and BRENT AC (2013) Assessing the sustainability of wastewater treatment technologies in the petrochemical industry. *S. Afr. J. Ind. Eng.* **24** (2) 1-11.

MENG X, LI H, SHENG Y, CAO H and ZHANG Y (2015) Analysis of a diverse bacterial community and degradation of organic compounds in a bioprocess for coking wastewater treatment. *Desalin. Water Treat.* 1-10 (doi: 10.1080/19443994.2015.1100556).

MERLO R, GERHARDT MB, BURLINGHAM F, DE LAS CASAS C, GILL E and FLIPPIN TH (2011) Petroleum refinery stripped sour water treatment using the activated sludge process. *Water Environ. Res.* **83** (11) 2067–2078.

MITRA A and MUKHOPADHYAY S (2016) Biofilm mediated decontamination of pollutants from the environment. *AIMS Bioeng* **3** (1) 44-49.

MOHAN SV, FALKENTOFT C, NANCHARAIAH YV, McSWAIN STURM BS, WATTIAU P, WILDERER PA, WUERTZ S and HAUSNER M (2009) Bioaugmentation of microbial communities in the laboratory and pilot scale sequencing batch biofilm reactors using the TOL plasmid. *Bioresour. Technol.* **100** 1746-1753.

MOHANTY SS (2012) Mixed microbial degradation of phenol: A comparative study. MSc dissertation, National Institute of Technology, Rourkela, India.

MOLVA M (2004) Removal of phenol from industrial wastewaters using lignitic coals. MSc dissertation, Izmir Institute of Technology, Izmir, Turkey.

MULCAHY G (1993) The characterization of *Pseudomonas* species from a commercial Bio-Augmentation product. PhD thesis, Dublin City University, Dublin, Ireland.

NAHED SG and SAAD AS (2008) Effect of environmental pollution by phenol on some physiological parameters of *Oreochromis niloticus*. *Global Veterinaria* **2** (6) 312-319.

NAKHLI SA, AHMADIZADEH K, FERESHTEHNEJAD M, HOSSEIN M, SAFARI RM and BORGHEI SM (2014) Biological removal of phenol from saline wastewater using a moving bed biofilm reactor containing acclimated mixed consortia. *SpringerPlus* **3** 112 (doi: 10.1186/2193-1801-3-112).

NAWAWI NM, AHMAD SA, SHUKOR MY, SYED MA and IBRAHIM AS (2014) Isolation and characterization of phenol-degrading microorganism: Recent advances. *JEBAT* **2** (1) 11-22.

NORMAN PE and TRAMBLE WW (2011) The use of bioaugmentation and ATP-based monitoring of bioactivity and stress to improve performance at a refinery WWTP. URL: http://.gewater.com/pdf/technical%20Papers_Cust/Americas/English/TP1187EN.pdf (Accessed 20 February 2013).

NOUBIGH A, MGAIDI A, ABDERRABBA M, PROVOST E and FURST W (2007) Effect of salts on the solubility of phenolic compounds: experimental measurements and modelling. *J. Sci. Food Agric*. **87** 783-788.

OECD (2010) Guidance document on horizontal gene transfer between bacteria. In: *Safety Assessment of Transgenic Organisms,* Volume **4**: *OECD Consensus Documents*. OECD Publishing, Paris. URL: http://dx.doi.org/10.1787/9789264096158-11-en (Accessed 12 March 2016).

OLAJIRE AA and ESSIEN JP (2014) Aerobic degradation of petroleum components by microbial consortia. *J. Pet. Environ. Biotechnol.* **5** (5) (doi: 10.4172/2157-7463.1000195).

OLSON ES, WORMAN JJ and DIEHL JW (1985) The formation of hydantoins in gasifier condensate water. *ASC Div. Fuel* **30** (2) 288–290.

O'SULLIVAN M (1998) The degradation of phenol and mono-chlorophenols by a mixed microbial population. PhD thesis, Dublin City University, Dublin, Ireland.

PAL P and KUMAR R (2014) Treatment of coke wastewater: A critical review for developing sustainable management strategies. *Sep. Purif. Rev.* **43** 89-123.

PARK D, LEE DS, KIM YM and PARK JM (2008) Bioaugmentation of cyanide-degrading microorganisms in a full-scale wastewater treatment facility. *Bioresour. Technol.* **99** 2082-2096.

PARKER D and WANNER J (2007) Review of methods for improving nitrification through bioaugmentation. *Water Practice* **1** (5) 1-15 (doi: 10.2175/193317707X256964).

PATIL BY (2013) Development of a bioremediation technology for the removal of cyanate from aqueous industrial wastes using metabolically active microorganisms. URL: http://dx.doi.org/10.5772/56975 (Accessed 2 March 2014).

PAVLOVICH GZ and LUTHY G (1988) Complexation of metals with hydantoins. *Water Res.* **22** (3) 327–336.

PERUMAL M, PRABAKARAN J and KAMARAJ M (2013) Isolation and characterization of potential cyanide degrading *Bacillus nealsonii* from different industrial effluents. *Int. J. Chem. Tech. Res.* **5** (5) 2357-2364.

PHALE PS, BASU A, MAJHI PD, DEVERYSHETTY J, VAMSEE-KRISHNA and SHRIVASTAVA R (2007) Metabolic diversity in bacterial degradation of aromatic compounds. *OMICS* **11** (3) 252-279.

PISHGAR R, MOUSAVI N, BAKHSHI Z and KHORRAMI M (2012) Phenol biodegradation kinetics in the presence of supplementary substrate. *Int. J. Eng. Transact. B: Appl.* **25** (3) 181-191.

PLATTES M, HENRY E, SCHOSSELER PM and WEIDENHAUPT A (2006) Modelling and dynamic simulation of a moving bed bioreactor for the treatment of municipal wastewater. *Biochem. Eng. J.* **32** 61-68.

POZO C, RODELAS B, DE LA ESCALERA S and GONZALEZ-LOPEZ J (2002) D, L-Hydantoinase activity of an *Ochrobactrum anthropi* strain. *J. Appl. Microbiol.* **92** 1028-1034.

PRADHAN B, MURUGAVELH S and MOHARTY K (2012) Phenol biodegradation by indigenous mixed microbial consortium: growth kinetics and inhibition. *Environ. Eng. Sci.* **29** (2) 86-92.

QIQI Y, QIANG H and IBRAHIM T (2012) Review on moving bed processes. *Pakistan J. Nutr.* **11** (9) 706–713.

QUAN F, YUXIAO W, TIANMIN W, HAO Z, LIBING C, CHONG Z, HONGZHANG C, XIUQIN K and XIN-HUI X (2012) Effects of packing rates of cubic-shaped polyurethane foam carriers on the microbial community and the removal of organics and nitrogen in moving bed biofilm reactors. *Bioresour. Technol.* **117** 201-207.

RAMASAMY S, MATHIYALAGAN P and CHANDRAN P (2014) Characterization and optimisation of EPS-producing and diesel oil-degrading *Ochrobactrum anthropi* MP3 isolated from refinery wastewater. *Pet. Sci.* **11** 439-445.

RATCLIFFE M, ROGERS C, MERDINGER M, PRINCE J, MABUZA T and JOHNSON CH (2006) Treatment of high strength chemical industry wastewater using moving bed biofilm reactor (MBBR) and powdered activated carbon (PAC) technology. *WEFTEC* **18** 1677–1694.

RAVA E, CHIRWA E, ALLISON P, VAN NIEKERK M and AUGUSTYN MP (2015) Removal of hard COD, nitrogenous compounds and phenols from a high strength coal gasification wastewater stream. *Water SA* **41** (4) 441-447.

RAVA E and CHIRWA E (2016) Effect of carrier fill ratio on biofilm properties and performance of a hybrid fixed-film bioreactor treating coal gasification wastewater for the removal of COD, phenols and ammonia-nitrogen. *Water Sci. Technol.* **73** (10) 2461-2467.

RAVA E, CHIRWA E, ALLISON P, VAN NIEKERK M and AUGUSTYN MP (2016) The use of exogenous microbial species to enhance the performance of a hybrid fixed-film

bioreactor treating coal gasification wastewater to meet discharge requirements. *Water SA* **42** (3) 483-489.

REVANURU S and MISHRA IM (2011) Chemical characteristics of the granular sludge from an UASB reactor treating binary mixture of catechol and resorcinol in an aqueous solution. In: *Proceedings of 2nd International Conference on Environmental Engineering and Applications* – ICEEA, August 19-21, Shangai, China, pp 128-133.

RIGO M and ALEGRE RM (2004) Isolation and selection of phenol-degrading microorganisms from industrial wastewaters and kinetics of the biodegradation. *Folia Microbiol.* **49** (1) 41-45.

ROHRBACHER F and ST-ARNAUD M (2016) Root exudation: The ecological driver of hydrocarbon rhizoremediation. *Agronomy* **6** (10) 1-25.

RORKE DCS, SUINYUY TN and KANA EBG (2017) Microwave-assisted chemical pre-treatment of waste sorghum leaves: process optimization and development of an intelligent model for determination of volatile compound fractions. *Bioresour. Technol*. **224** 590-600.

ROSE SJ and BERMUDEZ LE (2016) Identification of bicarbonate as a trigger and genes involved with extracellular DNA export in mycobacterial biofilms. MBio. **7** (6) e01597-16.

ROSSO D, LOTHMAN SE, JEUNG MK, PITT P, GELLNER WJ, STONE AL and HOWARD D (2011) Oxygen transfer and uptake, nutrient removal, and energy footprint of parallel full-scale IFAS and activated sludge processes. *Water Res*. **45** 5987-5996.

SABS (SOUTH AFRICAN BUREAU OF STANDARDS) (2007) SANS 6051:2007 (Edition 2): Water - Oil and grease content. South African National Standard (SANS) issued by Standards South Africa, a division of the South African Bureau of Standards (SABS), Pretoria, South Africa. ISBN 978-0-626-19714-8.

SANCHEZ O, FERRERA I GONZALEZ JM and MAS J (2013) Assessing bacterial diversity in a seawater-processing wastewater treatment plant by 454-pyrosequencing of the 16 rRNA and *amo*A genes. *Microbiol. Biotechnol.* **6** 435-442.

SARKAR S and MAZUMDER D (2014) Feasibility of hybrid bioreactor in the treatment of wastewater containing slowly biodegradable substances. *Int. J. Environ. Sci.* **5** (2) 383-400.

SCHAUER-GIMENEZ A, ZITOMER DH, MAKI JS and STRUBLE CA (2010) Bioaugmentation for improved recovery of anaerobic digesters after toxicant exposure. *Water Res.* **44** (12) 3555-3564.

SCHMIDT CE, SHARKEY AG and FRIEDEL RA (1974) Mass spectrometric analysis of product water from coal gasification.
URL: http://babel.hathitrust.org/cgi/pt?id=mdp.39015077582776;view=1up;seq=3
(Accessed 8 February 2014).

SEMRANY S, FAVIER L, DJELAL H, TAHA S and AMRANE A (2012) Bioaugmentation: Possible solutions in the treatment of bio-refractory organic compounds (Bio-ROCs). *Biochem. Eng. J.* **69** 75-86.

SEN D, RANDALL CW, COPITHORN RR, HUHTAMAKI M, FARREN G and FLUORNOY W (2007) The importance of aerobic mixing, biofilm thickness control and modelling on the success or failure of IFAS systems for biological nutrient removal. *Water Pract.* **1** (5) 1-16.

SEN D and RANDALL CW (2008) Improved computational model (Aquifas) for activated sludge, integrated fixed-film activated sludge, and moving-bed biofilm reactor systems, Part II Multilayer biofilm diffusion model. *Water Environ. Res.* **80** (7) 624–632.

SEWSYNKER Y and KANA EGB (2016) Intelligent models to predict hydrogen yield in dark microbial fermentations using existing knowledge. *Int. J. Hydrogen Energy* **41** 12929-12940.

SHAH MP, SEBASTIAN S, MATHUKIYA HM and DARJI AM (2012) Biodegradation of phenol by an application of *Pseudomonas* spp. ETL-2414. *Int. J. Bio. Eng. Technol.* **3** (2) 6-11.

SHAHOT K, IDRIS A, OMAR R and YUSOFF HM (2014) Review of biofilm processes for wastewater treatment. *Life Sci. J.* **11** (11) 1-13.

SHARMA NK and PHILIP L (2014) Treatment of phenolics, aromatic hydrocarbons, and cyanide-bearing wastewater in individual and combined anaerobic, aerobic, and anoxic bioreactors. *Appl. Biochem. Biotechnol.* **175** (1) 300-322.

SILVA CC, VIERO AF, DIAS AC, ANDREOTE FD, JESUS EC, DE PAULA SO, TORRES AP, SANTIAGO VM and OLIVEIRA VM (2010) Monitoring the bacterial community dynamics in a petroleum refinery wastewater membrane bioreactor fed with high phenolic load. *J. Microbiol. Biotechnol.* **20** (1) 21-29.

SILVA CC, HAYDEN H, SAWBRIDGE T, MELE P, DE PAULA SO, SILVA LCF, VIDIGAL PMP, VICENTINI R, SOUSA MP, TORRES APR and SANTIAGO VMJ (2013) Identification of genes and pathways related to phenol degradation in metagenomics libraries from petroleum refinery wastewater. *PLoS ONE* **8** (4) e61811 (doi: 10.1371/journal.pone.006 1811).

SIMON MA, BONNER JS, PAGE CA, TOWNSEND RT, MUELLER DC, FULLER CB and AUTENRIETH RL (2004) Evaluation of two commercial bioaugmentation products for enhanced removal of petroleum from a wetland. *Ecol. Eng.* **23** 263-277.

SKEPU ZG (2000) Characterization of amide bond hydrolysis in novel hydantoinase-producing bacteria. MSc dissertation, Rhodes University, Grahamstown, South Africa. URL: http://hdl.handle.net/10962/d1003970 (Accessed 5 January 2014).

SKONDE MP (2009) Sulphur behaviour and capturing during a fixed bed gasification process of coal. PhD thesis, North-West University, Potchefstroom, South Africa. URL: https://repository.nwu.ac.za/handle/10394/2333 (Accessed 6 March 2013).

SLADE AH, THORN GJ and DENNIS MA (2011) The relationship between BOD:N ratio and wastewater treatability in a nitrogen-fixing wastewater treatment system. *Water Sci. Technol.* **63** (4) 627-632.

SOLJAN MG, BAN S, DRAGICEVIC L, SOLJAN V and MATIC V (2001) Granulated mixed microbial culture suggesting successful employment of bioaugmentation in the treatment of process wastewaters. *Chem. Biochem. Eng. Q.* **15** (3) 87-94.

SOROKIN DY, TOUROVA TP, LYSENKO AM and KUENEN JG (2001) Microbial thiocyanate utilization under highly alkaline conditions. *Appl. Environ. Microbiol.* **67** (2) 528-538.

STAMOUDIS VC and LUTHY RG (1980) Biological removal of organic constituents in quench water from a slagging, fixed-bed coal gasification pilot plant. United States Department of Energy (contract W-32-109-Eng-38).
URL: http://www.osti.gov/scitech/servlets/purl/5531569 (Accessed 2 January 2014).

STEPHENSON D and STEPHENSON T (1992) Bioaugmentation for enhancing biological wastewater treatment. *Biotechnol. Adv.* **10** 549-559.

SZÉKELY AJ (2008) Analysis and application of bacterial diversity methods in wastewater microbiology research. PhD thesis, Eötvös Loránd University, Budapest, Hungary.

TAN CH, KOH KS, XIE C, ZHANG J, TAN XH, LEE GP, ZHOU Y NG WJ, RICE SA and KJELLEBERG S (2015) Community quorum sensing signalling and quenching: microbial granular biofilm assembly. *NPJ Biofilms Microbiomes* **1** (doi: 10.1038/npjbiofilms.2015.6).

TATARKO M (2008) Waste water treatment. United States Patent Application Publication US 2008/0251450 A1.

TATARKO M (2010) Waste water treatment. United States Patent Application Publication US 2010/0213122 A1.

TODAR K (2006) *Todar's Online Textbook of Bacteriology*. Department of Bacteriology, University of Wisconsin-Madison, Madison, WI, USA.

TOERIEN A and VAN NIEKERK A (2013) Sasol gasification effluent treatment process: Conceptual engineering review. Report No 12614862, Unpublished internal document, Golder Associates Africa (Pty) Ltd, South Africa.

TOP EM, SPRINGAEL D and BOON N (2002) Catabolic mobile genetic elements and their potential use in bioaugmentation of polluted soils and rivers. *FEMS Microbiol. Ecol.* ***42*** 199-208.

TORRESI E, FOWLER SJ, POLESEL F, BESTER K, ANDERSEN HR, SMETS BF, PLOSZ BG and CHRISTENSSON M (2016) Biofilm thickness influences biodiversity in nitrifying MBBRs - Implications on micropollutant removal. *Environ. Sci. Technol.* **50** (17) 9279-9288.

TURNER C, DIEPOLDER P and STRAIN J (1985) Biological nitrification and hydantoin removal in coal gasification wastewater. In: *Proceedings of the 40th Industrial Waste Conference*, 14–16 May 1985, Indiana, USA.

TURNER C and WERNBERG K (1985) Biological treatment of high strength ammonia wastewater using a four stage RBC. In: *Proceedings of the North Dakota Academy of Science – 77th Annual meeting*, 26-28 April 1985, Dakota, USA.

TZIRITA M (2012) A characterisation of bioaugmentation products for the treatment of waste fats, oils and grease (FOG). PhD thesis, Dublin City University, Dublin, Ireland.

USEPA (UNITED STATES ENVIRONMENTAL PROTECTION AGENCY) (1983) EPA Method 300.0: Determination of Inorganic Anions by Ion Chromatography. In: *Methods for Chemical Analysis of Water and Wastes*, US EPA Report-600/4-79-020. Environmental Monitoring and Support Laboratory, US Environmental Protection Agency, Washington, DC, USA.

VAN ZYL J (2008) Anaerobic digestion of Fischer-Tropsch reaction water. PhD thesis, University of Cape Town, Cape Town, South Africa.

VAN DER WERF MJ, KEIJZER PM and VAN DER SCHAFT PH (2001) *Xanthobacter* sp. C20 contains novel bioconversion pathway for limonene. *J. Biotechnol.* **84** (2) 133-143.

WAGNER M, LOY A, NOGUEIRA R, PURKHOLD U, LEE N and DAIMS H (2002) Microbial community composition and function in wastewater treatment plants. *Anton. Leeuw. Int. J.* **81** 665-680.

WANG S and LOH K (1999) Modeling the role of metabolic intermediates in kinetics of phenol biodegradation. *Enzyme Microbiol. Technol*. **25** 177–814.

WANG X, HU M, XIA Y, WEN X and DING K (2012) Pyrosequencing analysis of bacterial diversity of 14 wastewater treatment systems in China. *Appl. Environ. Microbiol.* **78** (19) 7042-7047.

WARD JP and KING JR (2012) Thin-film modelling of biofilm growth and quorum sensing. *J. Eng. Math*. **73** (1) 71-92.

WASILKOWSKI D, SWĘDZIOŁ Z and MROZIK A (2012) The applicability of genetically modified microorganisms in bioremediation of contaminated environments. *CHEMIK* **8** (66) 822-826.

WEI I and GOLDSTEIN DJ (1977) Biological treatment of coal conversion. URL: https://repository.library.northeastern.edu/files/neu:329980 (Accessed 5 June 2014).

WERNBERG KB, STRAIN JH, TURNER CD and GALLAGHER JR (1984) Treatment of coal gasification wastewater using rotating biological contactors.
URL: http://65.54.113.26/Publication/60401434 (Accessed 3 February 2015).

WHITEMAN RJ (2010) Methods for reducing the cost required for coming into compliance. United States Patent Number US2010/0096323 A1.

WHITEMAN JK and KANA EBG (2014) Comparative assessment of the artificial neural network and response surface modelling efficiencies for biohydrogen production on sugar cane molasses. *Bioenerg. Res.* **7** 295-305 (doi: 10.1007/s12155-013-9375-7).

WIJEYEKOON S, MINO T, SATOH H and MATSUO T (2004) Effects of substrate loading rate on biofilm structure. *Water Res*. **38** (10) 2479-2488.

WORLD BANK GROUP (2007) *Environmental, Health and Safety (EHS) Guidelines for Petroleum Refining*. URL: http://www.ifc.org/wps/wcm/connect/f73fca004e7bd2ce97b1bffce

4951bf6/2013+Working+Doc_Petroleum+Refining.pdf?MOD=AJPERES (Accessed 6 June 2014).

WOZNICA A, NOWAK A, KARCZEWSKI J, KLIS C and BERNAS T (2010) Automatic biodetector of water toxicity (ABTOW) as a tool for examination of phenol and cyanide contaminated water. *Chemosphere* **81** 767-772.

YANG C, QIAN Y, ZHANG L and FENG J (2006) Solvent extraction process development and on-site trial-plant for phenol removal from industrial coal-gasification wastewater. *Chem. Eng. J.* **117** 179-185.

YANG C, YANG S, QIAN Y, GUO J and CHEN Y (2013) Simulation and operation cost estimate for phenol extraction and solvent recovery process of coal-gasification wastewater. *Ind. Eng. Chem. Res.* **52** 12108-12115.

YELEBE ZR and PUYATE YT (2012) Effect of bioaugmentation on aerobic digestion of biodegradable organic waste. *J. Appl. Technol. Environ. Sanit.* **2** (3) 165-174.

YONG YC and ZHONG JJ (2013) Regulation of aromatics biodegradation by *rhl* quorum sensing system through induction of catechol meta-cleavage pathway. *Bioresour. Technol.* **136** 761-765.

YU Z, CHEN Y, FENG D and QIAN Y (2010) Process development, simulation and industrial implementation of a new coal-gasification wastewater treatment installation for phenol and ammonia removal. *Ind. Eng. Chem. Res*. **49** 2874-2881.

ZACHOPOULOS SA and HUNG YT (1990) Effect of bioaugmentation on activated sludge biokinetics. *Acta Hydrochim. Hydrobiol*. **18** (5) 591-603.

ZHANG Y, CHEN L, SUN R, DAI T, TIAN J, LIU R and WEN D (2014) Effect of wastewater disposal on the bacterial and archaeal community of sea sediment in an industrial area in China. *FEMS Microbiol. Ecol.* **88** 320-332.

ZHANG W and LI C (2016) Exploiting quorum sensing interfering strategies in gram-negative bacteria for the enhancement of environmental applications. *Front. Microbiol.* **6** (doi:10.3389/fmicb.2015.0135).

ZHANG W, RAO P, ZHANG H and XU J (2009) The role of diatomite particles in the activated sludge system for treating coal gasification wastewater. *Chinese J. Chem. Eng.* **17** (1) 161-170.

ZHAO L, MA F, GUO J and ZHOA Q (2007) Petrochemical wastewater treatment with a pilot-scale bioaugmented biological treatment system. *J. Zhejiang Univ. Sci. A.* **8** (11) 1831-1838.

ZHAO Q, HAN H, XU C, ZHUANG H, FANG G and ZHANG L (2013) Effect of powdered activated carbon technology on short-cut nitrogen removal of coal gasification wastewater. *Bioresour. Technol.* **142** 179-185.

ZHAO Q, HAN H, HOU B, ZHUANG H, JIA S and FANG F (2014) Nitrogen removal from coal gasification wastewater by activated carbon technologies combined with short-cut nitrogen removal process. *J. Environ. Sci*. **26** 2231-2239.

ZHOU X, LI Y, ZHAO Y and YUE X (2012) Pilot-scale anaerobic/anoxic/oxic/oxic biofilm process treating coking wastewater. *J. Chem. Technol. Biotechnol.* **8** 305-310.

ZHOU X, LI Y and ZHAO Y (2014) Removal characteristics of organics and nitrogen in a novel four-stage biofilm integrated system for enhanced treatment of coking wastewater under different HRTs. *RSC Adv.* **4** 51620-15629.

ZIMMERMAN J, JAHN R and GEMEINHOLZER B (2011). Barcoding diatoms: evaluation of the V4 subregion on the 18S rRNA gene, including new primers and protocols. *Org. Divers. Evol.* **11** 173-192 (doi: 10.1007/s13127-011-0050-6).
URL: http://www.bgbm.org/sites/default/files/documents/Zimmermann%20et%20al%202011%20Barcoding%20diatoms.pdf (Accessed 4 October 2015).

APPENDICES

Appendix A

Table A-1: Organic compounds detected in the feed and effluent (>80% fit by GC-MS)

Organic compound	Empirical formula
2-Butenoic acid	$C_4H_6O_2$
2-Pentenoic acid	$C_5H_8O_2$
2-Methyl-2-pentenoic acid	$C_6H_{10}O_2$
Hexanoic acid	$C_6H_{12}O_2$
Heptanoic acid	$C_7H_{14}O_2$
Octanoic acid	$C_8H_{16}O_2$
Hexadecanoic acid	$C_{16}H_{32}O_2$
Octadecadienoic acid	$C_{18}H_{36}O_2$
2-Methylbenzoic acid; 3-methylbenzoic acid; 4-methylbenzoic acid	$C_8H_8O_2$
3,4-Dimethylbenzoic acid; 2,5-dimethylbenzoic acid;3,5-dimethylbenzoic acid	$C_9H_{10}O_2$
4,1-Methylethylbenzoic acid	$C_{10}H_{12}O_2$
4-Ethylbenzoic acid	$C_{11}H_{14}O_2$
2-Methylcyclopentanone; 3-methylcyclopentanone; Phenol	C_6H_6O
1,2-Benzenediol (catechol)	$C_6H_6O_2$
2-Methyl-1,4-benzenediol	$C_7H_8O_2$
2,5-Dimethylfuran; 2-Methyl-2-cyclopenten-1-one; 3-Methyl-2-cyclopenten-1-one	C_6H_8O
3,4-Dimethyl-2-cyclopenten-1-one; 2,3-Dimethyl-2-cyclopenten-1-one	$C_7H_{10}O$
4-Phenyl-3-buten-2-one	$C_{10}H_{10}O$
2-Methyl-p-benzoquinone	$C_7H_6O_2$
2,5-Dimethyl-p-benzoquinone; 2,6-Dimethyl-p-benzoquinone	$C_8H_8O_2$
Aniline	$C_6H_5NH_2$
2-Methyl-1H-benzimidazole	$C_8H_8N_2$
3-Methylpyridine	C_6H_7N
1(2H)-isoquinolinone	C_9H_7N
6-Methyl-1H-indole	C_9H_9N
4-Methylbenzamide	C_8H_9NO
2,6-Dimethylphenyl isocyanate	C_9H_9NO
5-Isoquinolinol	$C_{10}H_7NO$
2-Methyl-8-quinolinol	$C_{10}H_9NO$
1-Methyl-2-acetylindole	$C_{11}H_{11}NO$
5-Ethyl-5-methyl-hydantoin (EMH)	$C_6H_{10}N_2O_2$
5,5-Dimethyl-hydantoin (DMH)	$C_5H_8N_2O_2$

[a] Detection limit: 25 µg/L

Table A-2: SVOC and PAHs in the feed and effluent samples

SVOC-PAHs	Result (µg/L)
Naphthalene	<24
Acenaphthylene	<26
Acenaphthene	<34
Fluorene	<19
Phenanthrene	<28
Anthracene	<46
Fluoranthene	<38
Pyrene	<30
Benzo(a)anthracene	<34
Chrysene	<33
Benzo(b)fluoranthene	<44
Benzo(k)fluoranthene	<45
Benzo(a)pyrene	<44
Indeno (1;2;3-cd)pyrene	<70
Dibenzo (a;b) anthracene	<75
Benzo (ghi) perylene	<56

[a] < below test method detection limit

Appendix B

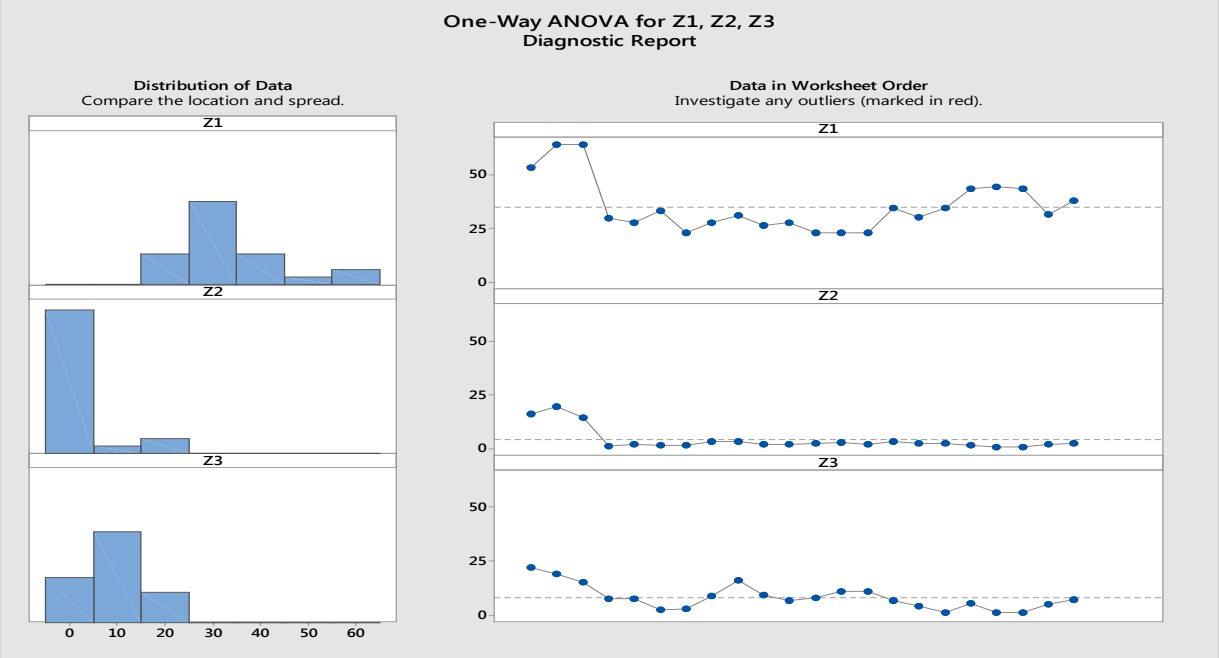

Figure B-1: Biofilm thickness (µm) in Zone (Z1), Zone 2 (Z2) and Zone 3 (Z3) during the operation of the H-FFBR (Week 1 to Week 12)

x-axis: Weekly samples (2 data points per week except week 11 and week 12 only 1 data point);

y-axis: Biofilm thickness (µm)

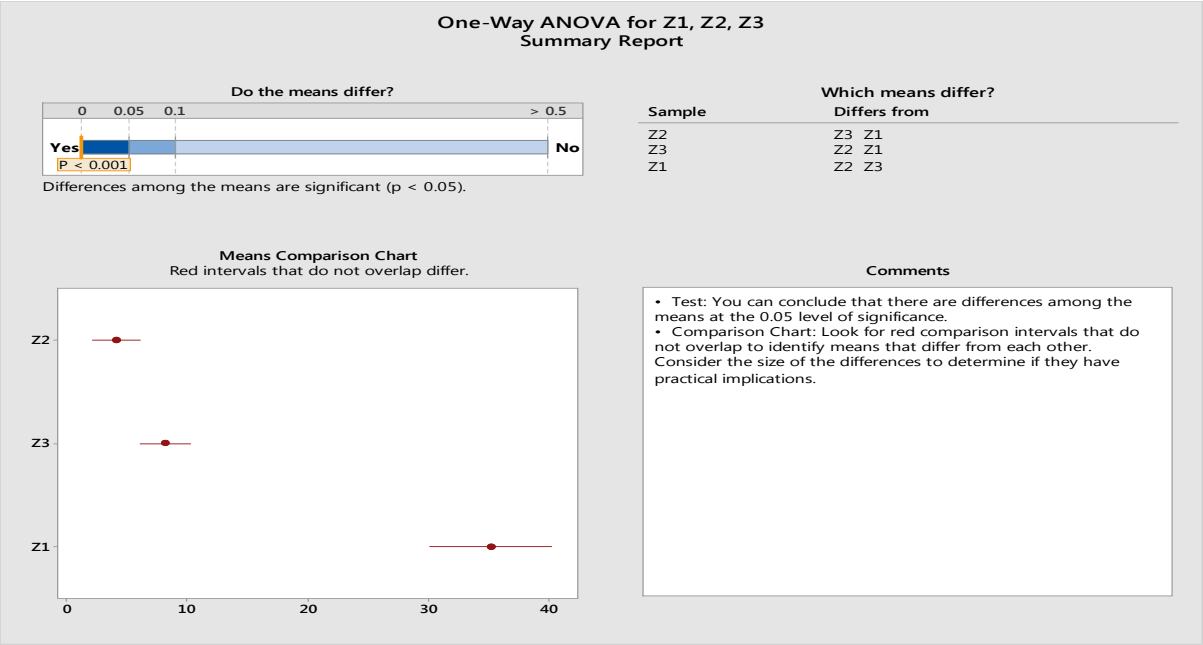

Figure B-2: Significance of difference in biofilm thickness (µm) between Zone 1 (Z1), Zone 2 (Z2) and Zone (Z3) during the operation of the H-FFBR (Week 1 to Week 12)

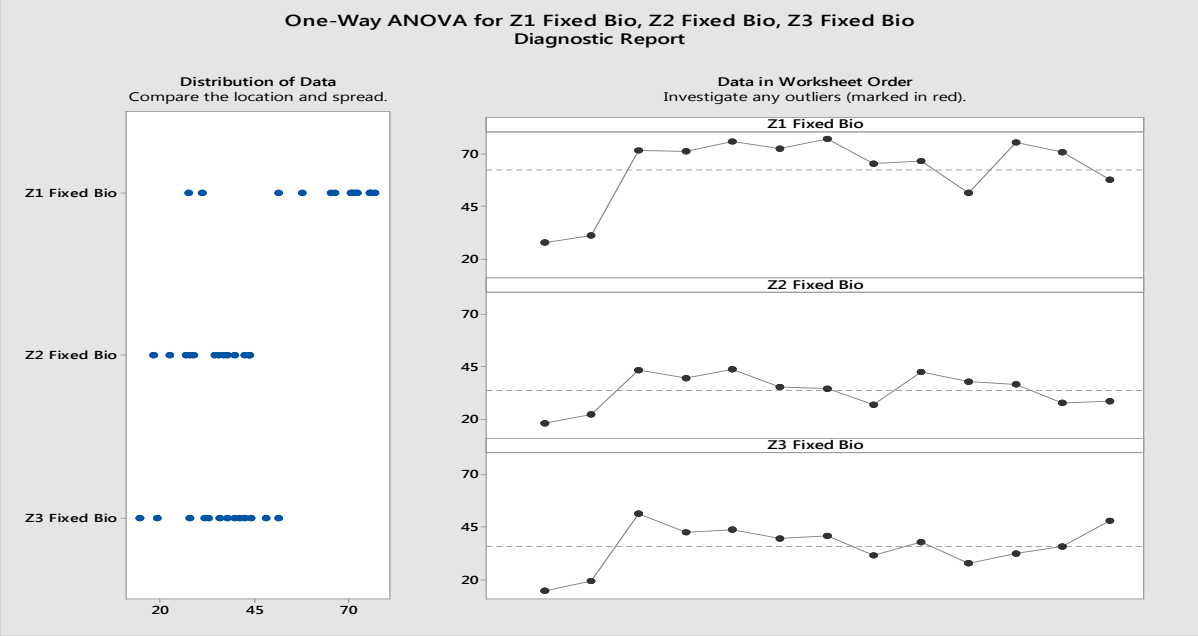

Figure B-3: Fixed biomass OUR (mg O_2/L.h) in Zone 1 (Z1), Zone 2 (Z2) and Zone 3 (Z3) during the operation of the H-FFBR (Week 1 to Week 12)

x-axis: Weekly samples (each data point represents the weekly sample result; 2 samples tested in Week 12); **y-axis**: OUR (mg O_2/L.h)

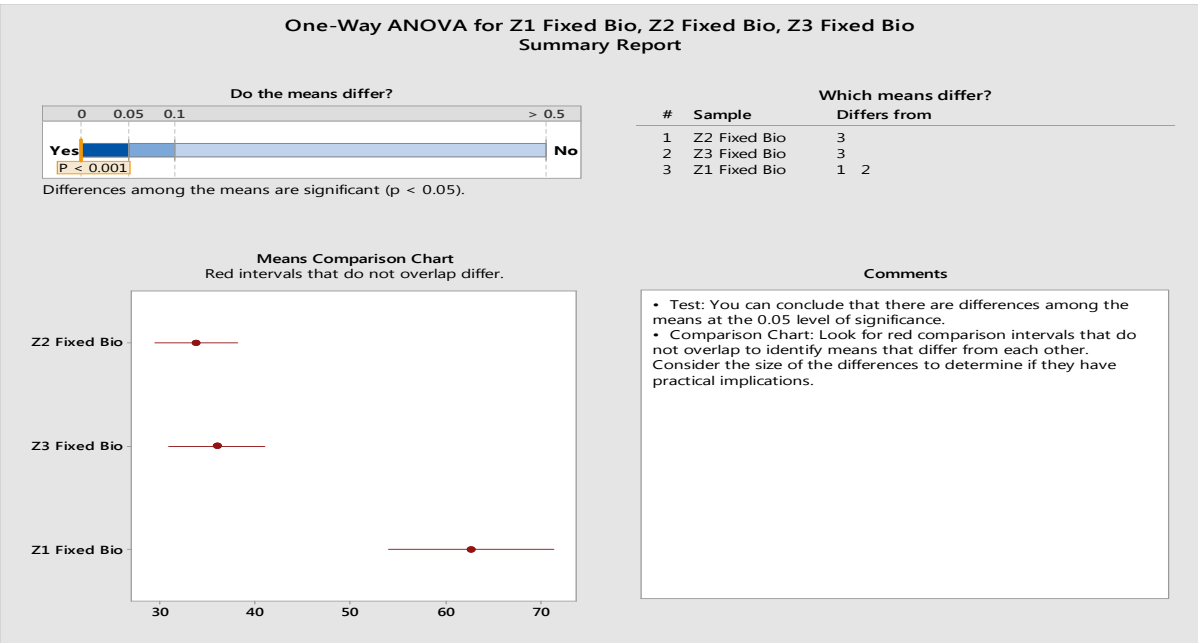

Figure B-4: Significance of difference in fixed biomass OUR (mg O_2/L.h) between Zone 1 (Z1), Zone 2 (Z2) and Zone 3(Z3) during the operation of the H-FFBR (Week 1 to Week 12)

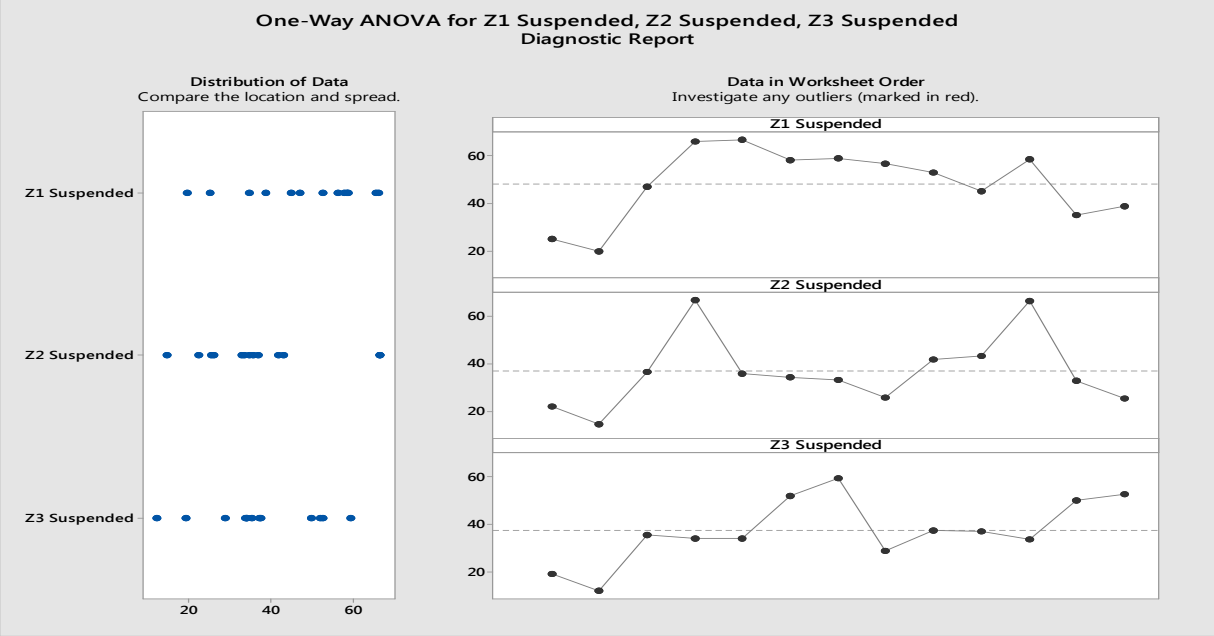

Figure B-5: Suspended biomass OUR (mg O_2/L.h) in Zone 1 (Z1), Zone 2 (Z2) and Zone 3 (Z3) during the operation of the H-FFBR (Week 1 to Week 12)

x-axis: Weekly sample (each data point represents the weekly result; 2 samples tested in week 12); **y-axis**: OUR (mg O_2/L.h)

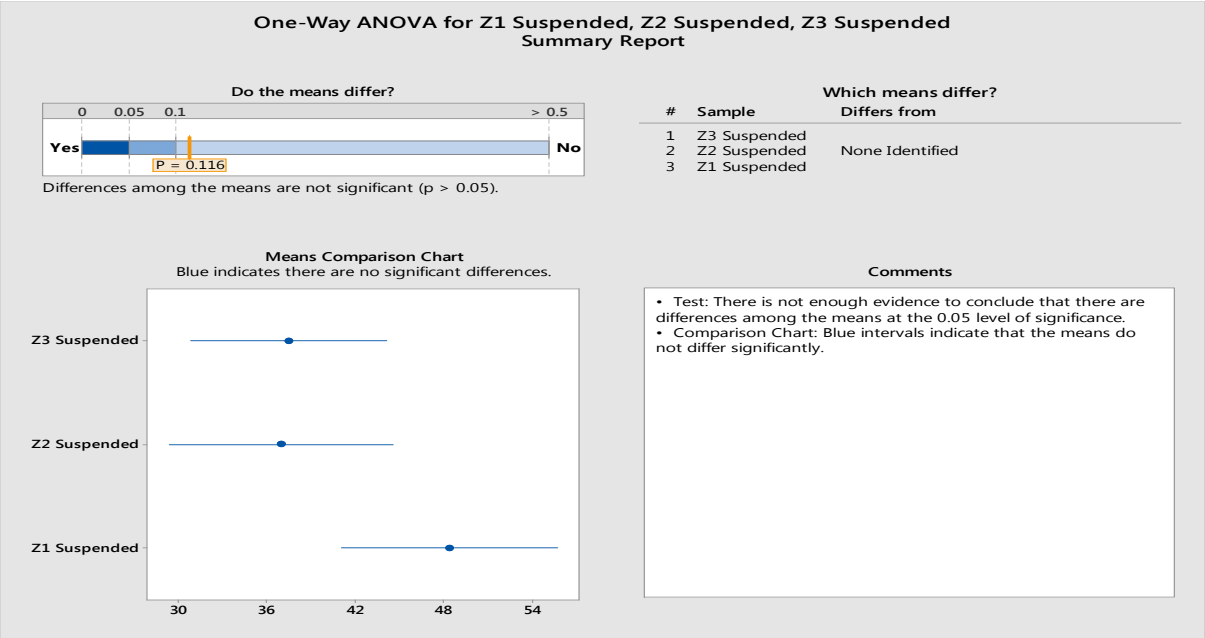

Figure B-6: Significance of difference in suspended biomass OUR (mg O_2/L.h) in Zone 1 (Z1), Zone 2 (Z2) and Zone 3 (Z3) during the operation of the H-FFBR (Week 1 to Week 12)

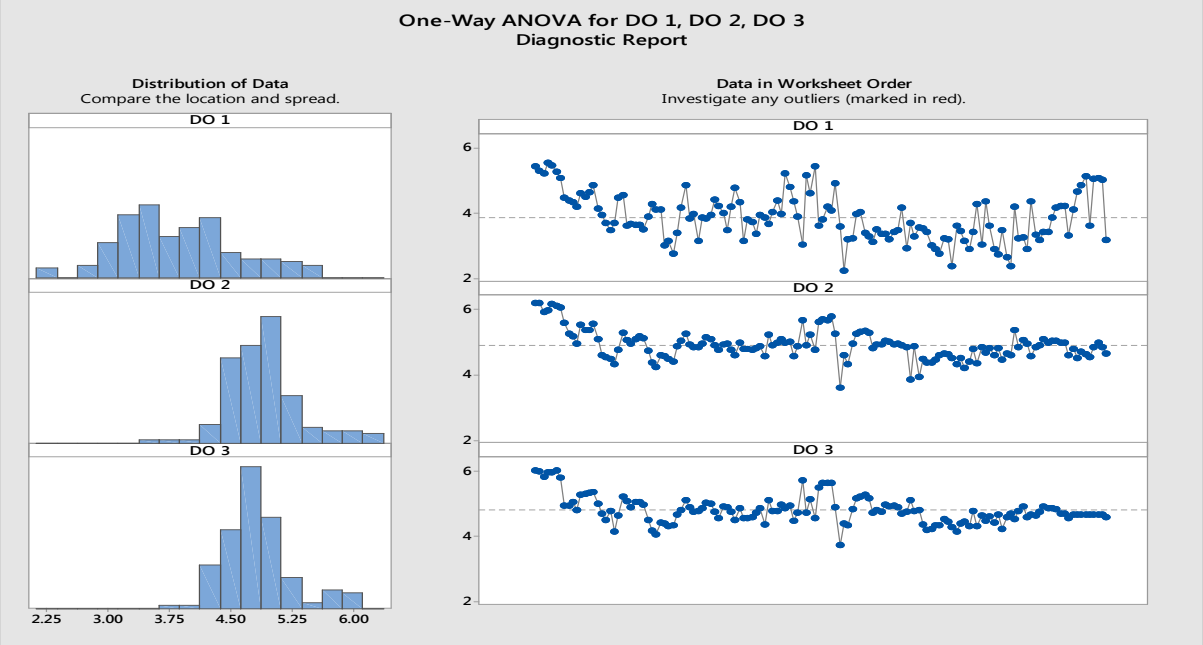

Figure B-7: DO (mg O_2/L) in Zone 1 (DO2), Zone 2 (DO2) and Zone 3 (DO3) during the operation of the H-FFBR (Week 1 to Week 12)

x-axis: Individual daily samples (each data point is the daily result); **y-axis**: DO (mg O_2/L)

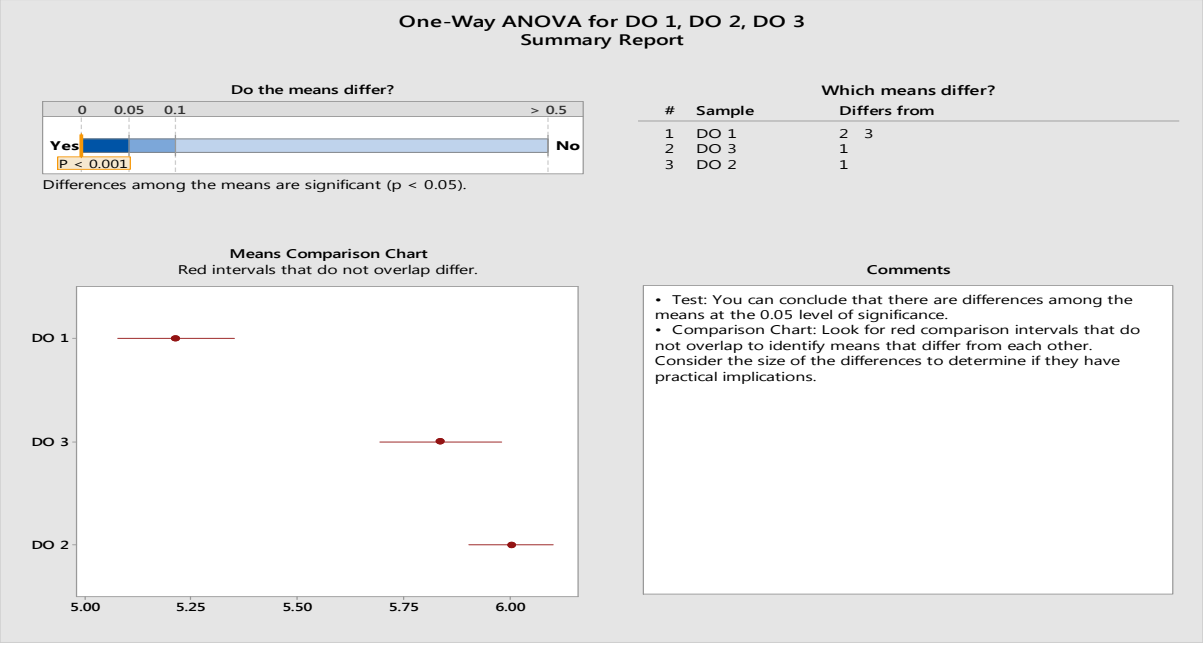

Figure B-8: Significance of difference in DO between Zone 1 (DO1), Zone 2 (DO2) and Zone 3 (DO3) during the operation of the H-FFBR (Week 1 to Week 12)

Appendix C

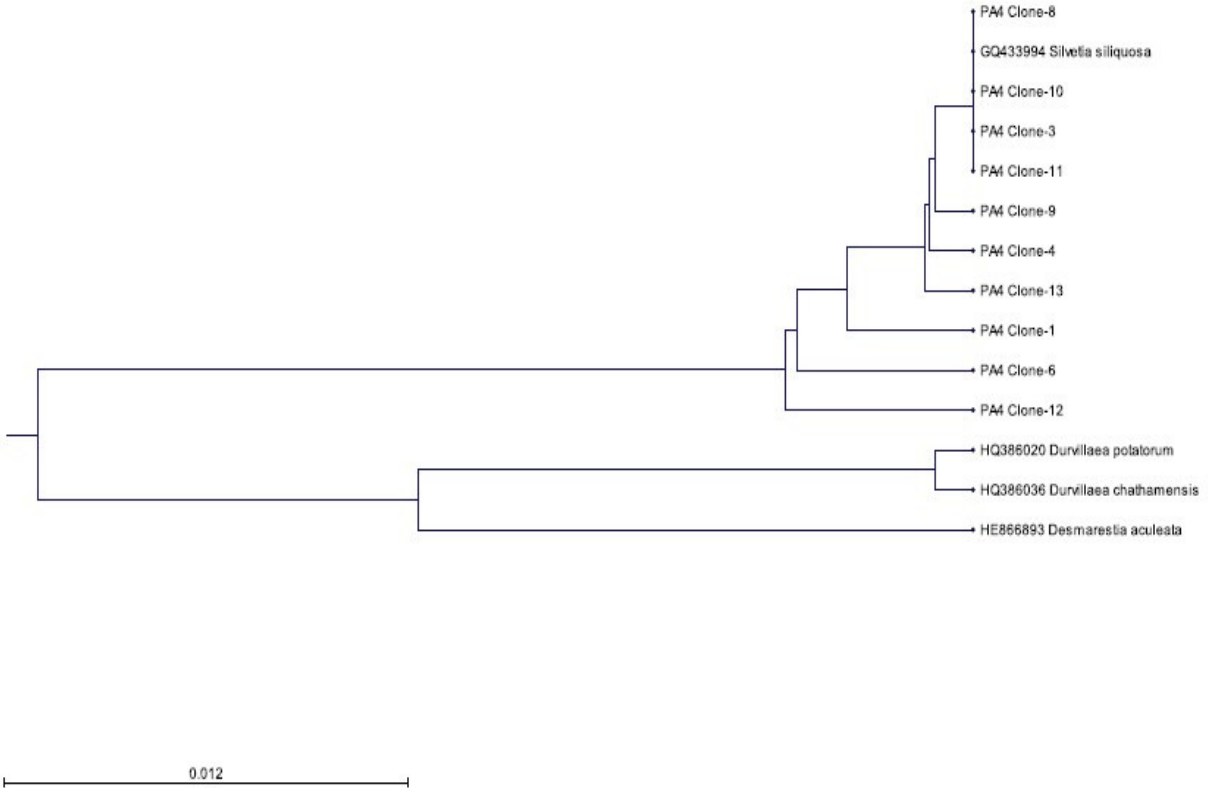

Figure C-1: Phylogenetic tree for inoculum PA4. The scale bar (0.012) represents evolutionary distance.

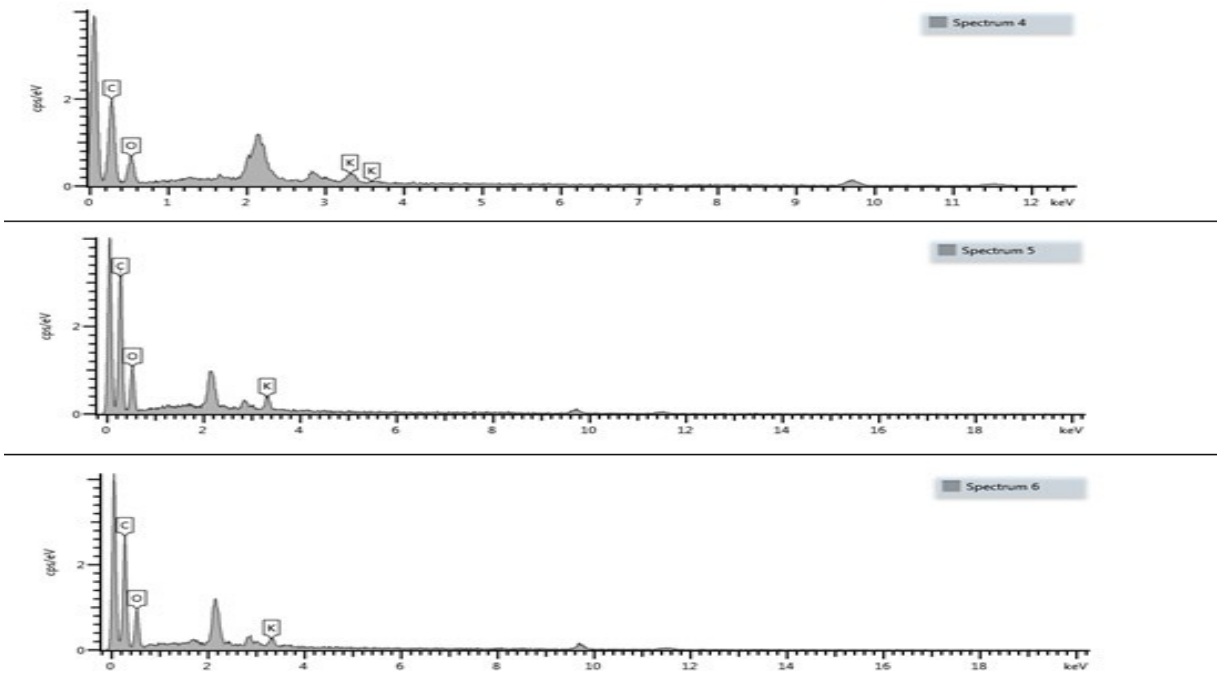

Figure C-2: EDX of inoculum PA1 performed in triplicate (EDX Spectrum 4, 5, and 6)

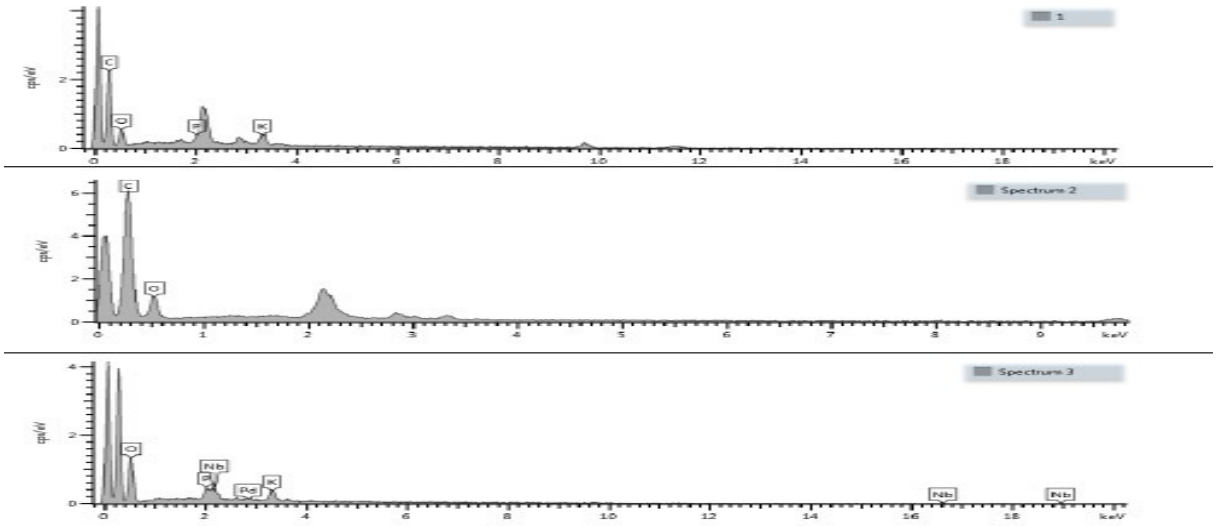

Figure C-3: EDX of inoculum PA2 performed in triplicate (EDX Spectrum 1, 2, and 3)

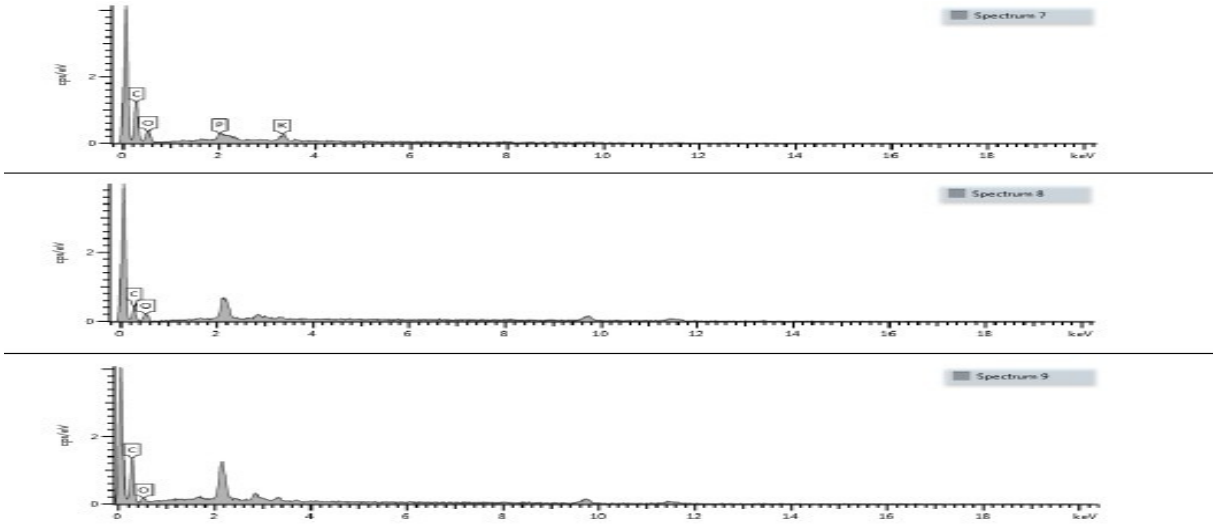

Figure C-4: EDX of inoculum PA3 performed in triplicate (EDX Spectrum 7, 8 and 9)

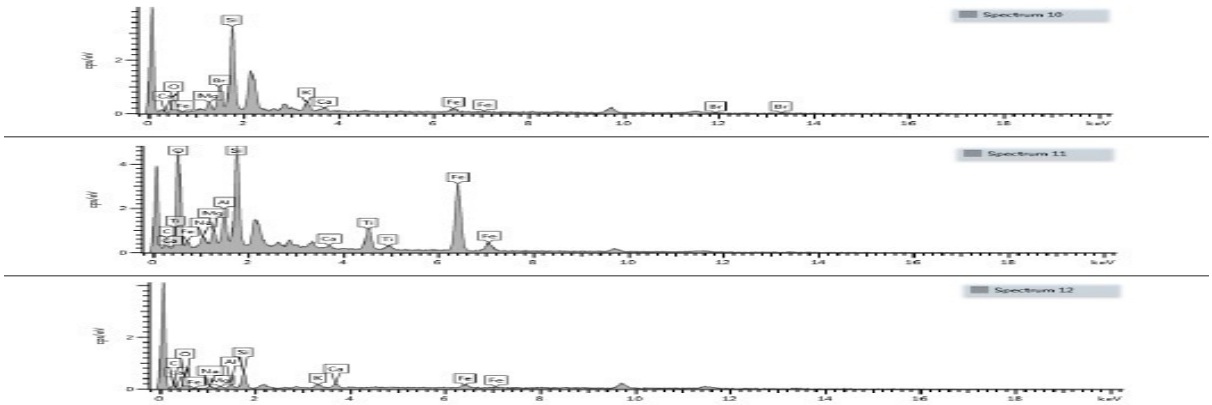

Figure C-5: EDX of inoculum PA4 performed in triplicate (EDX Spectrum 10, 11 and 12)

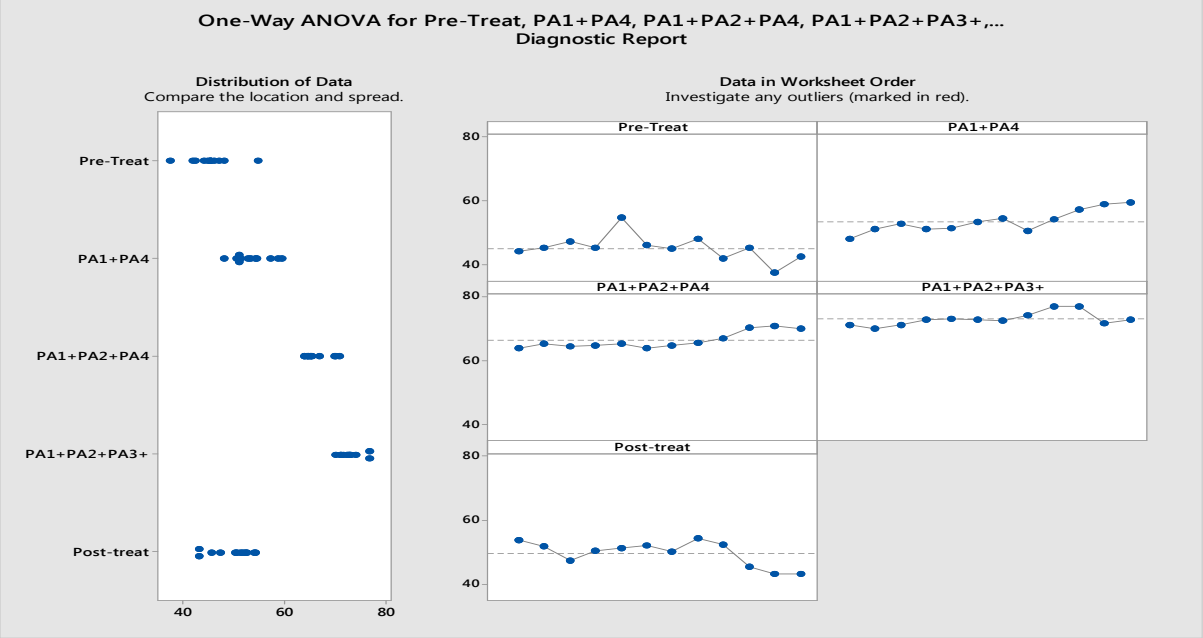

Figure C-6: COD removal during the operation of the H-FFBR with and without bioaugmentation (Week 1 to Week 65)

x-axis: Weekly average COD value (each data point represents the average of 5 samples tested per week); **y-axis**: % COD removal

Where:

Week 1-12: Pre-treatment (baseline data; no bioaugmentation)

Week 13-24: PA1+PA4 (Bioaugmentation Regime 1)

Week 24-36: PA1+PA2+PA4 (Bioaugmentation Regime 2)

Week 37-48: PA1+PA2+PA3+PA4 (Bioaugmentation Regime 3)

Week 49-65: Post-treatment (no bioaugmentation)

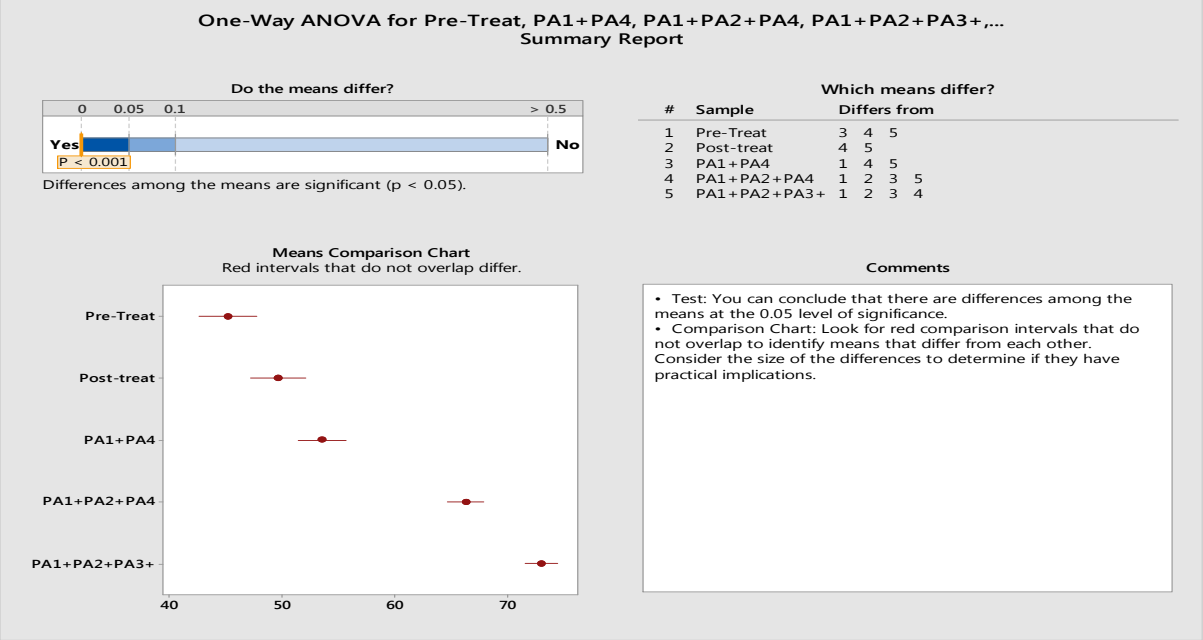

Figure C-7: Significance of difference in COD removal during the operation of the H-FFBR with and without bioaugmentation (Week 1 to Week 65)

Appendix D

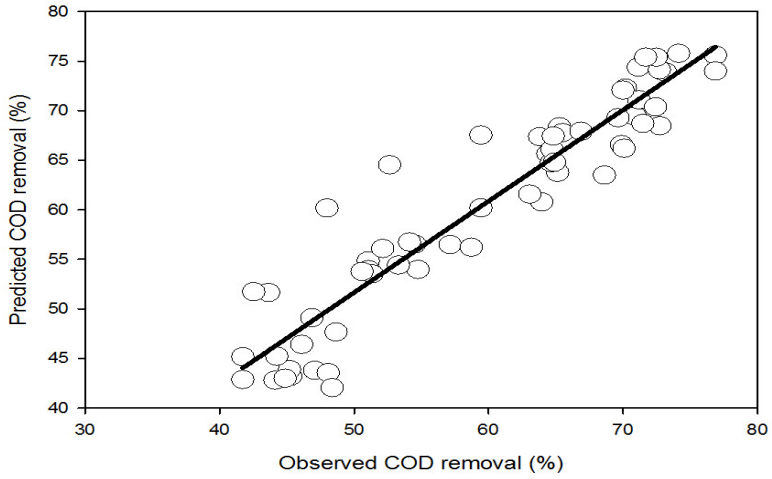

Figure D-1: Regression plot showing the predicted versus observed COD removal values, exhibiting an R^2 value of 0.89

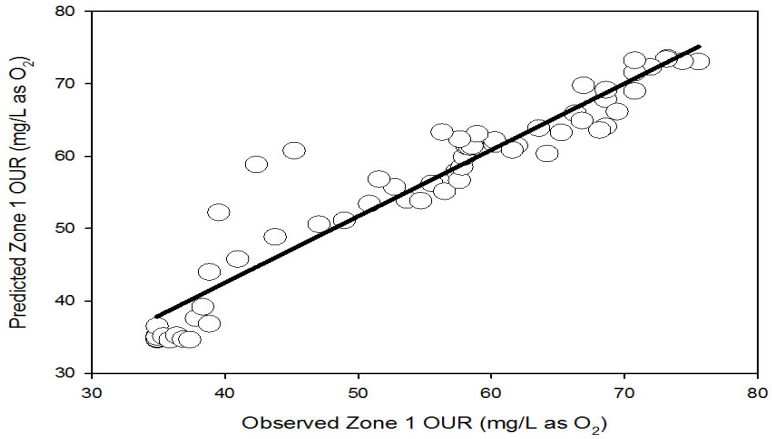

Figure D-2: Regression plot showing the predicted versus observed Zone 1 oxygen uptake rate values, exhibiting an R^2 value of 0.91

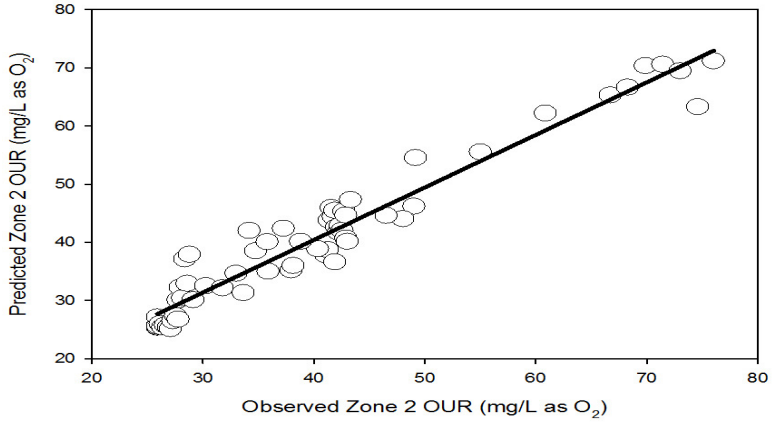

Figure D-3: Regression plot showing the predicted versus observed Zone 2 oxygen uptake rate values, exhibiting an R^2 value of 0.94

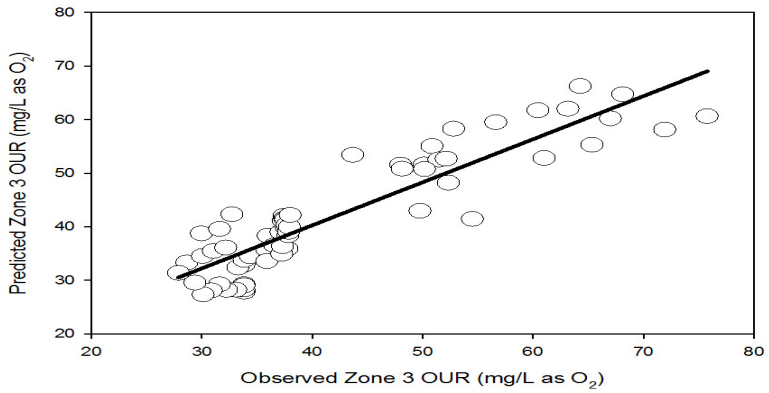

Figure D-4: Regression plot showing the predicted versus observed Zone 3 oxygen uptake rate values, exhibiting an R^2 value of 0.82

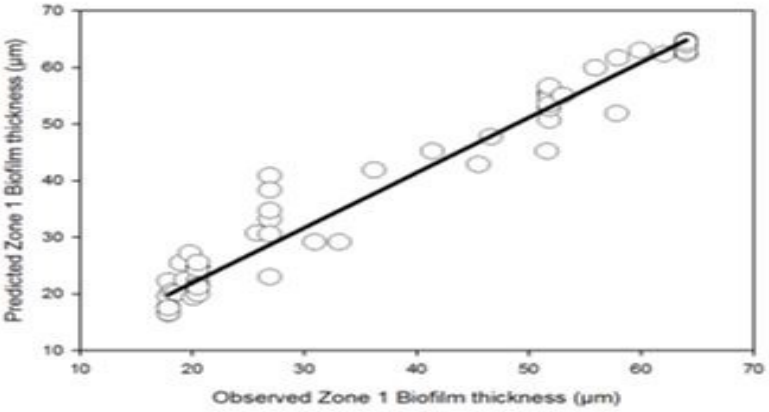

Figure D-5: Regression plot showing the predicted versus observed Zone 1 biofilm thickness values, exhibiting an R^2 value of 0.96

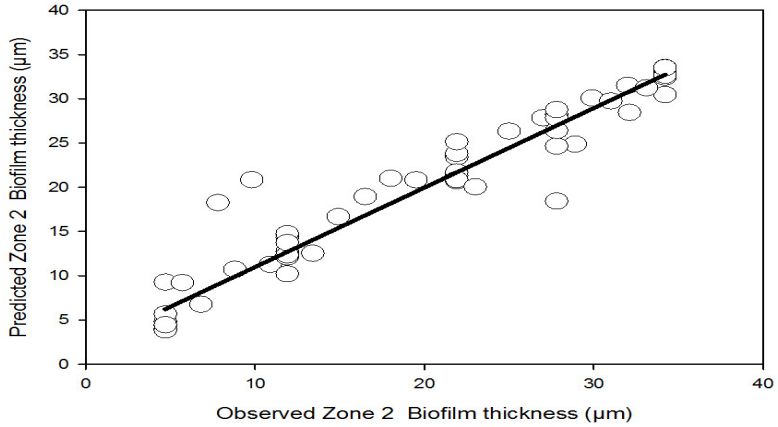

Figure D-6: Regression plot showing the predicted versus observed Zone 2 biofilm thickness values, exhibiting an R^2 value of 0.93

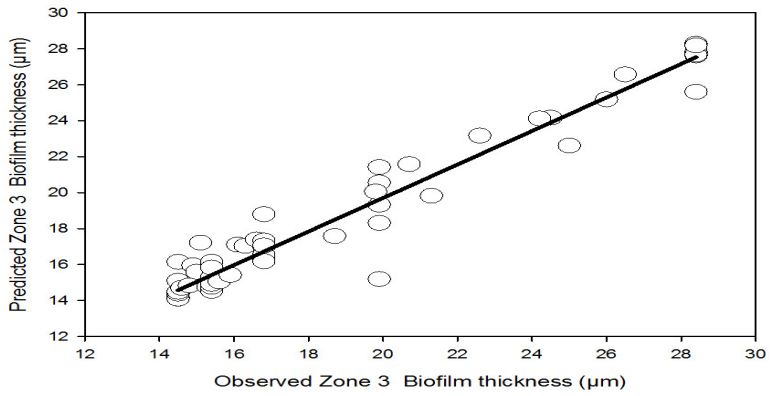

Figure D-7: Regression plot showing the predicted versus observed Zone 3 biofilm thickness values, exhibiting an R^2 value of 0.95

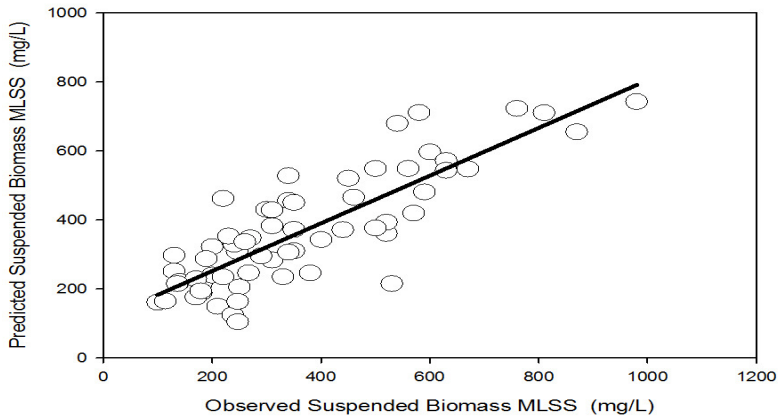

Figure D-8: Regression plot showing predicted versus observed suspended biomass values, exhibiting an R^2 value of 0.70

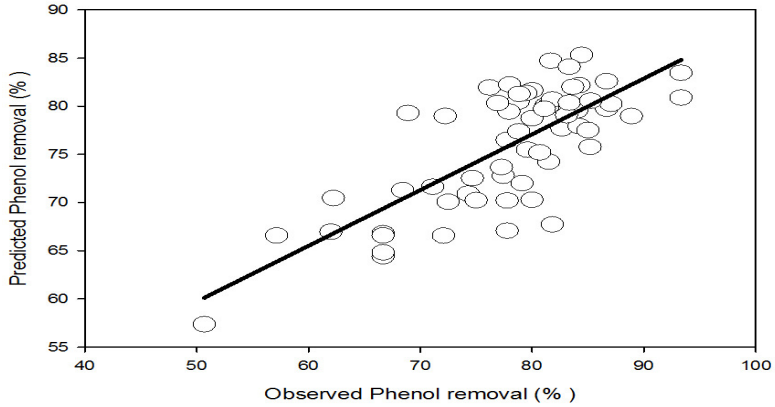

Figure D-9: Regression plot showing the predicted versus observed phenol removal values, exhibiting an R^2 value of 0.57

Appendix E

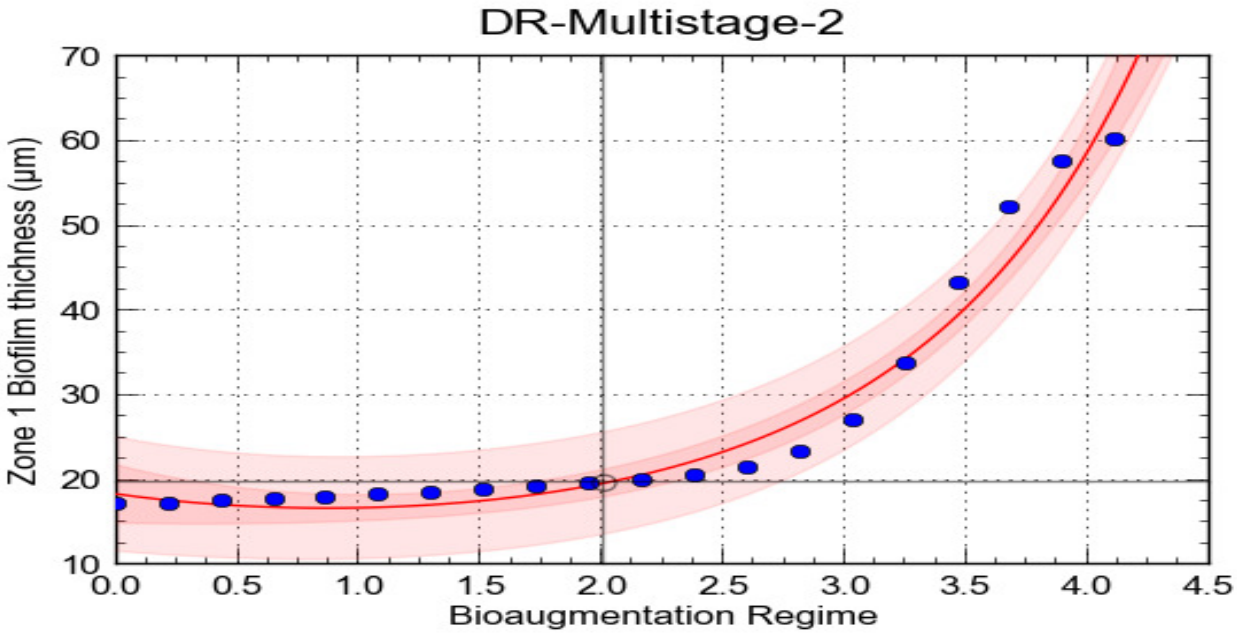

Figure E-1: Graph illustrating the model response of Zone 1 biofilm thickness as a function of Bioaugmentation Regimes 0, 1, 2, 3 and 4

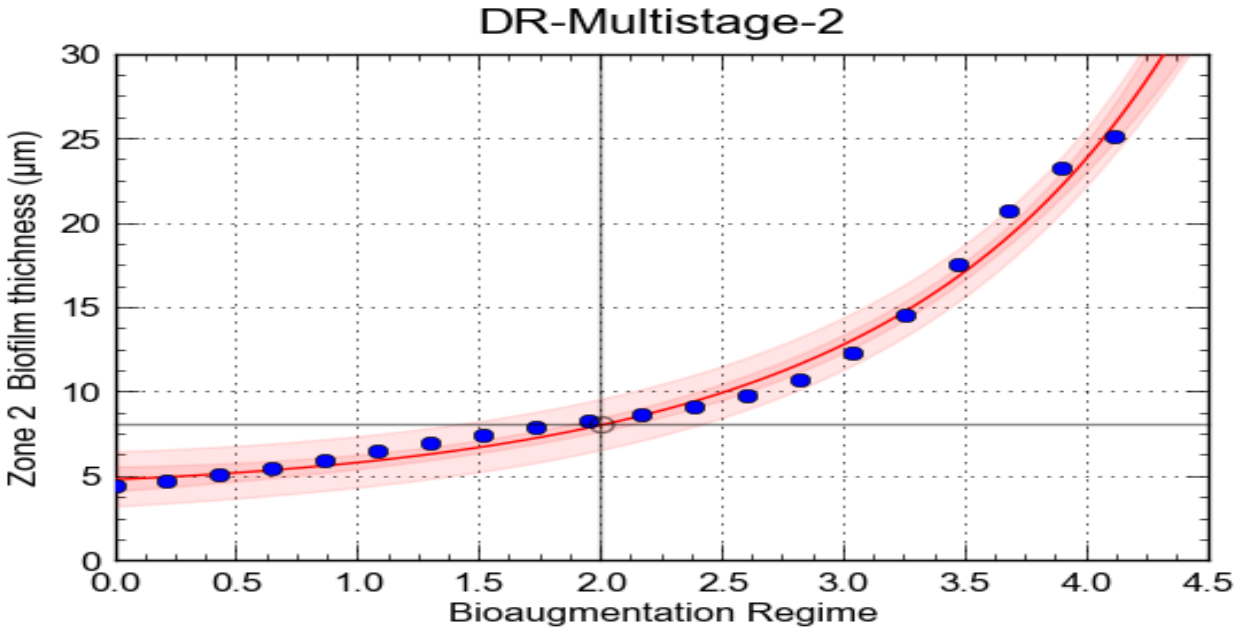

Figure E-2: Graph illustrating the model response of Zone 2 biofilm thickness as a function of Bioaugmentation Regimes 0, 1, 2, 3 and 4

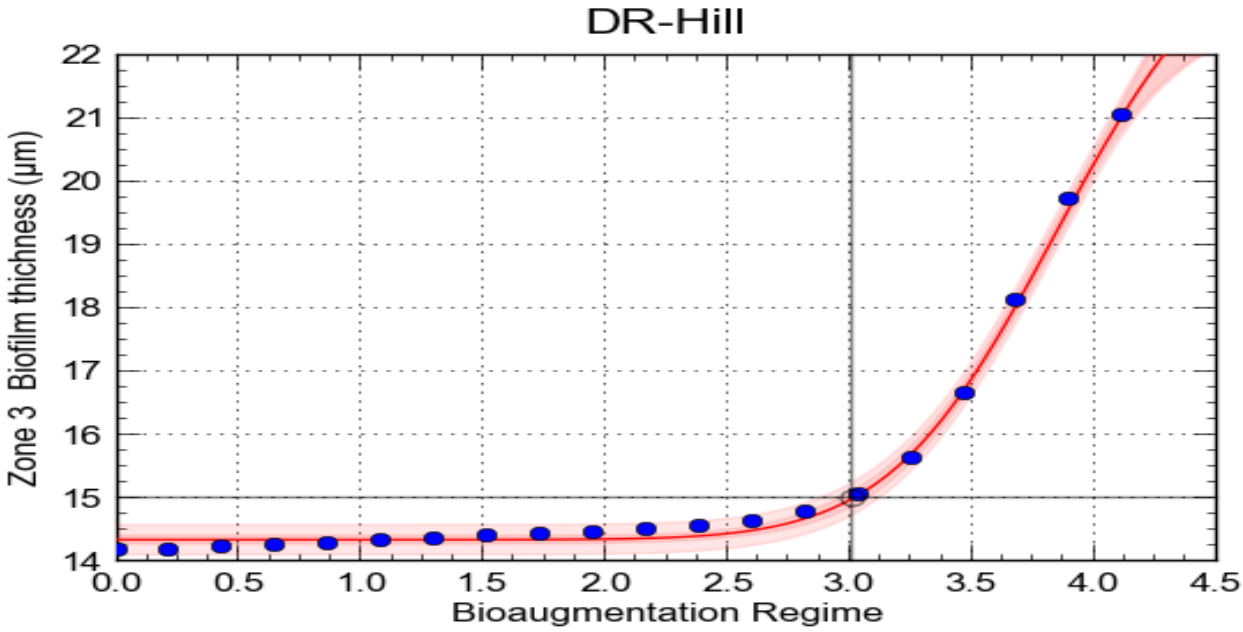

Figure E-3: Graph illustrating the model response of Zone 3 biofilm thickness as a function of Bioaugmentation Regimes 0, 1, 2, 3 and 4

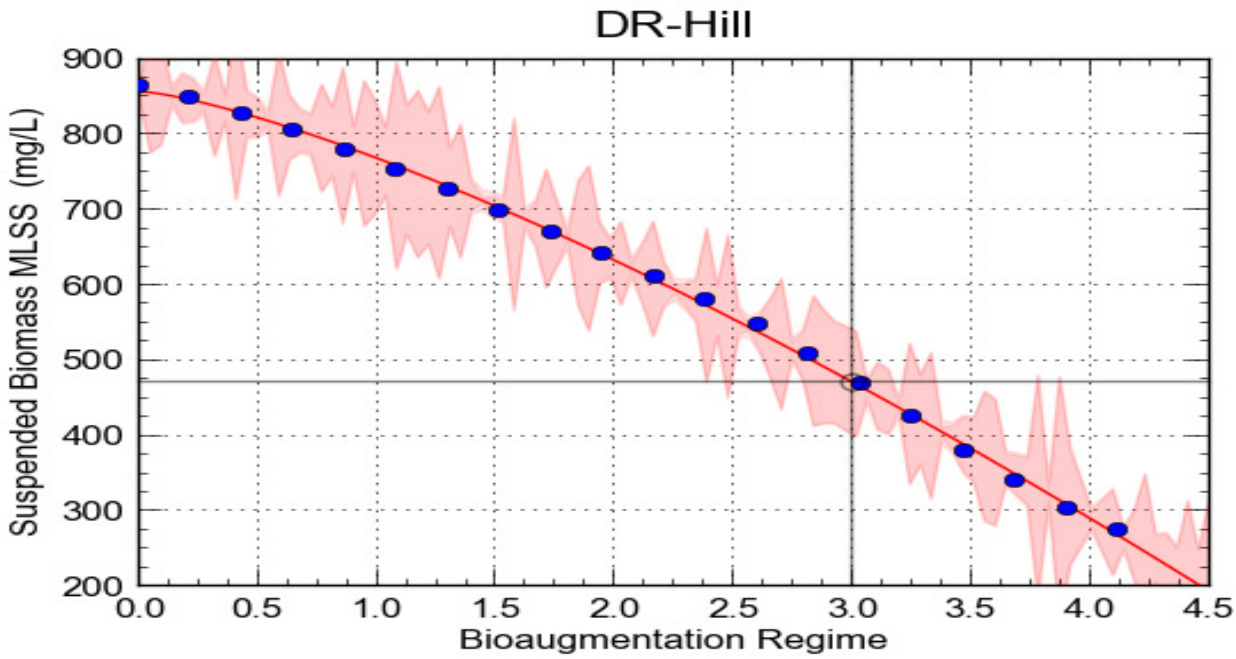

Figure E-4: Graph illustrating the model response of suspended biomass as a function of Bioaugmentation Regimes 0, 1, 2, 3 and 4

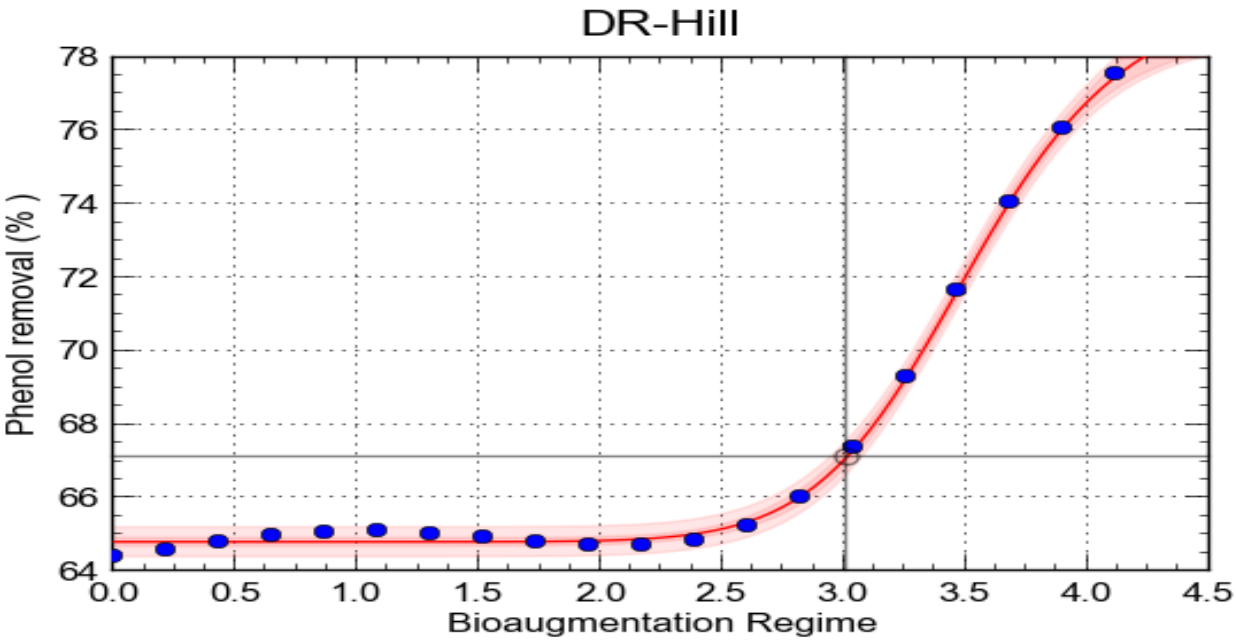

Figure E-5: Graph illustrating the model response of phenol removal as a function of Bioaugmentation Regimes 0, 1, 2, 3 and 4

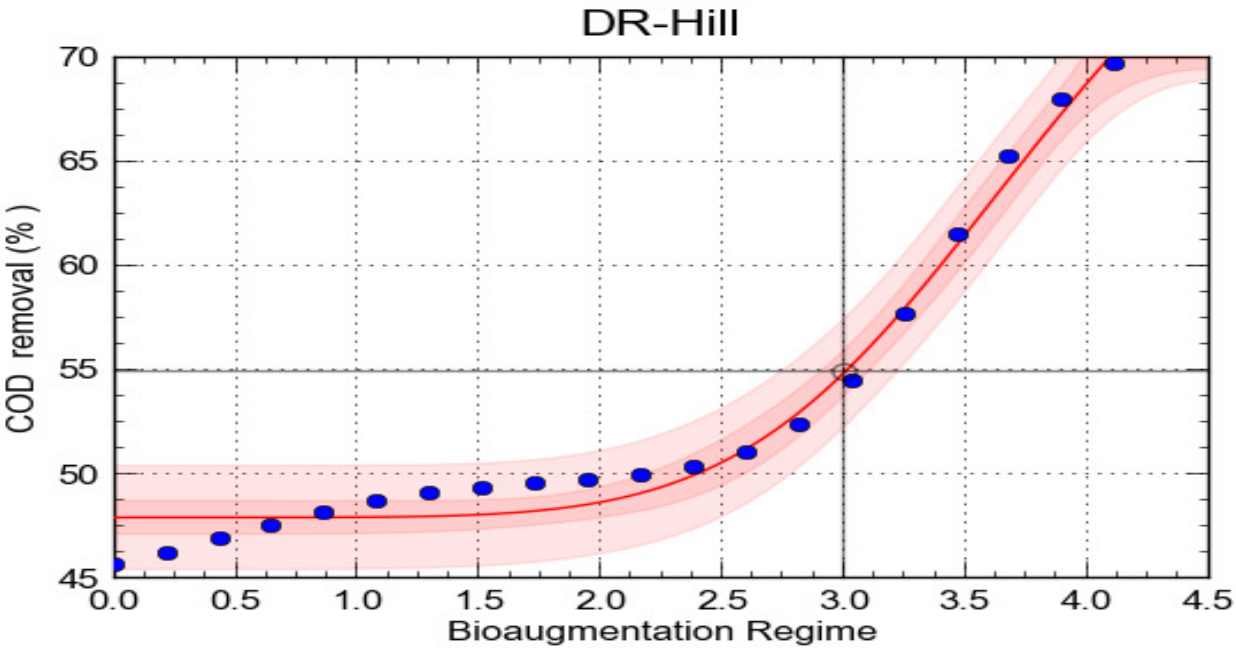

Figure E-6: Graph illustrating the model response of COD removal as a function of Bioaugmentation Regimes 0, 1, 2, 3 and 4

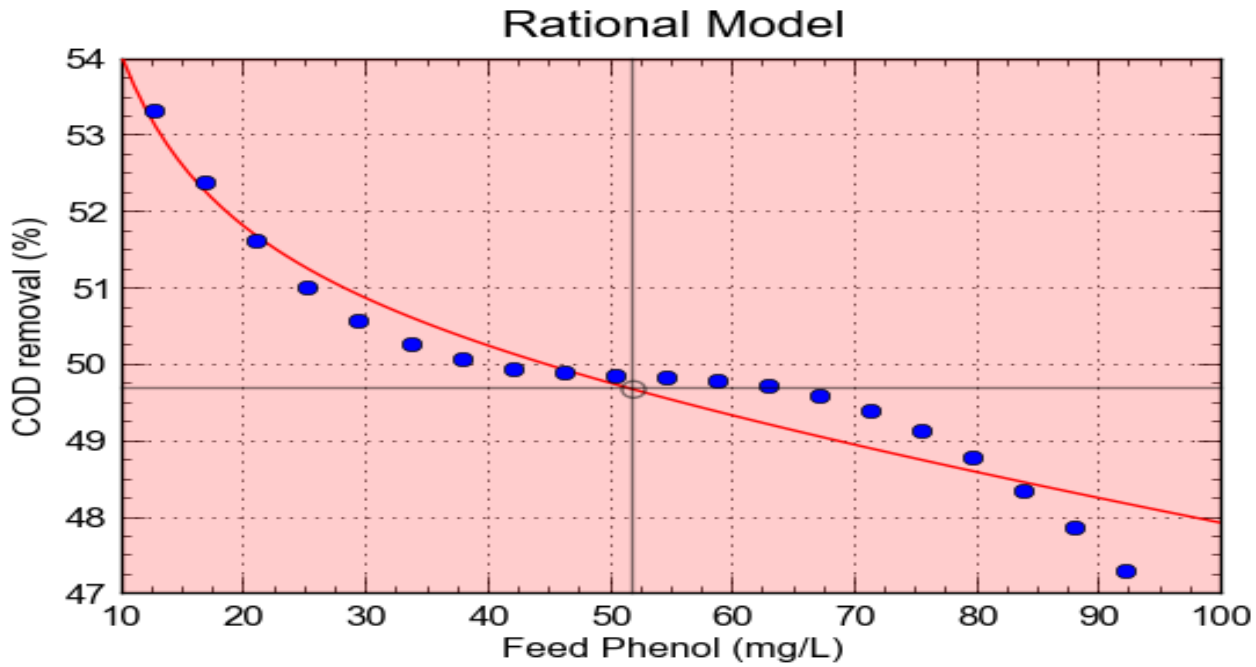

Figure E-7: Graph illustrating the model response of COD removal as a function of feed phenol

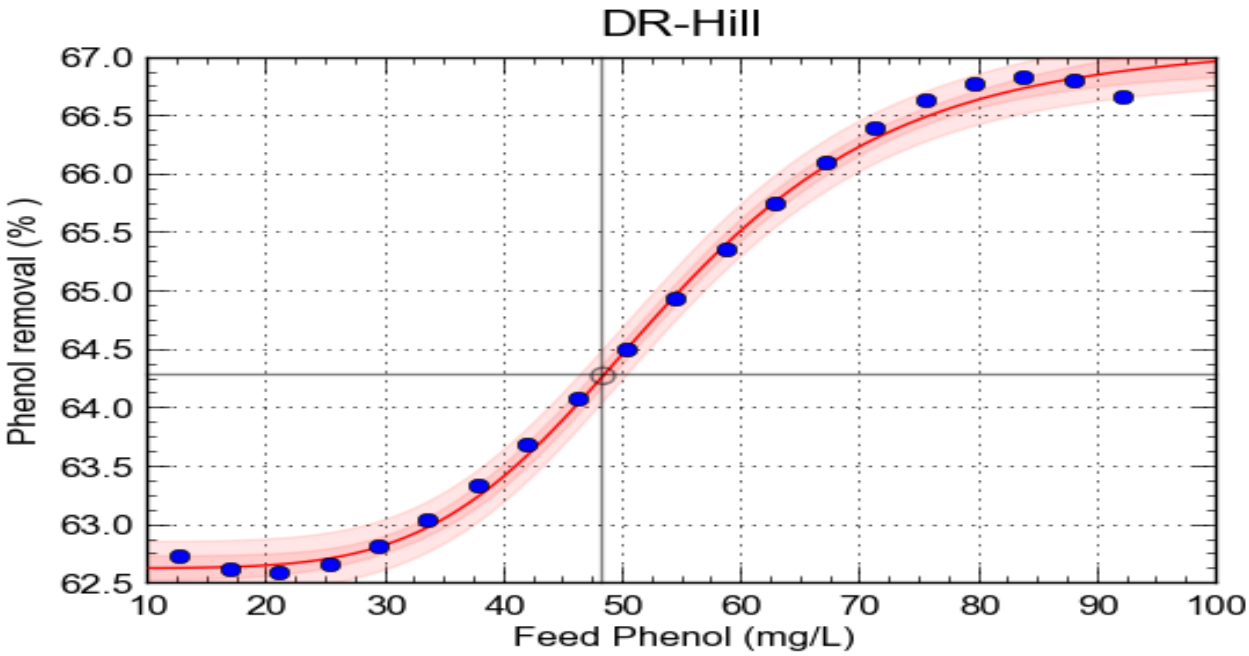

Figure E-8: Graph illustrating the model response of phenol removal as a function of feed phenol

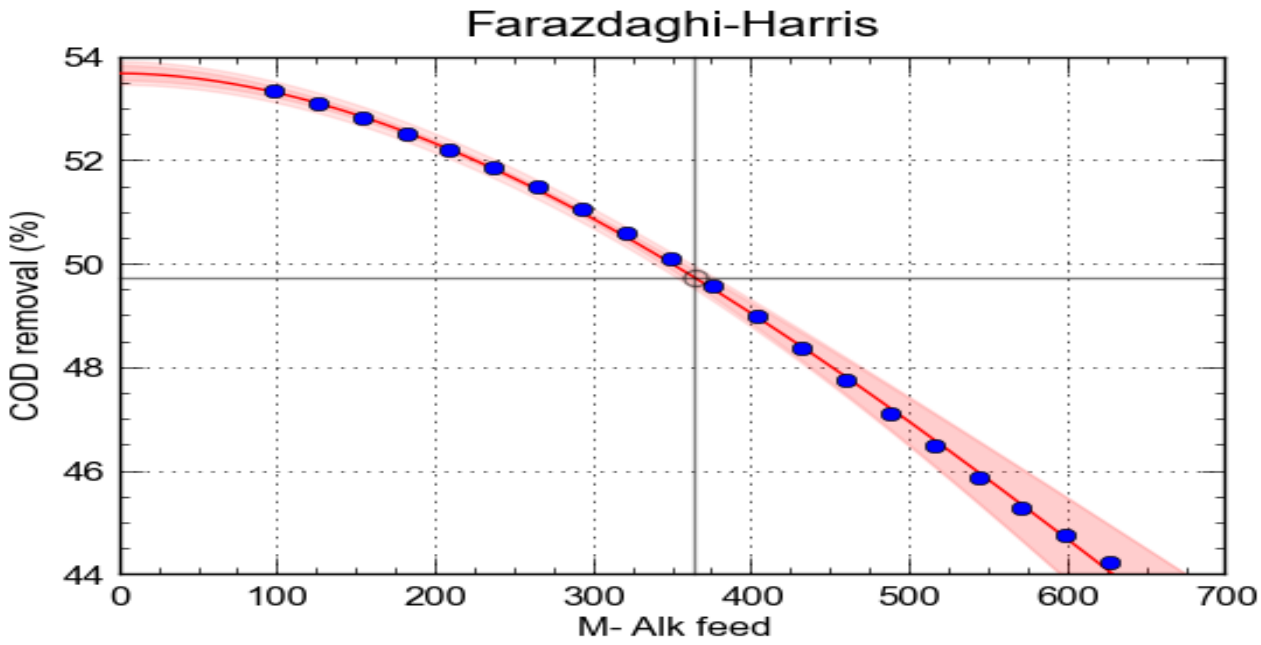

Figure E-9: Graph illustrating the model response of COD removal as a function of feed M-alkalinity

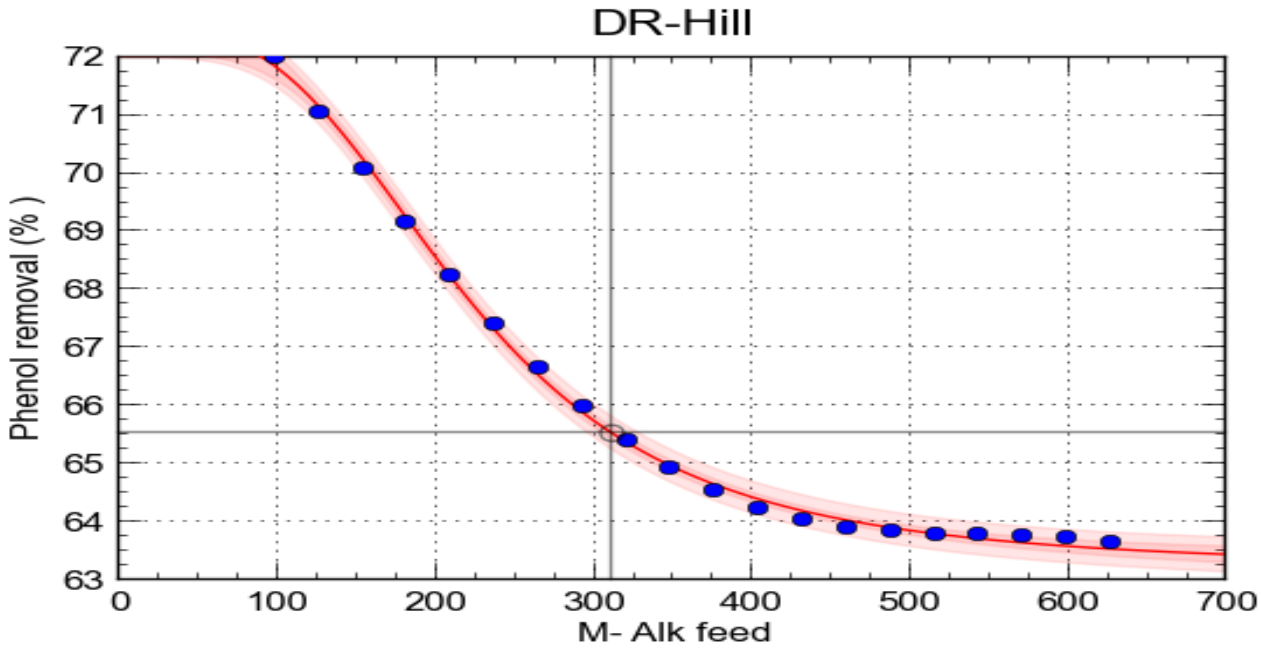

Figure E-10: Graph illustrating the model response of phenol removal as a function of feed M-alkalinity

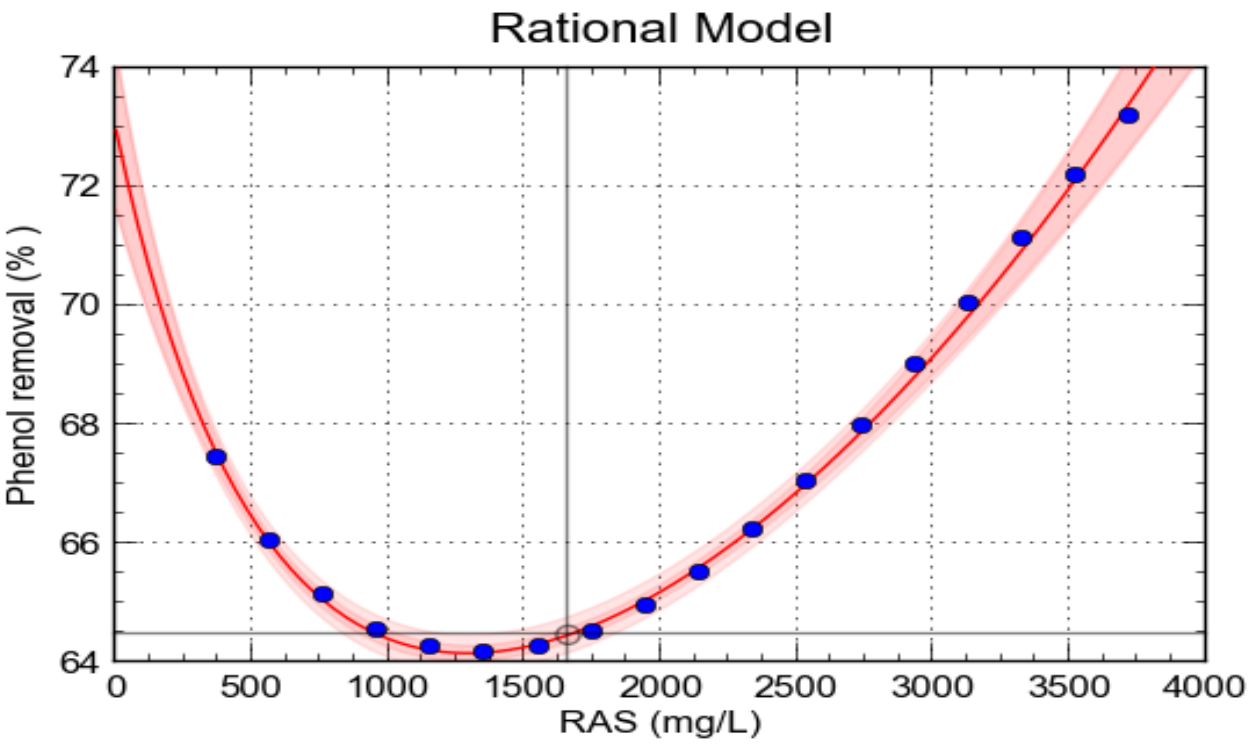

Figure E-11: Graph illustrating the model response of phenol removal as a function of RAS (feed suspended solids)

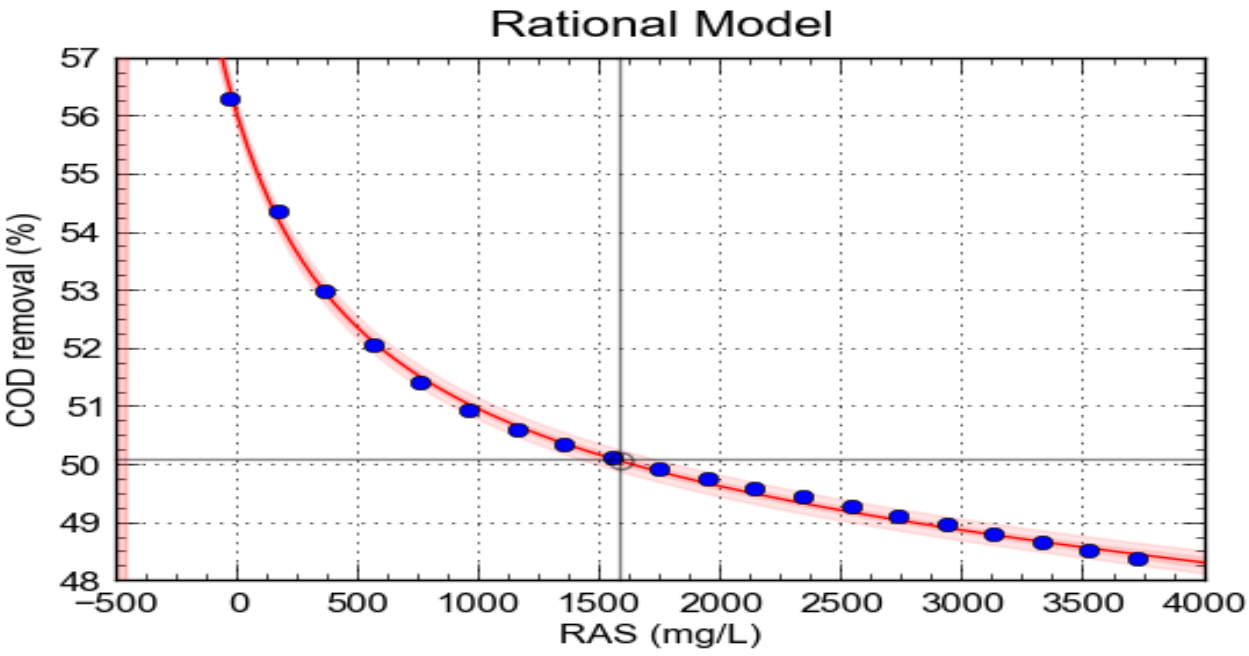

Figure E-12: Graph illustrating the model response of COD removal as a function of RAS (feed suspended solids)

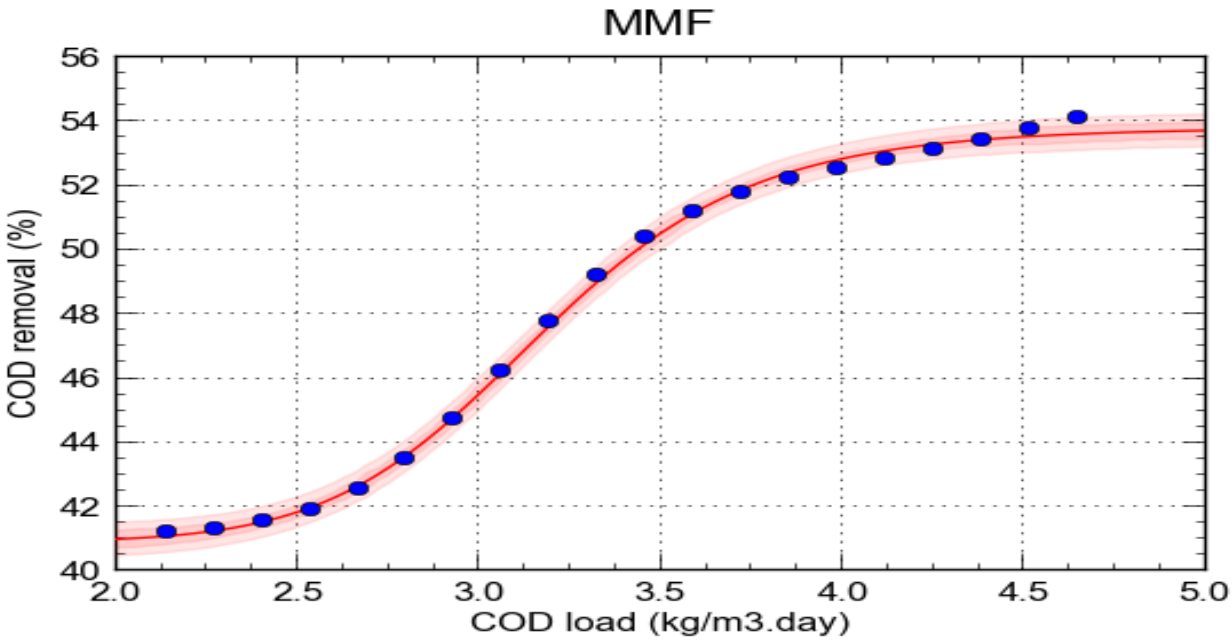

Figure E-13: Graph illustrating the model response of COD removal as a function of COD load

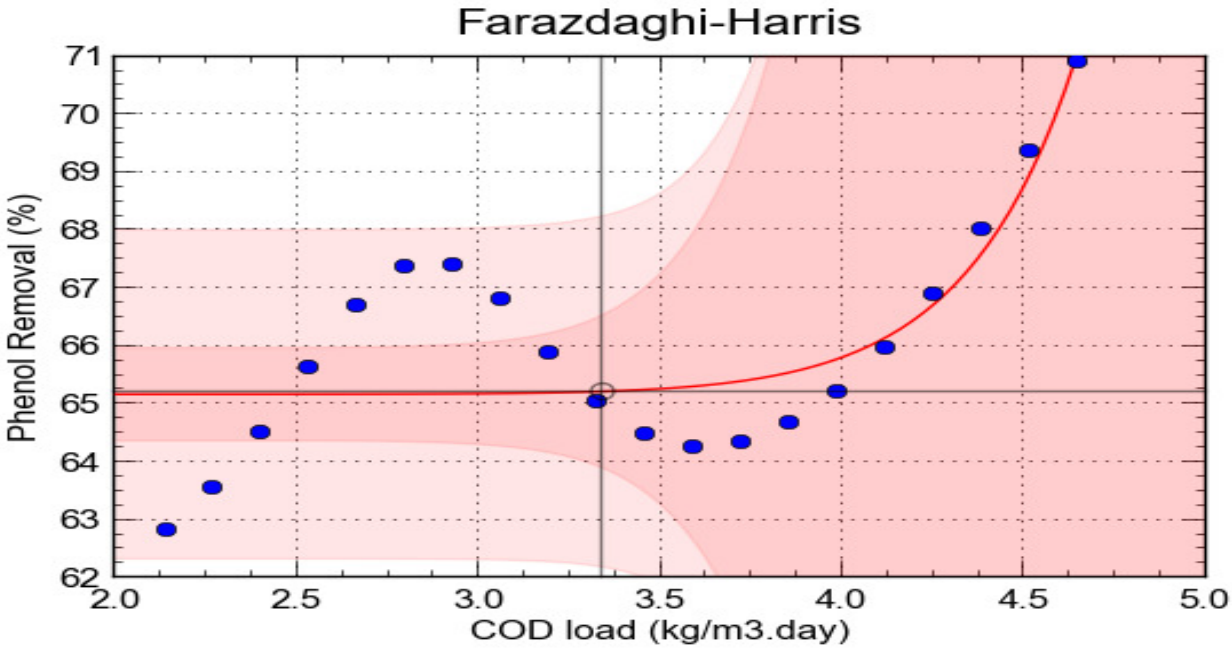

Figure E-14: Graph illustrating the model response of phenol removal as a function of COD load

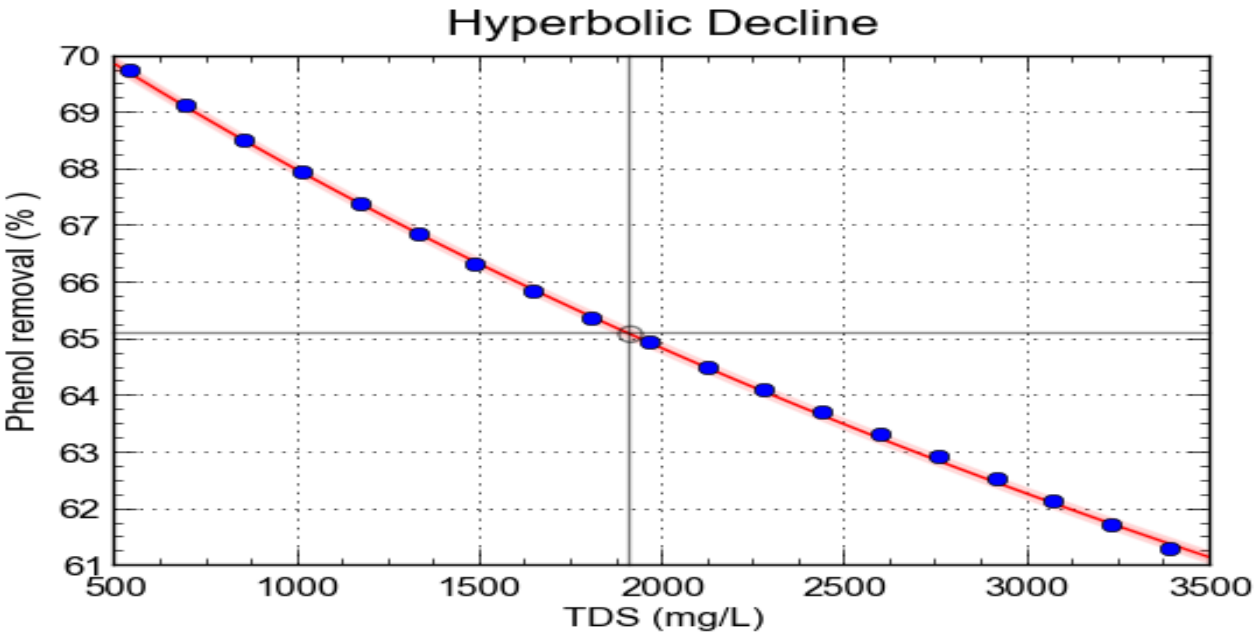

Figure E-15: Graph illustrating the model response of phenol removal as a function of TDS

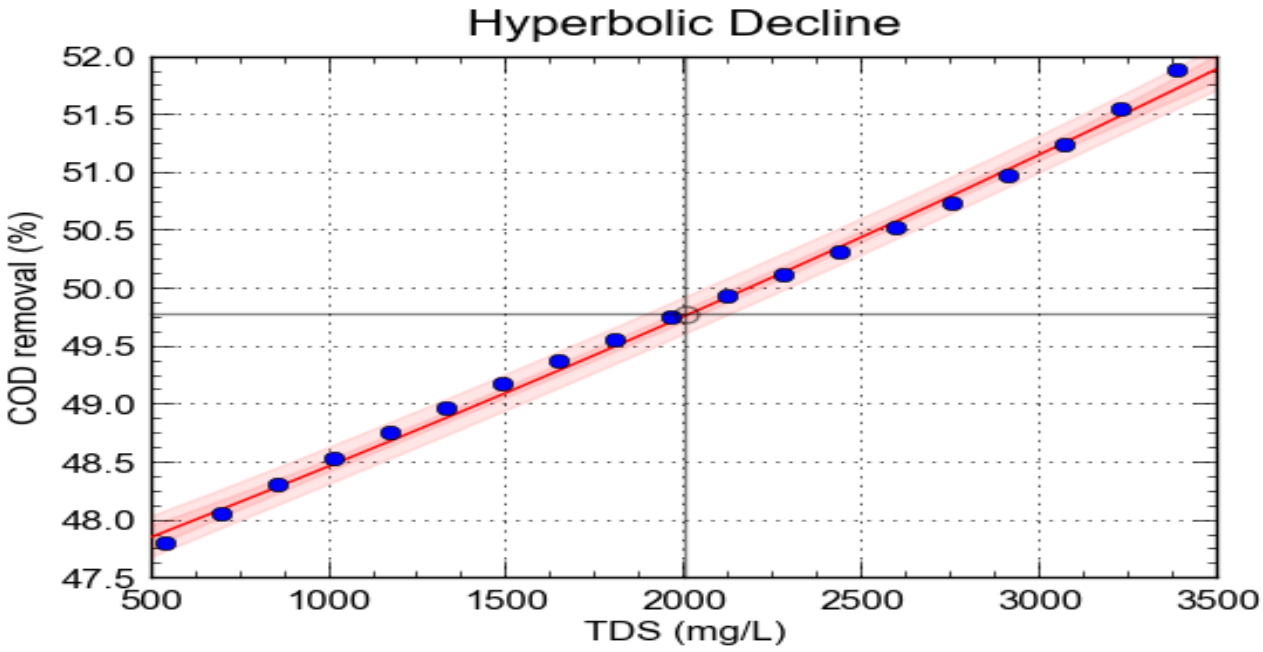

Figure E-16: Graph illustrating the model response of COD removal as a function of TDS

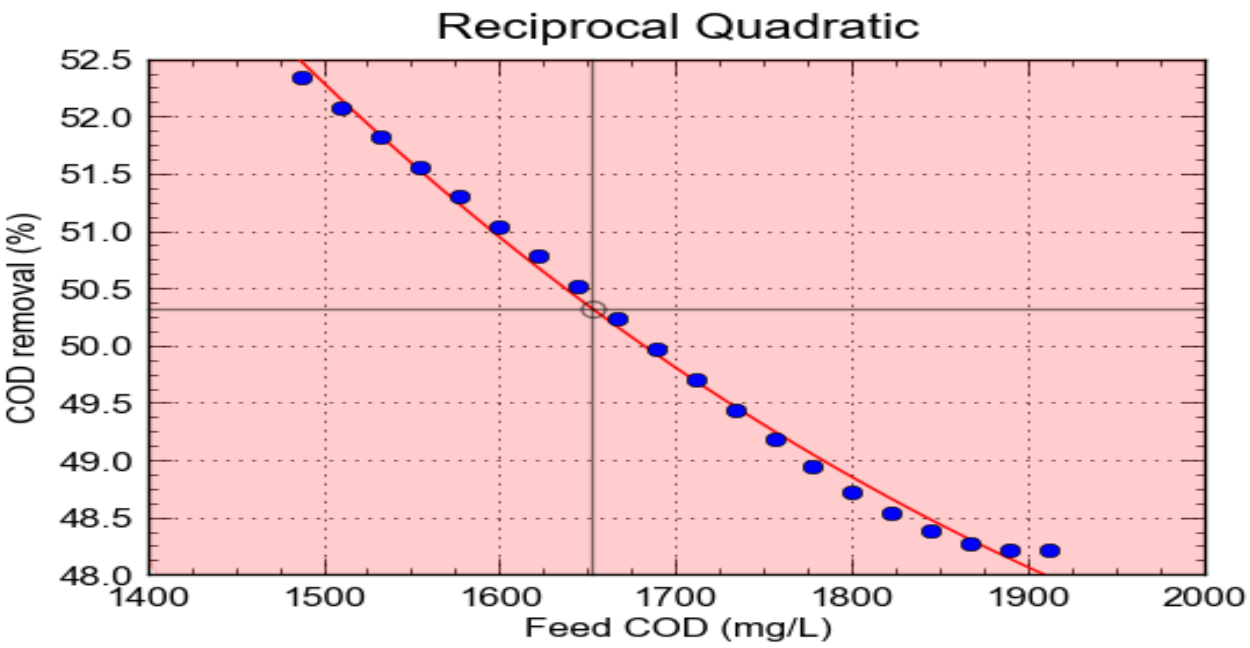

Figure E-17: Graph illustrating the model response of COD removal as a function of feed COD

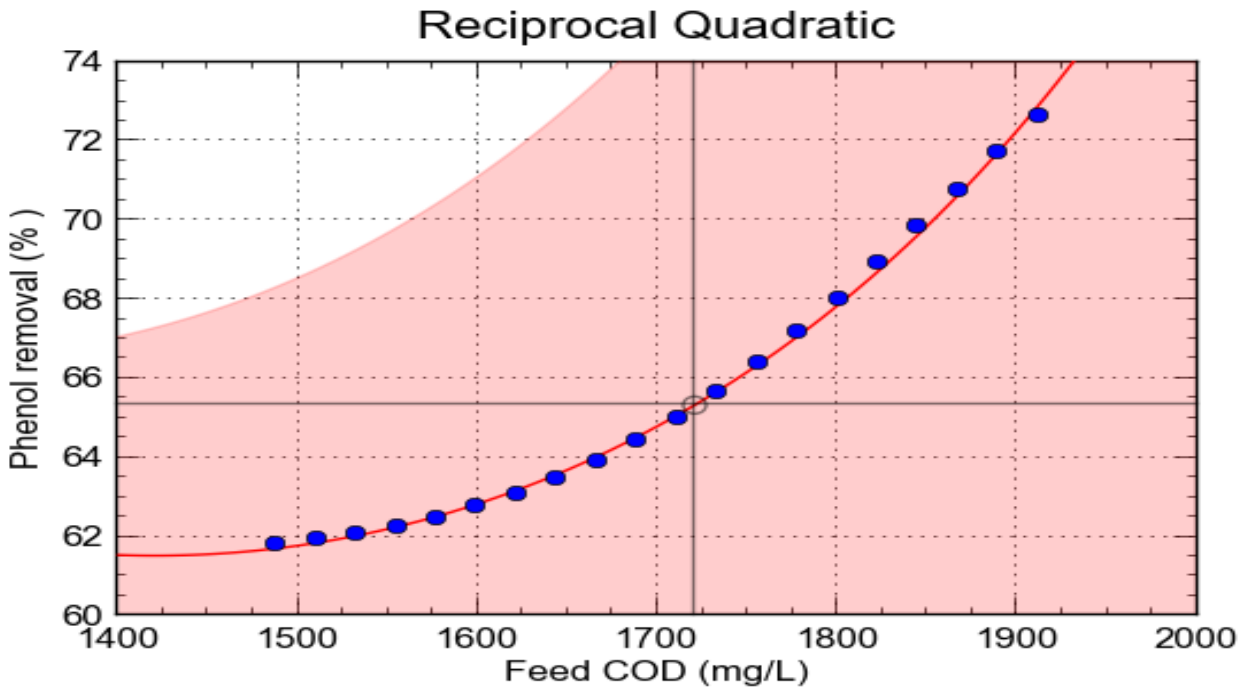

Figure E-18: Graph illustrating the model response of phenol removal as a function of feed COD